UNIVERSITEIT VAN PRETORIA
UNIVERSITY OF PRETORIA
YUNIBESITHI YA PRETORIA

An investigation into the fluorination capabilities of ammonium acid fluoride under microwave radiation with respect to zircon

---

Tryphine Nurse Nhlabathi

28722605

Department of Chemical Engineering

University of Pretoria

Dissertation submitted in partial fulfilment of the requirements of the degree Master of Science in the Faculty of Engineering, Built Environment and Information Technology, University of Pretoria

Supervisor : Prof. P.L. Crouse

Co-supervisor : Dr J.T. Nel

June 2012

Declaration

I declare that this dissertation is my own work and has not been submitted before for any degree or examination in any other university, and that all the sources I have used or quoted have been indicated and acknowledged as complete references.

Tryphine Nurse Nhlabathi

Signature: …… Date: ……...

Acknowledgements

This dissertation would not have been possible without the guidance and support of several individuals who contributed and extended their valuable assistance in the preparation and completion of this study.

I especially want to thank my supervisor Prof. P.L. Crouse for his supervision, guidance, and willingness to help throughout the research.

I would like to acknowledge my co-supervisor Dr J.T. Nel for the advice, support and guidance he has given me throughout the study.

I would like to thank my mentor Wilna du Plessis who supported me throughout my studies.

I gratefully thank Dr Hester Oosthuizen for editing and gave constructive comments on this thesis.

I am much indebted to Nols Jansen for his valuable advice in science discussion and editing this thesis.

I would also like to convey thanks to the Necsa for providing the laboratory facilities.

Thanks to my colleagues and staff in Applied Chemistry for moral support.

Special thanks go to Mpho Lekgoathi, without his assistance this study would not have been successful

I acknowledge the National Research Foundation (NRF), Graduate-in-Training Programme and for their financial support on this project.

I also acknowledge the DST via AMI for funding this project.

Lastly, I would like to thank my family members, especially Thapelo. Without their encouragement I would not have finished this thesis.

Abstract

South Africa is the second largest producer of zircon ($ZrSiO_4$) in the world, Australia being the largest. Zircon is notorious for its chemical inertness. Extreme processing conditions such as alkaline fusion (NaOH at 600 °C or Na_2CO_3 at 1200 °C) are used to extract the zirconium values from the mineral. The purpose of this study was to investigate the use of microwave digestion as an alternative process, and to determine the parameters for this technique for the digestion of zircon with ammonium acid fluoride (AAF) under various conditions. Ammonium acid fluoride is more convenient and safer to use than conventional fluorination methods such as HF and F_2.

In this study zircon was treated with ammonium acid fluoride ($NH_4F{\cdot}1.5HF$) by means of microwave assisted digestion. Reaction times ranged from 10 to 330 minutes at temperatures between 100 °C and 240 °C. Successive microwave digestion steps, interrupted by an aqueous wash procedure, resulted in a >99 % conversion of zircon to the water soluble intermediates $(NH_4)_3ZrF_7$ and $(NH_4)_2SiF_6$. XRD and Raman spectroscopy confirm that zircon was the major phase present in the insoluble fraction of the product after washing. Arrhenius rate laws are derived for both reaction control (progressively shrinking particle) and diffusion control by the product layer. Both models show reasonably good agreement with the experimental data, but diffusion control was accepted as the most probable. The derived diffusion coefficient corresponds to a solid-liquid case.

Publications emanating from this research

1) T.N Nhlabathi, A model for the kinetics of the reaction of zircon with ammonium acid fluoride enhanced by microwave digestion, AMI Light Metals Conference, Muldersdrift, October 2010.

2) J.T. Nel, W. du Plessis, T.N. Nhlabathi, C.J. Pretorius, A.A. Jansen, P.L. Crouse, Reaction kinetics of the microwave enhanced digestion of zircon, Journal of Fluorine Chemistry (2011) 132, 258-262.

List of abbreviations and acronyms

Abbreviations	Description
AAF	Ammonium acid fluoride
ABF	Ammonium bifluoride
AMI	Advanced Metals Initiative
AZST	Acid zirconium sulphate tetrahydrate
CSIR	Council for Scientific and Industrial Research
DST	Department of Science and Technology
ICP-OES	Inductively coupled plasma optical emission spectroscopy
LMDN	Light Metals Development Network
NMDN	New Metals Development Network
PCM	Progressive conversion model
PDZ	Plasma Dissociated Zircon
PMDN	Precious Metals Development Network
SCM	Shrinking core model
SEM	Scanning electron microscope
XRD	X-ray diffraction
ZBS	Zirconium basic sulphate
ZOC	Zirconium oxychloride

Table of Contents

List of figures

List of tables

CHAPTER 1

Introduction

1.1. Background information

South Africa supplies more than 30% of the global demand for zircon, of which more than 95% is exported (Industrial Minerals, 2010). Beneficiated products are then imported at high cost for industrial applications locally. In an effort to develop processes for the beneficiation of South Africa's mineral reserves, the Department of Science and Technology (DST) introduced the Advanced Metals Initiative (AMI). The AMI is structured in three legs, namely the Light Metals Development Network (LMDN), the Precious Metals Development Network (PMDN) and the New Metals Development Network (NMDN). The LMDN is responsible for the development of Ti, Mg and Al technology and is co-ordinated by the CSIR. The PMDN is co-ordinated by Mintek.

Necsa is responsible, *via* the NMDN, for the manufacture of Zr, Hf, Ta and Nb. All of these are expected to find application in the nuclear industry. The aim of the AMI is to develop new cost-effective and environmentally-friendly processes for the manufacture of the above mentioned metals. Necsa has developed a process whereby zircon ($ZrSiO_4$) is dissociated in a plasma to form $ZrO_2{\cdot}SiO_2$ or plasma dissociated zircon (PDZ). PDZ is chemically reactive, in contrast with the inert raw material. PDZ is the feedstock material of choice for the manufacture of both Zr and Hf. The process is unique and its development has been a considerable technological contribution.

1.2. Problem statement

Traditional mineral beneficiation processes to extract Zr, Hf, Ta and Nb from the associated minerals involve high temperature alkaline smelting and digestion with

mineral acids. These minerals are notoriously difficult to get into solution. Ammonium acid fluoride (AAF) has been identified as an alternative fluorinating agent as it may provide a method by which a broad spectrum of anhydrous metal fluorides can be synthesized. The anhydrous metal fluorides might be useful as metal precursors if further applications of the corresponding metals are considered. AAF is expected to be more convenient and safer to use than conventional methods. In addition the potential for regeneration and recycling of the reagents exists.

1.3. Strategy

Initial trials of zircon and AAF with microwave assisted digestion proved to be very promising. AAF couples very effectively with microwave radiation and heating is extremely rapid. The high pressures achieved in the vessel accelerate the reaction considerably. This study was planned to focus on the microwave-accelerated reactions with the metal compounds applicable to the New Metals Development Network (i.e. Zr, Hf, Ta and Nb).

A microwave system was purchased by Necsa. All other resources such as instrumentation, equipment, tools, reagents, analysis and technical assistance were available at, or would be procured by, Necsa. Existing specialist equipment and expertise with regard to XRD analyses and Raman spectroscopy at Necsa would be used.

The main thrust of the work has been:

- The generation of kinetic data for the reaction between zircon and AAF.
- Determination of the exact rate-determining mechanism, and comparison with conventional processes.

Existing literature on the properties and reactions of ammonium bifluoride and the respective ammonium fluorometallates has been supplemented, where possible, by results obtained through thermogravimetric studies. Reagents and products were characterized by means of various analytical techniques such as Raman, XRD, etc. Isolation and characterization of reaction products, especially where PDZ is concerned, may prove to be a challenge. Finally, experience gained in the experimental work would be used for developing guidelines for the construction of a larger-scale reactor for treatment of > kg quantities.

1.4. The aim of the study

The purpose of this study is to determine the kinetic parameters for the microwave digestion of zirconium compounds with ammonium acid fluoride (AAF) under various conditions. The following were investigated:

1.4.1. Effect of temperature and pressure with reaction time.
1.4.2. Spectroscopic investigation of the reaction products.
1.4.3. Investigation into the morphology of the products.

From the data above, a kinetic rate law and Arrhenius parameters will be extracted.

CHAPTER 2

Literature review

Methodology used in this literature review

The search for information was made using the following database and web search engines: Science direct, Scopus and Google. The key words used were “microwave chemistry”, “dielectric properties”, “microwave assisted leaching”, “microwave processing”, “microwave enhanced chemistry”, “microwave effects”, “microwave digestion of zircon”, “fundamentals of microwave heating”, “microwave dissolution of minerals”, ‘‘closed and open techniques”, “microwave applicators” and “hot spots in microwave irradiation”. The following books were also used: Metaxas and Meredith (1993) “Industrial microwave heating” and Kingston (1988) “Introduction to microwave sample preparation’’. Discussions with a number of Necsa specialists were also conducted on regular basis.

2.1. The chemistry of Zr and Hf

2.1.1. Introduction

South Africa is the second largest producer of zircon ($ZrSiO_4$) in the world, Australia being the largest (Tyler and Minnitt, 2004). In 2009 South Africa supplied about 400 000 tonnes (29% of the global demand). Zircon concentrate is separated from ilmenite ($FeTiO_3$) and rutile (TiO_2) in beach sand dredgings (U_xC Consulting, 2010; TZ Minerals, 2001). The main heavy mineral sand industries in South Africa are located on the KwaZulu Natal coast at Richards Bay, and on the west coast at Namakwa Sands (Roskill, 2004). Figure 2.1 shows typical sea zircon sand.

Figure 2.1: Zircon sand (source: Manufacturer. *s.a*.)

Zircon is mainly used as an opacifier in the ceramic tile industry and this accounts for more than 80% of all zircon mined. Zircon must be milled to an average particle size of less than 5 µm to be suitable for opacifier applications. The different opacifier grades of zircon depend mainly on the particle size and particle size distribution. Purity also plays a role and prime grade zircon is usually used in these applications (Snyders, 2007). Chemicals such as acid zirconium sulphate tetrahydrate (AZST), zirconium oxychloride (ZOC), zirconium acetate, zirconium basic sulphate (ZBS), and zirconium metal are usually manufactured from zircon (Abdelkader *et al*., 2008). In 2009 the global market for zirconium chemicals was about 10 000 tonnes and for zirconium metal between 5 000 and 10 000 tonnes (U_xC Consulting, 2010; Puclin *et al*., 1995). Zirconium metal is almost exclusively used as a cladding material for nuclear fuel in nuclear reactors (Puclin *et al*., 1995). Hafnium, which is always present in zircon in concentrations of 1 to 3%, has to be removed from zirconium intended for nuclear applications because of its high neutron capture cross section (Etherington *et al*., 1955).

Zircon is notorious for its chemical inertness (Wilks *et al*., 1974). In order to extract the zirconium values from the mineral, extreme processes like alkaline smelting with NaOH at 600 °C or with Na_2CO_3 at 1200 °C have to be applied. These reactions proceed according to Equations 2.1 and 2.2.

$$ZrSiO_4 + 4NaOH \xrightarrow{600^\circ C} Na_2ZrO_3 + Na_2SiO_3 + 2H_2O \quad (2.1)$$

$$ZrSiO_4 + 2Na_2CO_3 \xrightarrow{1200^\circ C} Na_2ZrO_3 + Na_2SiO_3 + 2CO_2 \quad (2.2)$$

Separation of the sodium zirconate from the sodium silicate is achieved by dissolution in water, filtration and precipitation.

Zirconium tetrachloride is produced by carbo-chlorination of zircon at >800 °C according to Equation 2.3.

$$ZrSiO_4 + 4Cl_2 + 2C \xrightarrow{>800^\circ C} ZrCl_4 + SiCl_4 + 2CO_2 \quad (2.3)$$

The $ZrCl_4$ and $SiCl_4$ both liquids are separated by distillation. $ZrCl_4$ serves as a starting material for the manufacture of several zirconium chemicals as well as the metal. Zircon can also be made chemically more tractable by dissociation in a plasma flame at >1700 ºC. This product is called plasma dissociated zircon (PDZ, $ZrO_2 \cdot SiO_2$). Compared to zircon, PDZ is chemically very reactive. The amorphous silica can be dissolved selectively with concentrated NaOH solutions, or reacted with anhydrous HF (Stevens, 1986; Bidaye *et al*., 1999; Williamson and Evans, 1979; Wilks *et al*., 1972; McPherson and Shafer, 1985). The processes are represented by Equations 2.4, 2.5 and 2.6.

$$ZrSiO_4 \xrightarrow{>1700\ ^\circ C} ZrO_2.SiO_2 \quad (2.4)$$

$$ZrO_2 \cdot SiO_2 + 2NaOH\ (aq) \rightarrow ZrO_2 + Na_2SiO_3 + H_2O \quad (2.5)$$

$$ZrO_2 \cdot SiO_2 + 4HF(g) \rightarrow ZrO_2\ (s) + SiF_4 + 2H_2O \quad (2.6)$$

PDZ can also be fully dissolved in 40% HF as follows: (Monnahela, 2008).

$$ZrO_2 \cdot SiO_2 + 12HF(aq) \rightarrow H_2ZrF_6 + H_2SiF_6 + 4H_2O \quad (2.7)$$

The H_2ZrF_6 and H_2SiF_6 are separated by evaporative crystallization. The crystallization also serves as a purification step for the H_2ZrF_6. Pure ZrO_2 can be produced from H_2ZrF_6 by steam pyrolysis at 600 to 800 °C, according to Equation 2.8.

$$H_2ZrF_6 + 2H_2O \xrightarrow{600\text{-}800^{\circ}C} ZrO_2 + 6HF \qquad (2.8)$$

The present work investigates the reaction of zircon with ammonium acid fluoride (AAF) under microwave assisted digestion conditions. The reaction kinetics under these conditions is reported.

2.1.2. Occurrence of zircon

Zircon ($ZrSiO_4$) occurs in nature as an additional mineral deposited over time on the earth's crust. It is found in igneous rocks, metamorphic rocks and also in sedimentary rocks (Finch and Hanchar, 2003; Rasmussen, 2005). Weather processing and erosion of these rocks by action of wind and water have led to zircon deposits to concentrate in ocean beaches, deltas and river sands. Zircon is mined from unconsolidated sands in beach deposits as an ore. The mineral sands are primarily mined in Australia, South Africa, the USA, Canada, and India. In South Africa, the Richards Bay mineral reserves are rated among the largest in the world (Kotzé *et al*., 2006).

2.1.3. Production of zircon

The leading zircon producers are presented in Table 2.1.

Table 2.1: Leading zircon producers in 2008

Producer	Home Country	Principal operations	2008 production share (%)
Iluka Resources	Australia	Australia; U.S.A (VA)	34
Exxaro Resources	South Africa	South Africa; Australia	15
Rio Tinto Group	UK	South Africa; Canada	9
BHP Billiton	Australia	South Africa	9
Bemax Resources	Australia	Australia	4
Du Pont	U.S.A.	U.S.A. (FL)	3
TiWest JV	Australia	Australia	2
Others			24

Source: U_xC Consulting, 2010

2.1.4. Properties of zircon

Zircon is a good refractory material, which has been applied regularly in the steel industry. Zircon does not undergo any structural transformation until at about 1450-1700 °C. It demonstrates many attractive properties such as excellent chemical stability with a very low thermal expansion co-efficient (4.1 x 10^{-6} °C^{-1} from room temperature to 1400 °C) (Rendtorff *et al*., 2009) and low thermal conductivity (5.1 W/m °C at room temperature and 3.5 W/m °C at 1000 °C) (Shi *et al*., 1997).

The mineral zircon occurs in nature in a variety of green, yellow, red, and brown colours. The heat-treatment process produce blue and golden crystals and colourless materials are produced in this manner too (Roskill, 2004).

Zircon is the only feasible mineral as starting material for the manufacture of zirconium (Zr) metal. However, this mineral is chemically very inert; and thus considerable energy is needed to break the bonds necessary for its reduction into zirconia (ZrO_2) and zirconium metal (Elijofor *et al*., 1997).

2.2.1. Chemistry of ammonium acid fluoride

The fluorinating actions of elemental fluorine, halogen fluorides and hydrogen fluoride are well known and these compounds are widely applied for synthesizing inorganic fluorides (Opalovsky *et al.,* 1973). However the high cost of F_2 and HF and their corresponding corrosive behaviour, and also the liberation of SiF_4 result in fewer industrial applications of this process. Lately, however, interest in solid fluorinating agents has continually grown, since they possess many advantages. Ammonium fluorides are easier to use because they are solid crystalline substances under normal conditions, unlike fluorine and hydrogen fluoride which are gases. Metal fluorides, when treated with ammonium hydroxide, result in ammonium fluorides, which are the basis for recycling and conversion of the ammonium fluorides (Guzeev and D'yackenko, 2006).

Much attention has been paid to ammonium bifluoride as a potential fluorinating agent, because the melting and evaporation temperatures of this compound are relatively low. The reactivity of $NH_4F.HF$ is close to that of anhydrous hydrofluoric acid and the compound can be successfully applied as a fluorinating agent in many reactions. Ammonium bifluoride melts without perceptible decomposition, and on further heating decomposes, hydrogen fluoride being split off (Opalovsky *et al.,* 1973).

The knowledge of the activities of the components of the NH_4HF_2-HF mixtures for various compositions and temperatures, offers a particular interest in the study of the electrowinning of fluorine and nitrogen trifluoride from these mixtures. From the HF activity corresponding to a given composition and temperature, we can deduce, using the Gibbs-Duhem relation, the activity of the second component of the melt ($NH_4F{\cdot}HF$). Subsequently, the equilibrium constant of the following equilibrium enables us to calculate the activity of NH_4F.

$$NH_4F{\cdot}HF \rightleftharpoons HF + NH_4F \qquad (2.9)$$

From the activities of these three molecular species, equilibrium diagrams such as potential –p(HF) diagram [with p(HF) = -log p(HF)] can be set up (Filliaudeau and Picard, 1991).

2.2.2. Properties of ammonium fluorides

Two known stable compounds of ammonium with hydrogen fluoride under ordinary conditions are NH_4F and NH_4HF_2. Ammonium fluoride normally is a clear, colourless and a transparent substance which forms hexagonal crystals with the wurtzite lattice (space group *P6mc*). This is related to the formation of strong hydrogen bonds by NH_4F and accounts for the fact that the NH_4^+ groups are immobile in the crystal and this also distinguishes it from other ammonium halides, which have cubic structures. The crystal lattice of NH_4F at 23 °C has the following lattice constants: a = 0.4439 nm, c = 0.7165 nm, z = 2. The respective calculated and measured values of the density are 1.006 $g.cm^{-3}$ and 1.002 $g.cm^{-3}$. While the boiling point of NH_4F is not yet known, when heated in the temperature range 343 – 383 K, the compound decomposes according to Equation 2.10.

$$2NH_4F\ (crystalline) \rightarrow NH_4HF_2\ (crystalline) + NH_3(gas) \qquad (2.10)$$

This also helps to differentiate it from other ammonium halides (Rakov and Mel'nichenko, 1984).

Ammonium bifluoride while also colourless is a slightly hygroscopic substance and forms an orthorhombic crystal lattice with dimensions a = 0.840 nm, b = 0.816 nm, c = 0.367 nm, z = 4, the calculated density of ammonium bifluoride as per space group *Pman*, is 1.505 g. cm^{-3}. The NH_4^+ ion group is connected to the F^- anion by strong hydrogen bonds: with each fluorine atom forming two hydrogen bonds with the nitrogen atom, and one with another fluorine atom. The melting point of NH_4HF_2 is 126.45 °C, and the enthalpy of fusion is 4.564$\pm$ 0.002 kcal $mole^{-3}$. Ammonium bifluoride is readily soluble in water and is of greatest interest as a fluorinating agent (Rakov and Mel'nichenko, 1984).

According to Vorotynstev *et al*. (2004) $NH_4F.HF$ can contain $NH_4F.HF$, $NH_4F.3HF$, and $NH_4F.5HF$ both in the solid and liquid states and $NH_4F.2HF$ in the solid state, determined by thermal analysis, density, viscosity and heat capacity measurements. However because $NH_4F.3HF$ and $NH_4F.5HF$ easily start evaporating at 23.2°C and -8°C respectively, the melt composition at elevated temperatures includes only NH_4F, $NH_4F.HF$, and HF. Electrolytic dissociation in a melt of acidic ammonium fluorides is due to the dissociation of HF stimulated by ammonium fluorides, while NH_4F itself virtually does not dissociate. Hence, the chemical equilibrium in a melt of ammonium polyfluorides at elevated temperatures can be described by Equations 2.11 and 2.12.

$$NH_4F{\cdot}HF \rightarrow NH_4F + HF \qquad (2.11)$$

$$3HF \rightarrow H_2F^+ + HF_2^- \qquad (2.12)$$

2.3.1. Process improvement

The technology used for the processing and breakdown of zircon is still labor-consuming, although efforts have been made to improve it (Guzeev and D'yachenko, 2006). Necsa has developed a processing route for zircon which is based on plasma and fluorochemical technology (Nel, 1995). In this study we have used microwave digestion as an alternative method or source of energy for the breakdown of zircon. Ammonium acid fluorides (AAF) have been identified as alternative fluorinating agents because they are found to be relatively safe to use compared to hydrogen fluoride (HF) and fluorine (F_2). The main objective for choosing microwave digestion in this study is to reduce processing costs, time, and improve the yield of extracted metals.

The beneficial effects of microwave radiation can be utilized to improve processes, especially if classical methods require harsh conditions, prolonged reaction times or high temperatures. Where processes involve sensitive reagents or where an increase in reaction temperature could cause product decomposition, microwave radiation can also be used (Langa *et al*., 1997).

Microwave heating was used as an industrial process technique as far back as the 1960s (Galema, 1997; Metaxas and Meredith, 1983). Microwave is a broad name for electromagnetic (EM) waves (Tada *et al*., 1998). Microwave energy has been applied extensively in the processing of food, communication, and leaching of metals to increase the yield during extraction. Microwave energy has been found to be better than conventional heating, which is known to overcure the external surface; while undercuring the interior (Clarke *et al*., 2000; Al-Harahsheh and Kingman, 2004). It is because with microwaves radiation heat is generated inside the material and simultaneously distributed to the bulk of the material due to excitation of molecules. It is radiated outwards, making this type of energy source non-conventional (Baeraky, 2002; Callebaut, 2007).

The microwave heating technique was first used in 1975 as a heating source, under atmospheric conditions, for acid digestion applications in the chemistry laboratory. Microwave heating has brought significant improvements in the rate of chemical reactions, and reduced the sample preparation time from hours to a few minutes. This has resulted in an overall reduction in experimental time as compared to conventional methods (LeBlanc, 2000). Yet, microwave heating is not suitable for all types of compounds, for example, alkanes, ethers, glycols, ketones and explosives because they are highly reactive with oxidizing acids.

Microwave digestion has gained considerable attention during the last two decades in the processing of ceramics. The advantages that account for microwave usage includes:

- rapid heating,
- enhanced densification rate,
- decreased sintering activation energy,
- improved product yield, and
- improved microstructure.

Microwave heating also has the prospect for energy and cost savings when compared to conventional heating (Xie *et al*., 1999; Das *et al*., 2008). Microwave heating is used predominantly in the synthesis of organic compounds. However, its application in inorganic chemistry has been well documented as various aspects of inorganic chemistry and polymer chemistry (specifically polymer curing) have also been investigated (Galema, 1997; Bookse *et al*., 1997).

The development of probes that could enter the microwave environment safely and without any considerable disruption to the reaction, still poses a serious challenge to the advancement of microwave enhanced chemistry. Pressure feedback controls were first introduced in 1989 and by 1992 temperature feedback control came into being used (Walter *et al*., 1998).

2.3.2. Temperature effects

2.3.2.1. Factors in microwave heating

The following factors play a role in microwave heating:

- Superheating in the presence of a larger number of ions;
- More rapid achievement of the reaction temperature;
- Efficient mixing and boundary effects.

These effects have been observed and have also been described as rapid heating effects, hot spots or surface effects and pressure cooler effects (Galema, 1997).

2.3.2.2. Hot spots and surface effects

Microwave heating alleged effects can be divided into two types, namely thermal and non-thermal effects. Thermal effects are those caused by the different temperature regions within a sample, which are as a result of microwave dielectric heating. Non-thermal effects are those caused by effects specifically inherent to the microwaves and are not caused by different temperature regimes. These effects (non-thermal) are normally associated with microwave spectroscopy. However, microwave dielectric heating differs from microwave spectroscopy, which is carried out in the gas phase and for which discrete energy levels of excitation can be observed. This is in contrast to dielectric heating during which no molecules can be excited into higher energy levels. Therefore microwave dielectric heating should not be confused with microwave spectroscopy (Galema, 1997).

In microwave ovens, specifically relating to cases of solids being heated, there are some dramatic effects with respect to heating rates and these are called hot spots or surface effects (Galema, 1997). Several researchers have detected or postulated the presence of hot spots in samples irradiated with microwaves. This effect, which is related to that observed with ultrasound, arises as a result of the inhomogeneity of the applied electromagnetic field as well as an impurity in the sample possessing higher thermal absorptivity (Hill and Marchant, 1996). Thus in certain sections within the sample, the temperature is much greater than the macroscopic temperature, and hence this is not representative of the reaction condition as a whole. This is a thermal effect and so has been described as the false microwave effect (Langa *et al*., 1997). In case of organic solvents no thermal effects have been observed (Galema, 1997).

2.3.3. Separating thermal and non-thermal effects

Despite the work that has been published in the field of microwave irradiation, there is still a considerable debate on the exact reasons why microwaves irradiation is able to improve chemical processes. Possible reasons are the following:

- It results from the kinetic effect as a consequence of the rapid heating;
- observed enhancement are associated to selective interactions of the electromagnetic field with specific substrate molecules;
- are catalyst or non-thermal effects (Obermayer *et al*., 2009; Al-Harasheh and Kingman, 2004).

2.4. Microwave theory

2.4.1. Microwave energy

Microwave energy is a type of electromagnetic energy, which travels in high frequency waves. The microwave radiation region is found between infrared radiation and radio waves in the electromagnetic spectrum (Figure 2.2) (Lidstrom *et al*., 2001). Similar to all electromagnetic radiation, microwaves have an electrical as well as a magnetic component, (Galema, 1997; Al-Harahsheh *et al*., 2005).

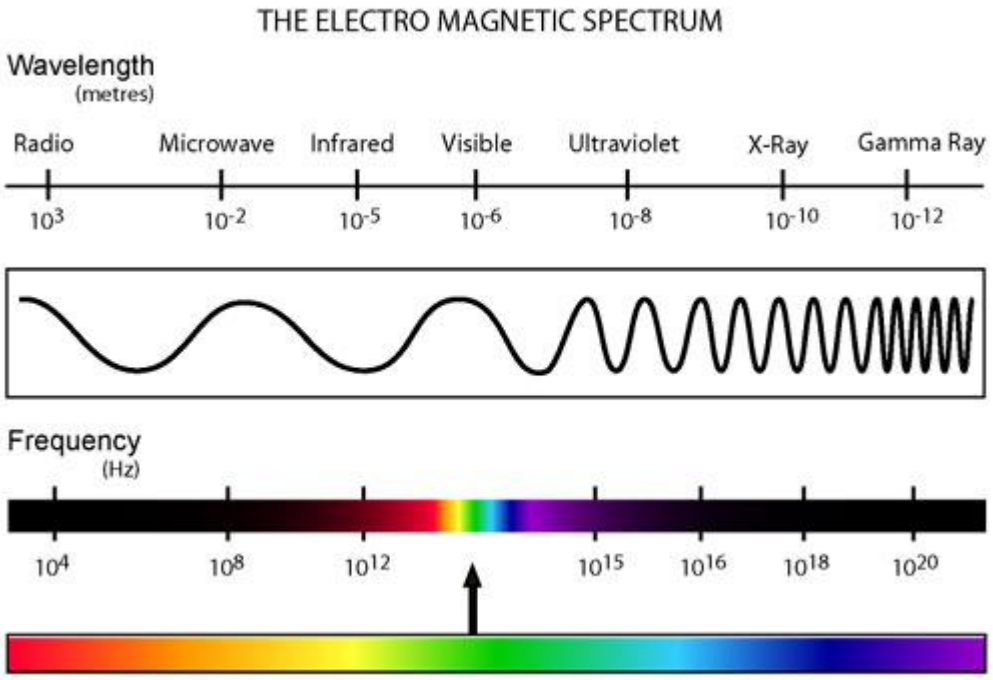

Figure 2.2. The electromagnetic spectrum (source: Kollewin, 2009)

The wavelengths of the microwave spectrum are between 1 mm and 1 m with corresponding frequencies between 300 MHz and 300 GHz. Within this range, microwaves have extensive use in communication, especially in radar, cellular phones, and television and satellite applications. The microwave heating process belongs to a group of electro-heating techniques, such as radio frequency, induction, direct

resistance, and infrared heating, which use definite sections of electromagnetic energy (Al-Harahsheh and Kingman, 2004).The most generally used frequencies for heating purposes are 915 MHz and 2.45 GHz, which correspond to wavelengths of 33.5 and 12.2 cm, respectively. These frequencies were internationally agreed upon to minimize the interference with communication services (Michael *et al*., 1991; Zhang and Hayward, 2006; Al-Harahshesh and Kingman, 2004; Thostenson and Chou, 1999).

2.4.2. Dielectric polarization

The largest contributing factor to microwave dielectric heating is the dipole moment of charged particles exposed to an alternating electric field (Lewis *et al*., 2007). The inability of partially bound charges to follow the rapid changes in a high frequency electric field gives rise to one mechanism of microwave heating (Whittaker, 2007). The total polarization, a_t of the material arising from the displacement of charges may be expressed as the sum of a number of components, as shown in Equation 2.13 (Lewis *et al*., 2007).

$$a_t = a_e + a_a + a_d + a_i \tag{2.13}$$

Where a_e is the electronic polarization, resulting from the displacement of electron charges in relation to the nuclei in a material, and the atomic polarization, a_a, resulting from the movement of a number of nuclei relative to each other in materials that have unequal charge distribution. Both these factors, a_e and a_a contribute a very small amount to the overall heating process at frequencies in the microwave region due to the displacement of the particles following the electric field component of the wave almost perfectly (Michael *et al*., 1991). a_d , results from the reorientation of polar molecules or other permanent dipoles in the material. Thus a_d is the most important of the polarization incidents in microwave heating as the timescale of its operation is in the order of those associated with microwaves. Lastly, a_i the interfacial polarisation (Maxwell - Wagner) effects results from interfacial phenomena in inhomogeneous

materials and is restricted to microwave frequencies, and its contribution is generally found to be limited. (Whittaker, 2007).

Ionic conduction is another important microwave heating mechanism that is employed. When a microwave field is applied to a solution containing ions, the ions move due to their inherent charge (Al-Harasheh and Kingman, 2004). As a result, the ions collide and their collisions result in the conversion of kinetic energy to thermal energy. The greater the concentration of ions in the solution, the more the collisions occurs, causing the solution to heat faster.

The physical size, the chemical composition, and shape of the material tend to affect how the material behaves in a microwave field. Materials can be classified into the following three principal groups with respect to their interaction with a microwave field:

1. Transparent (low dielectric loss) materials; microwaves pass easily through these materials with little observable change in electromagnetic energy;
2. Electrical conductors - microwaves are reflected without any penetration of the material;
3. Absorbing (high dielectric loss) materials which absorb microwaves and dissipate the electromagnetic energy as heat, depending on the value of the dielectric loss factor.

A fourth group exist, which occurs when a material contains two or more phases with different dielectric properties. In this case, microwaves can selectively heat the high loss phase and pass through the low loss one without significant absorption (Clark *et al*., 2000; Al-Harasheh *et al*., 2005; Haque, 1999; Zhao and Chen, 2008).

2.4.3. Dielectric properties

The physical properties in materials can be measured and used to predict their behaviour in a microwave field (Milestone, 2003). For example, thermal and dielectric properties of a material are considered in microwave processing (Janney *et al*., 1997; Michael *et al*., 1991). A microwave must be able to enter the material and transmit energy so that heat can be generated within the material (Thostenson and Chou, 1999). The dielectric constant, ε', and dielectric loss factor, ε'', are used to express the dielectric response of materials in an applied microwave field. The dielectric constant measures the ability of molecules of a material to store microwave energy that is the ability of the material to be polarized. The dielectric loss factor measures the ability of a material to dissipate the stored energy of electromagnetic radiation into heat (Michael *et al*., 1991). The loss factor is itself depends on variables such as the temperature of the sample and frequency of the electric field. It has been determined that loss the factor is directly proportional to temperature (Callebaut, 2007). These components namely dielectric constant and loss factor are often expressed in terms of the complex dielectric constant, ε^*, (Conner and Tompsett, 2008), as shown in Equation 2.14.

$$\varepsilon^* = \varepsilon' - i\varepsilon'' \tag{2.14}$$

where ε' and ε'' are the dielectric constant and dielectric loss factor of the complex dielectric constant , ε^*, (Thostenson and Chou, 1999).

The loss tangent provides an indication of how well a material can be penetrated by an electric field and how it dissipates energy into heat and is given by Equation 2.15,

$$\tan\delta = \frac{\varepsilon''}{\varepsilon'} \tag{2.15}$$

where δ is the loss angle directly associated to the phase shift between the orientation of the molecules and the changing electrical field as a result of their interaction

(Callebaut, 2007; Kingston and Jassie, 1988). Thus the ability of a material to absorb microwaves is directly proportional to its dissipating factor (Li and Yang, 2008).

The average dipole moment (μ) of a displayed dipole is given by the following equation:

$$\mu = qx_i \tag{2.16}$$

where q, is the charge and x_i is the charge separation (Metaxas and Meredith, 1983).

2.4.4. Dipolar loss mechanism

Dipolar polarisation or reorientation is the most significant factor in industrial microwave heating applications at frequencies above 1 GHz when compared to other forms of loss mechanisms. However it does influence the lower frequency band as well. The traditional approach to the treatment of permanent dipoles in solutions and in liquids of polar molecules containing non-polar solvents is to consider their behaviour in an alternating electric field as arising from the rotation of a spherical dipole in a viscous medium dominated by friction. In 1929 Debye, while working on electrolytes deduced the well-known equation:

$$\varepsilon^* = \varepsilon^{'} - j\varepsilon_d^{'} = \varepsilon_\infty + \frac{\varepsilon_s + \varepsilon_\infty}{1+j\omega\tau} \tag{2.17}$$

where ε_s and ε_∞ are the dielectric constants at distance cavity length (Metaxas and Meredith, 1983).

The theoretical examination of the frequency dependence of $\varepsilon^{'}$ and $\varepsilon^{''}$ began with the derivation of the Debye equations:

$$\varepsilon_d^{'} = \varepsilon_\infty^{'} + \frac{(\varepsilon_{0+}^{'} \varepsilon_\infty^{'})}{(1+\omega^2\tau^2)} \tag{2.18}$$

$$\varepsilon_d^{''} = \frac{(\varepsilon_0^{'} - \varepsilon_\infty^{'})\,\omega\tau}{(1 + \omega^2\tau^2)} \tag{2.19}$$

Here $\varepsilon^{'}{}_\infty$ is the static dielectric constant, $\varepsilon^{'}{}_0$ is the high frequency and ω and τ are defined as the frequency and relaxation times which characterize the rate of build up and decay of polarization. The results above apply to liquids and solids; however, different modes are used to derive it. The values of ε'_d and ε''_d at the frequency of which the dielectric loss in the Debye equation is the maximum and independent of both frequency and relaxation time:

$$\varepsilon''_{max} = (\varepsilon'_0 - \varepsilon^{'}{}_\infty) / 2 \tag{2.20}$$

where,

$$\varepsilon'_d = (\varepsilon^{'}{}_0 + \varepsilon^{'}{}_\infty) / 2 \tag{2.21}$$

Generally, in liquids the assumption is that the dipole can point in any direction and can continually change due to thermal agitation. Debye's interpretation for the relaxation is given in terms of the forces in the medium. Stokes' theorem is used to derive the following expression for the relaxation time of a spherical dipole:

$$\tau = 4\pi r^3\,\eta / kT \tag{2.22}$$

where η, is the viscosity of the medium, r is the radius of the dipolar molecule and k is the Boltzmann's constant.

In solids the dipole has a number of equilibria due to the variable interactions of a molecule with its neighbours (Michael *et al*., 1991).

2.4.5. Variation of ε* with temperature and moisture content

A number of investigations have been done in order to explain the temperature dependence of the loss factor in various materials (Metaxas and Meredith, 1983). However, since many applications involve the removal of moisture from the workload, the variation of ε^* and in particular ε''_{eff} with moisture content, play an important role in the design of microwave heating / drying devices. The penetration depth ($D_{p,}$) is the distance from the material surface where the absorbed electric field (e) falls to 1/e of the electric field at the surface. The penetration depth is inversely proportional to the frequency, whereas the greatest heating is achieved at high frequencies. For example, for water the greatest rate of heating occurs at 20 GHz, where the dielectric loss factor is at its maximum value. However, the penetration depth at such frequencies is so low that only the exterior of the material will be heated. The penetration depth (D_p) is given by (Al-Harasheh and Kingman, 2004; Al-Harasheh *et al*., 2005; Zhao and Chen, 2008)

$$D_p = \frac{C}{2\pi f \sqrt{2\varepsilon'} \left[\sqrt{1+ tan^2 \delta} -1\right]^{\frac{1}{2}}} \qquad (2.23)$$

where f is the frequency of the electric field (Hz) and *c* is the speed of light (m/s).

The penetration depth plays an important role of determining the uniformity of the heating across the material (Clark *et al*., 2000). In conventional furnaces, heat is transferred to the material by thermal electromagnetic radiation (Gupta and Wong Wai Leong, 2007). The penetration depth at infrared radiation ($f = 10^{13}\ s^{-1}$) is very small ($D_p \ll 10^{-4}$ m) in the majority of solids, which means a very thin layer of the material will be heated depending on the heat transfer properties of the material. Obviously, this can result in significant temperature gradients. In the microwave frequency range, D_p varies from metres to millimetres depending on the frequency, temperature, chemical composition and microstructure. Reducing the temperature gradient across a material

as a result of microwave heating can therefore give more uniform heating (Al-Harasheh and Kingman, 2004; Gupta and Wong Wai Leong, 2007).

An approximate relationship for penetration depth D_p, when the value of ε'' is small is given by

$$D_p \propto \lambda_0 \sqrt{(\varepsilon'/\varepsilon'')} \tag{2.24}$$

where λ_0 is the wavelength of the microwave radiation (Michael *et al*., 1991).

The average power density (P) (volumetric absorption of microwave energy $\mathrm{W/m^3}$) produced in a material when it is exposed to microwave energy is defined as

$$P = 2\pi f \varepsilon_0 \varepsilon''_{eff} E^2 \tag{2.25}$$

where ε_0 is the permittivity of free space, ε''_{eff} is the effective relative loss factor and E is the electric field strength inside the material.

The effect of the magnetic field must be considered if the material shows magnetic loss, especially for materials exhibiting high magnetic susceptibility (Al-Harahsheh and Kingman, 2004; Clark *et al*., 2000). The relevant equation can be re-written as

$$P = 2\pi f \mu_0 \varepsilon''_{eff} + 2\pi f \mu''_{eff} H^2 \tag{2.26}$$

where μ_0 is the permeability of free space, μ''_{eff} is the effective magnetic loss factor and H is the magnetic field strength.

2.5. Microwave technology

2.5.1. Comparison of domestic microwave ovens to commercial systems

The unsuitability of common domestic microwave ovens for usage in industrial applications has lead to a number of commercial dedicated systems to be specifically manufactured to overcome the inconvenience of acid fume damage, sample power reflection, field inhomogeneity, long time bases and safety concerns that cannot be adequately addressed by conventional heating methods (Stadler *et al*, 2002; Lamble and Hill, 1998).

2.5.2. Types of microwave digestions techniques

There are several microwave digestion techniques available for laboratory use, being classified as either closed or open digestion techniques. There are several suppliers of microwave systems including Aurora Biomed, Parr, CEM Corporation and Milestone.

2.5.2.1. Closed digestion technique

The closed digestion technique involves placing the sample in a vial (or bomb), usually constructed of a fluorinated polymer (Figure 2.3), such as polytetrafluoroethylene (PTFE) or perfluoroalkoxy (PFA). After addition of the digestion reagents, the bomb is tightly sealed and placed in the microwave oven for irradiation by microwave energy (Lamble and Hill, 1998),

Figure 2.3: Parr microwave acid digestion bombs (source: Parrin, 2009)

In closed vessels, the solvent is heated above its boiling point enhancing extraction speed and efficiency. Most commonly used closed digestions are carried out in multimode ovens where the microwaves are dispersed into a large cavity. This is because the electric field is not homogeneous, so the vessels are placed in a turntable cavity environment (Camel, 2000; Lamble and Hill, 1998). The closed system is easy to control and requires almost no supervision. In addition, the use of closed-vessels prevents sample contamination from the laboratory environment or cross-contamination from other samples and digested samples undergo accelerated decomposition as a result of increased pressure and temperature. This completely closed system does not expose laboratory personnel to potentially dangerous or undesirable acid fumes, thus safety is an important consideration (Tanase *et al*., 2004).

As the pressure is controlled in only one vessel, it is recommended that samples that are simultaneously digested should be similar (Camel, 2000). Productivity has increased, because, on the one hand, simultaneous digestions can by carried out in one

run and, one the other hand, the analysts can complete other tasks while the microprocessor-controlled unit runs through the digestion routine unattended (Tanase *et al*., 2004).

Another method widely reported in order to control pressure build-up within the reaction vessel, is to monitor the temperature and pressure throughout the course of the reaction and subsequently apply microwave power only when the reading is within the required level. This is achieved by placing a pressure transducer inside one of the digestion vessels to monitor the pressure continuously. The pressure can be controlled in this way, thus minimising venting of the digestion vessel. Temperature measurements are taken using an infrared probe attached to the bottom of the microwave oven. The output from the probe is fed to a computer which switches the magnetron on and off to attain a pre-set temperature–time programme. Thus this technology for monitoring the temperature or pressure of the digestion presents the potential to produce a more controllable and reproducible procedure (Lamble and Hill, 1998).

2.5.2.2. Open digestion techniques

Open digestion systems operate at atmospheric pressure and therefore do not suffer from the problems associated with pressure build-up. However, they do require an efficient fume removal system. In open digestion systems, extractions take place under atmospheric pressure and as a result, the maximum temperature is determined by the boiling point of the solvent at that pressure. Focused microwaves are used so that heating of the sample is efficient and homogeneous (Camel, 2000).

Figure 2.4: Example of microwave open-vessels digestion system (source: Milestone, 2009)

Most open vessel work has been carried out using single-mode (focused) microwave systems. Heating is more efficient than with conventional microwave designs (multimode) because the sample is placed within the waveguide, and thus directly within the path of the microwave energy. The potential loss of volatile species is controlled by condensation of vapours in a reflux column situated above the sample flask. The open vessel technique of microwave digestion find applications in the analysis of geological and environmental samples using for example inductively coupled plasma-mass spectroscopy (Taylor *et al*., 2002).

A potential disadvantage of the open single-mode system is that only one sample can be digested at a time, although this can be overcome by use of an auto-sampler unit with the ability to run up to 16 samples. A single-mode, multi-cavity system is also

available with the capability to digesting up to four samples for the determination of Kjedahl nitrogen. One of the commercially developed systems is a two- or six-cavity open microwave digestion system able to programme the desired temperature and the power output to each sample independently. Many open digestion procedures use a high boiling point acid such as sulphuric acid, by virtue of operating at atmospheric pressure, in order to completely decompose organic material in the sample (Lamble and Hill, 1998).

2.5.2.3. Advantages of closed digestion system

Although open vessel microwave digestion has proven to be a popular method because of its simplicity, it is however, still associated with the same drawbacks as conventional methods, such as risk of sample contamination, release of acid gases, loss of volatile elements, and maximum digestion temperatures limited by the boiling point of the acid mixture. In contrast, samples digested in closed-vessel environments are isolated from the atmosphere and undergo accelerated decomposition reactions as a consequence of increased pressure and temperature (Tanase *et al*., 2004; Levine *et al*., 1999).

The high heating efficiency obtainable by the closed microwave digestion technique is its major advantage. Heating results in the evaporation of digestion acids and the gases evolved during the decomposition of the sample matrix causes an increase in pressure. This is of particular importance as it increases the boiling point of the reagents, which aids in the breakdown of the sample matrix. The excessive build-up of pressure during the digestion of samples with a high organic content, can lead to the rupture of sealed vessels. Most digestion bombs are fitted with pressure relief valves, designed to open when the pressure becomes too great, and thus maintain safety (Lamble and Hill, 1998).

In addition, the high temperature possible in a closed vessel procedure increases the oxidising power of mineral acids and subsequently achieves the decomposition of sample matrix components that would otherwise not be possible in an open vessel or other conventional environment. Closed-vessel microwave digestion has been successfully implemented for many different types of organic sample matrixes (Tanase *et al*., 2004; Levine *et al*., 1999).

Closed vessel digestions have resulted in improvement of oxidation effectiveness and the time of digestion is greatly reduced. Different procedures, such as electrical current and infrared radiation, have been employed for ignition (Flores *et al*., 2007). The vessels used are transparent to microwave radiation and inert to reagents used (Luque-Garcia and Luque de Castro, 2003). The sample can realistically be heated above its boiling point at atmospheric pressure while enhancing both extraction speed and efficiency (Camel, 2000). Furthermore, microwaves only heat the liquid phase, while vapours are not heated. The temperature of the vapour phase is therefore lower than the temperature of the liquid phase and this allows for condensation of the vapour on the cool vessel walls to occur. Thus, the actual vapour pressure is lower than the predicted vapour pressure. This sustained dynamic, thermal non-equilibrium is a key advantage of microwave technology, as very high temperatures can be reached at relatively low pressures, which result in short digestion times (Agazzi and Pirola, 2000).

For closed vessels, if the rate of energy released by a chemical reaction is higher than the rate at which it can be absorbed by the vessel walls, this will result in temperature increases and, subsequently, the reaction rate and hence the rate of energy release also increases rapidly (Flores *et al*., 2007).

2.5.2.4. Advantages and disadvantages of open digestion system

The open vessel approach can generally accommodate larger samples (up to 15 g) and allows the delivery of digestion reagents at any stage of the procedure whereas with the closed system technique this is not possible. The ability to deliver digestion reagents at any stage of the open vessel approach may be advantageous for the effectiveness of the digestion, and is a distinct improvement over closed methods where the addition of reagents cannot readily be achieved without cooling and opening the vessels. The open system results in a sample to quickly and effectively evaporate to dryness, a particular advantage that is employed in the digestion of geological samples for the removal of HF (Lamble and Hill, 1998).

Despite the above mentioned advantages open systems are subjected to several shortcomings including the following:

- sample throughput is noticeably lower as most open systems cannot process multiple samples simultaneously when compared to closed systems which can handle 8 to 14 samples at a time;
- the operation times in open systems required to obtain identical results to closed systems are usually longer (Luque-Garcia and Luque de Castro, 2003).

2.6. Microwave instrumentation

2.6.1. Components of microwave digestion system

The microwave heating system consists of four major components, namely the magnetron, the waveguide, the applicator and the power supply (Haque, 1999).

2.6.1.1. The magnetron

The magnetron is where the microwave energy that heats the sample is produced (Luque-Garcia and Luque de Castro, 2003). A magnetron is a cylindrical diode comprising of an anode and a directly heated cathode (Kingston and Jassie, 1988). As the cathode is heated, this result in electrons being released which are attracted towards the anode (Figure 2.5).

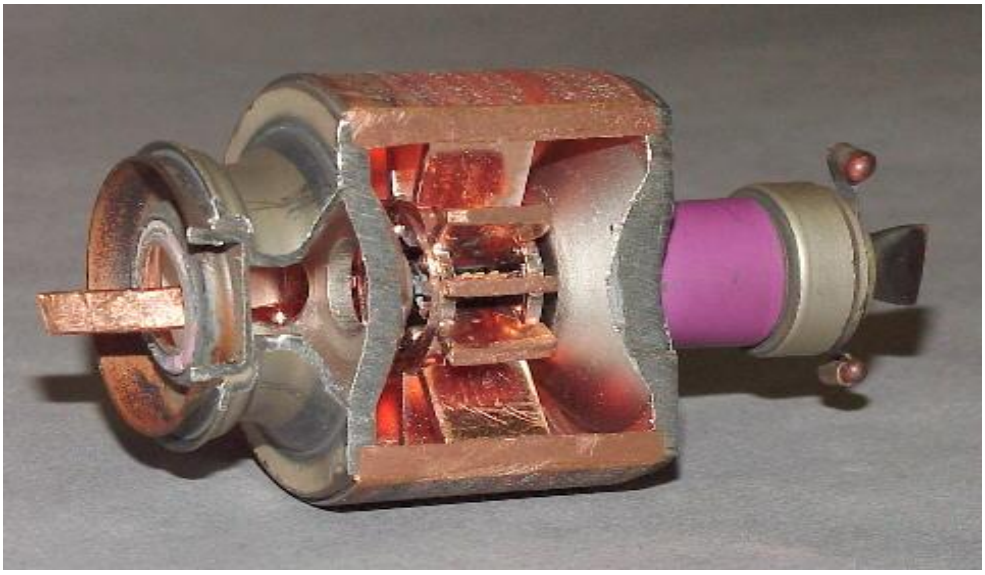

Figure 2.5: The magnetron of the microwave oven (source: Magnet Lab, *s.a*)

A very strong magnetic field is induced axially through the anode assembly and has the effect of bending the path of electrons as they travel from the cathode to the anode (Michael *et al*., 1991). Through the magnetron action, the microwave energy produced is projected along the waveguide into the cavity where a mode stirrer distributes the waves (Kuss, 1992).

2.6.1.2. The Waveguide

A waveguide is a rectangular channel made of sheet metal. Its reflective walls allow the transmission of the microwaves from the magnetron to the microwave cavity or applicator (Figure 2.6) (Luque-Garcia and Luque de Castro, 2003).

Figure 2.6: The waveguide of a microwave oven (source: Microwaves. *s.a*)

The minimum frequency which can be propagated is related to the dimensions of the rectangular cross section (Michael *et al*., 1991) given by the expression

$$c/f = 2d \tag{2.27}$$

Here c is the speed of light, f is the cut-off frequency and d is the larger of the two dimensions of the rectangular section of the waveguide.

2.6.2. Microwave applicators

2.6.2.1. Types of applicators

The applicator is where the sample is placed inside the microwave oven (Luque-Garcia and Luque de Castro, 2003). Currently, there are two types of microwave reactor design that are emerging: multimode and monomode (single mode) reactors (Kappe, 2002). The most common form of an applicator, comprising well over 50% of industrial systems, is the multimode type. In principle, it is an extension of the domestic microwave oven but is built for large scale material processing (Metaxas, 1991).

2.6.2.2. Multimode oven applicators

These are the most widely used type of all the oven applicators (Metaxas, 1991). The first commercial laboratory multimode microwave oven was introduced to the market in 1985 (Walter *et al*., 1998). In the past, laboratory tests were exclusively performed using a simple multimode oven as the starting point with regard to the evaluation of an industrial heating process. The apparent simplicity of this approach unfortunately often leads to misleading results, due to the variation in dielectric properties of the material with change in temperature and complexity of the field distribution within the oven, moisture content, density and other parameters (Metaxas, 1991).

2.6.2.3. Single-mode oven applicators

The single mode applicator consists of a microwave source and a rectangular waveguide (Will *et al*., 2004). The microwave irradiation is projected through an accurately designed waveguide and is directed onto the reaction vessel mounted at a fixed distance (Kappe, 2002). The resulting superposition of incident and reflected waves give rise to a well defined standing wave pattern. This allows the dielectric

material to assume a favourable position in the electric field which results in optimal electromagnetic energy transfer (Metaxas, 1991).

2.6.3. Applications of microwave digestion

Microwave radiation has found usage in various fields such as sintering and joining of ceramics, synthesis of compounds using assisted digestion procedures (Chou *et al*., 2009). Microwave digestion is an influential tool for converting diverse types of samples into a solution ready for instrumental measurement (Harzdorf *et al*., 1998). It has been pointed out that microwave energy could have a possible application in comminution, leaching, pre-treatment of refractory gold ores, roasting, drying, carbon reactivation, coal desulphurisation, carbothermic reduction of oxides and waste and slag management (Al-Harahsheh *et al*., 2006; Jafarifar *et al*., 2005).

It has also found usage in treatment of infectious wastes and hazardous industrial sludge. Microwave irradiation may catalyze chemical reactions through a process of selective heating and catalysis mechanism. Microwave assisted cracking has been successfully explored, at pilot plant scale, for the segregation of oil from petro-chemical processing sludge containing highly stable oil emulsions (Gan, 2000).

2.6.4. Advantages of microwave heating over conventional heating

Microwave irradiation techniques have led to improvement and simplification of organic reactions as it sometimes results in shorter reaction times, higher yields, and cleaner reactions as compared to conventional methods (Sosnowski and Skulki, 2005). A classic microwave acid digestion can be completed in a matter of minutes, whereas the same conventional hot plate digestion can take hours to complete. This is due to a

higher conversion rate observed for reactions under microwave digestion as compared to conventional digestion.

Other advantages of microwave processing include the following (Clark *et al*., 2000; Haque, 1999; Agazzi and Pirola, 2000):

- Decreased sintering temperatures;
- High speed and reaction efficiency;
- Rapid heating;
- Volumetric and selective heating;
- Lower contamination levels;
- Improved physical and mechanical properties;
- Better production quality;
- Reduced hazards to humans and the environment;
- Less expensive, and
- Decreased energy consumption.

Microwaves represent a radical procedure for heating materials which is clearly different from the classical methods. The main advantages of microwave heating are derived from the almost instantaneous "in core" heating of materials, in a homogeneous and selective manner, especially those with poor heat conduction properties. This technique proves to be excellent in cases where conventional heating has a low efficiency because of poor heat transmission, and hence local overheating is a major inconvenience (Deshayes *et al*., 1999).

2.6.5. Differences between microwave and conventional systems

In conventional heating methods, energy is transferred to the material through convection, conduction, and radiation of heat to the surface of the material by a medium

and by conduction to the rest of the material, whereas in microwave heating energy is delivered directly to the material through mass molecular interaction with the electromagnetic field from within the material itself. In conventional heat transfer, energy is transferred due to thermal gradients, but in microwave heating electromagnetic energy is converted to thermal energy, therefore it is energy conversion rather than heat transfer (Li *et al*., 2008; Acierno *et al*., 2004). This difference in the way energy is delivered can result in many potential advantages using microwaves for the processing of materials. Because microwaves can penetrate materials and deposit energy, heat can be generated throughout the volume of the material (Thostenson and Chou, 1999; Li *et al*., 2008).

The energy transfer does not depend on diffusion of heat from the surfaces, and it is possible to achieve rapid and uniform heating of thick materials (Thostenson and Chou, 1999). In conventional heating, the cycle time is regularly dominated by slow heating rates that are chosen to reduce steep thermal gradients that result in process-induced stresses (Das *et al*., 2008).

The main points of interests can thus be listed as the rapid transfer of energy into the bulk of the reaction mixture, since only the product is selectively heated, and the ease of energy utilization. Furthermore, microwaves interact with substances of appreciable thickness (about 10 cm), as the depth of penetration in materials is of the same order of magnitude as the wavelength (Deshayes *et al*., 1999). The temperature required to achieve a given sintered density for microwave heating is lower compared to conventional heating (Gupta and Wong Wai Leong, 2007).

The electromagnetic microwaves differs from conventional thermal treatment and incineration as it can energize, mitigate and assist chemical binding of dipolar molecules and metal ions within a solid structure (Gan, 2000).

2.6.6. Measuring temperature and pressure in microwave heating

According to Janney *et al*. (1997) the temperature required to achieve a given sintered density is lower for microwave heating compared to conventional heating in these systems. The magnitude of this temperature differential is often used as a measure of the enhancement caused by microwave processing.

One of the major shortcomings identified is how the power of the microwave transducer should be adjusted as a function of the two process parameters, namely temperature and pressure, which can be measured during the microwave digestion process. These two parameters are vital factors that affect the overall safety of the process in addition to being used as feedback for the control of the microwave radiation. This is particularly important, since the heating of the acid sample mixture occurs in most applications to as high as possible temperatures, while being carried out in closed containers.

Temperature and pressure sensors are used to monitor only a reference vessel in microwave digestion systems. The microwave power is then adjusted as a function of the measurements based on this reference sample. The assumption is that other samples processed simultaneously in the microwave digestion, behave in the same way as the reference sample (Kramer, 2003).

2.7. Microwave dissolution literature

Several studies have been undertaken on microwave dissolution of various materials using different acid digestion methods.

Zhao and Chen (2008) conducted a study on the kinetics of dissolution of uranium dioxide (UO_2) particles with nitric acid by microwave heating. A Mars 5 microwave assisted reactor system was used under a 600 W and 2.45 GHz microwave field. UO_2

(0.05 g) and 20 ml nitric acid (HNO_3) was used. The solution was heated rapidly to a selected temperature for a certain time (90 to 110 min). Their results showed that the dissolution rate of UO_2 particles is directly dependent on the temperature and concentration of HNO_3. As the temperature and concentration of HNO_3 were increased, so did the dissolution rate.

Ma and Li (2006) investigated a study on the microwave digestion of zirconium dioxide (ZrO_2) powder to determine trace elements such as iron (Fe), hafnium (Hf), manganese (Mn), sodium (Na), silicon (Si) and titanium (Ti). Microwave digestion at high pressure in a closed system was applied to the dissolution of ZrO_2 based powder using a combination of many acids including nitric acid (HNO_3), hydrofluoric acid (HF), sulphuric acid (H_2SO_4), hydrochloric acid (HCl) and ammonium sulphate ($(NH_4)_2SO_4$). Results were compared with those obtained by conventional digestion in an open system. The results showed that only with $(NH_4)_2SO_4$ and H_2SO_4, the powder could be completely dissolved in a microwave digestion. The conclusion was that a combined microwave assisted digestion using H_2SO_4-$(NH_4)_2SO_4$, allow fast and satisfactory determination of trace elements in high purity ZrO_2. The time required for sample preparation was greatly reduced. The accuracy and precision of the analytes and the detection limits for Fe, Mn, Si and Ti could be significantly improved compared to a conventional open vessel digestion.

Tripathi and Chattopaddhyay (2007) conducted a study on microwave digestion of titanium bearing complex matrices which were carried out in a closed digestion vessel by a combination of HNO_3, H_2SO_4, HF and HCl. The titanium sample (0.10 g) and 9 ml of the acid mixture were placed in a vessel. A series of six samples were digested simultaneously at different time intervals and at fixed temperature of 200 °C. The results showed that titanium and its ores can be best decomposed by HNO_3, HF, H_2SO_4 and HCl or a mixture of these. They concluded that a successful microwave digestion procedure was carried out for titanium bearing complex matrices with the aid of HNO_3, HF and HCl mixture. The microwave digestion procedure developed provides low

sample and reagent consumption with a higher frequency of sample analysis per unit time. The dissolution of ilmenite and other titanium bearing complex matrices were found to be 99 to 100% when digestion was carried out at 600 W for 17 min with 9 ml of the acid mixture. Although sulphuric acid proved to be a good decomposing agent for the refractory titanium ores, it cannot be recommended in microwave systems as they cause damage to the vessels at such, because high temperatures are required for its digestion.

In an effort to improve the amount of extracted metal produced and reduce processing time, a study on the influence of microwaves on the leaching kinetics of chalcopyrite was investigated by Al-Harahsheh *et al.* (2005). The microwave accelerated MARS 5 was used as an alternate system to experiment with. The experimental sample was consequently divided into different size fractions using wet sieving. The size fractions were -106+75, -75+53, -53+38 and -38 µm. The total digestion of samples from each size fraction was used to determine the chemical composition of chalcopyrite per sample. The system temperature range was set between 50 °C and 90 °C and power was set at 300 W for each temperature. The sample was continuously leached for a set of time with microwave energy and the sample was taken for copper analysis. The results showed that the leaching rate was inversely proportional to the particle size. However the reproducibility of the results was poor compared to that of particle sizes of less than 38 µm. They then concluded that application of microwave heating on chalcopyrite leaching has a positive effect on the reaction kinetics.

2.7.1. Conclusion

From the above literature studies, it can be concluded that microwave digestion is a quick and efficient method that is able to digest compounds that are notoriously difficult to dissolve such as zirconium dioxide, uranium oxide, chalcopyrite and titanium when compared to other heating methods. Although experimental conditions were not the same among the various studies undertaken, the results obtained were consistent for all

of them. It also shows that microwave digestion couples very well with different acids and time can be reduced from hours to minutes. Microwave heating is indeed a superior method compared to conventional heating for digestion of minerals, ceramics, etc., higher conversion rates can be obtained.

In this study the use of microwave digestion for zircon in AAF was investigated in order to prepare zirconium products.

2.8. Kinetic theory

2.8.1. Reaction mechanism and kinetic model

The term mechanism is somewhat inconsistent, when used relative to crystolysis reactions. The word mechanism is consistently used in the traditional sense, to describe the sequence of elementary steps involved in which the reactants are converted into products. This definition includes all aspects of the interface geometry (based on the interpretation of yield-time measurements) and the bond redistribution processes that do occur at an active reaction interface (often inferred indirectly from magnitudes of Arrhenius parameters), coupled with any re-crystallization and re-texturing processes. The more restricted mechanistic inferences about reaction geometry that are based on the best fit of yield-time data to one from a group of rate equations that have found application to decomposition of solids are described by the kinetic model. Therefore the kinetic model is the mechanism that accounts for rate characteristics by employing interface advance with possible involvement of diffusion processes and nucleation and growth. This mechanism, however, is not inclusive of the chemical changes that occur within the active interfacial zone which may include any re-crystallization or bond rearrangements (Galwey, 2000).

The kinetics of competing chemical reactions are usually described by:

$$\frac{d\alpha}{dt} = \sum_{p=1}^{q} f_p\ (\propto) k_p\ (T) \tag{2.28}$$

In the simplest case, the reaction is represented by only one function f and one rate constant k:

$$\frac{d\alpha}{dt} = f(\propto) k(T) \tag{2.29}$$

where $\propto$ is the extent of reaction (conversion), $f(\propto)$ the conversion function describing the reaction model, and $k(T)$ corresponds to the Arrhenius law,

$$k(T) = k_o\ \exp\frac{-E_a}{RT} \tag{2.30}$$

where E_a denotes the activation energy of the reaction and R the gas constant (Schawe, 2002).

The end of the nineteenth century saw the formation of basic kinetic concepts such as ‘reaction order’, ‘activation energy’, ‘reaction rate’ and ‘rate constant’. The concept of heat (or energy) of activation was introduced by Arrhenius to describe the dependence of the reaction rate on the temperature. All these mentioned kinetic concepts are generalizations of empirical knowledge about homogeneous reactions and as such it should not generally be expected to provide an accurate phenomenological description to results from the application of these concepts to reactions of solids. These concepts have nevertheless, been used extensively since the early twentieth century in solid-state kinetics (Vyazovkin, 2000).

The activation energy (E_a), because it possesses theoretical value in relating the temperature coefficient of reaction rate to the crest of the energy barrier opposing reaction through the Arrhenius equation, has proved to be an important parameter in the

interpretation of rate data throughout chemical kinetics. On the other hand, other rate / temperature relationships have been found to be lacking theoretically. For some thermal reactions of initially solid reactants, the variable values of the calculated magnitudes of E_a have been recognized simply because it was found that as the reaction advances, the measured temperature coefficient of the overall reaction rate exhibits change. (Galwey, 2003).

2.8.2. Selection of a model

Every model for the progression of a chemical reaction can be mathematically represented by a rate equation. Thus if a particular model is chosen, then its corresponding rate equation must be accepted as well and *vice versa*. If a model corresponds closely to the actual chemical reaction, then the actual kinetics can be described and predicted by the corresponding rate expression. Similarly if a model differs greatly from reality, then its kinetic expressions will be meaningless. It should be noted that it is worthless to the best in the field of science to make design prediction based on a model which does not conform to reality even when utilizing well designed and ambitious mathematical analysis. Thus a model holds is expected to surpass expectations in all areas of engineering. A good engineering model needs, as a requirement, to be treated with less mathematical complexities. A model should be chosen on the basis that it closely mirrors reality yet even simple enough to apply in the industry. The shrinking unreacted core model and the progressive-conversion model are two of the models that can be considered for non-catalytic reactions involving fluid as the surrounding media (Levenspiel, 1999).

2.8.3. Modelling of fluid-solid systems

To gain a closer understanding into reaction mechanisms and to interpret the corresponding experimental results, mathematical modelling of fluid-solid systems is

most often employed. It is also useful also to quantify rate parameters in the design of fluid-solid reactors. For non-catalytic fluid-solid reactions, shrinking particle, shrinking core, grain and homogeneous models are the major models that were developed. The shrinking core model (SCM) is applicable to a primarily impermeable particle, which when reacting with a reagent, leaves a reacted layer surrounding the un-reacted core see Figure 2.7. The shrinking particle model (SPM) displays similar characteristics to the SCM except that the un-reacted core is minus the product layer. The shrinking core model is extensively used in the discipline of hydrometallurgy to assist in modelling leaching systems (Gbor and Jia, 2004).

2.8.3.1. The shrinking core model

Yagi and Kunii (1955) are credited to be the first to develop the shrinking core model. In the development of the SCM, the solid reactant is regarded as being impermeable and is originally surrounded by a film of fluid which facilitates mass transfer to take place between the solid particle and the rest of the fluid. The assumption is that the initial point of the reaction occurs at the outer boundary of the particle. The reaction then moves into the body of the particle, with the material left behind completely converted and un-reactive solid. This ash-like, non reactive layer forms around the un-reacted core, as the reaction proceeds further. The general chemical reaction shown in Equation (2.31) is used in the development of the SCM.

$$A\ (\text{fluid}) + bB\ (\text{solid}) \rightarrow \text{fluid and solid products} \qquad (2.31)$$

The rate limiting step determines the rate equation and can at any stage be one of the following: (1) chemical reaction occurring at the surface of the un-reacted core, (2) diffusion through the liquid film surrounding the solid reactant particle and lastly (3) diffusion through the ash / inert solid product layer.

The first assumption here is that the solid reactant particle is spherical and its reaction with the fluid is isothermal. Secondly it is assumed that the concentration of the reacting fluid is in excess or constant (Gbor and Jia, 2004). The two most probable rate limiting mechanisms in this work were both ash-layer diffusion control and chemical reaction control.

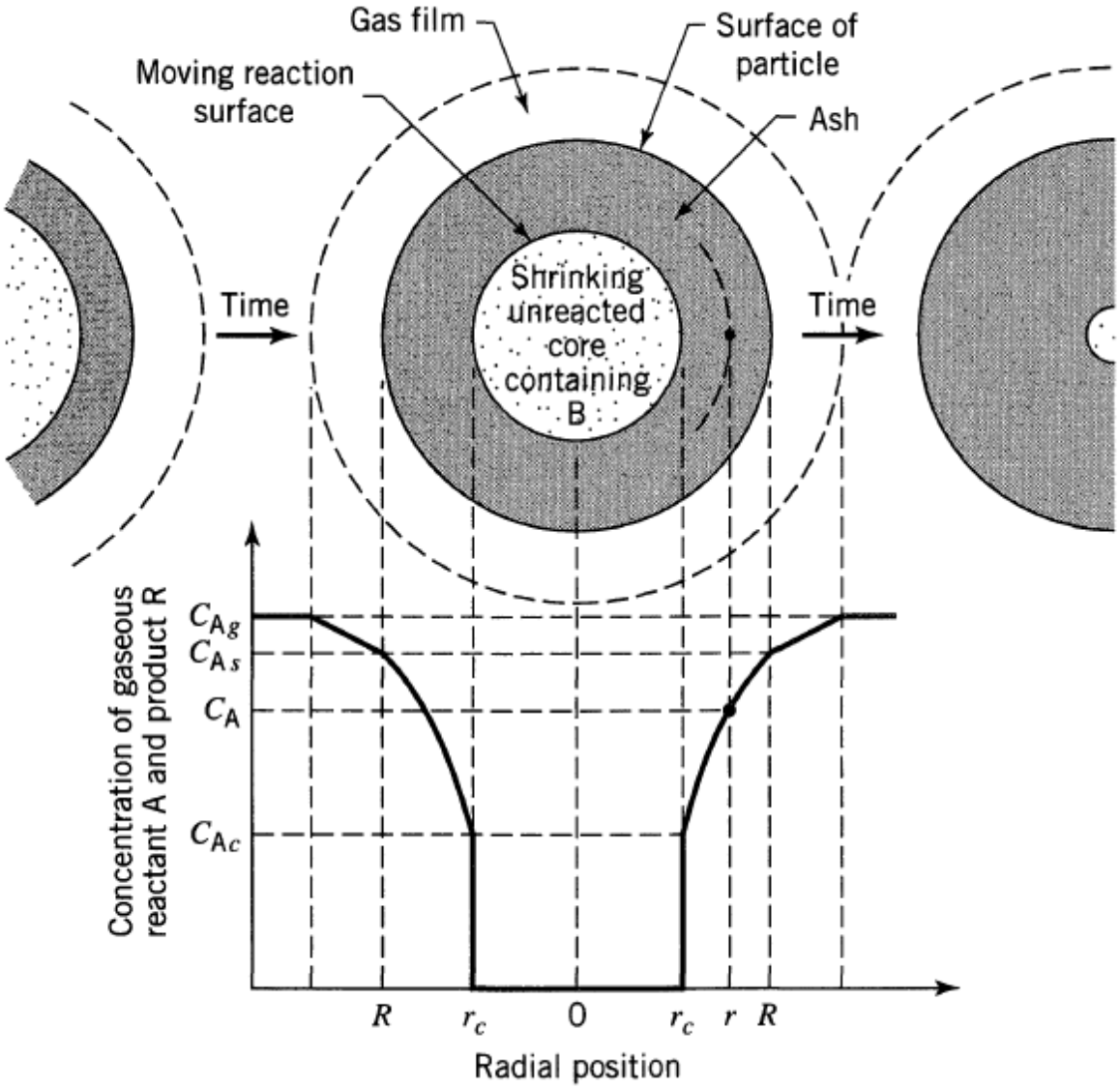

Figure 2.7: Shrinking-core model (source: Levenspiel, 1999)

2.8.4. Kinetics of solid-liquid reactions

For solid particles to dissolve in liquids, the solute molecules on the solid surface will dissociate first through a surface reaction, with these disintegrated solute molecules subsequently diffusing toward the bulk liquid phase. The rate of dissolution is directly depended upon the rates of the dissociation and the diffusion processes (Hsu and Liu, 1993).

2.8.5. Kinetics of solid particles reactions

The process of dissolution of solid particles is one of the typically important industrial processes, for example in ceramics, hydrometallurgy and environmental precipitation processes. The particle structural properties as well as the reaction media significantly influence the progress of dissolution process. Thus, in general, the dissolution kinetics of solid particles is dependent on the structural properties of the particles, the concentration of the fluid reactants as well as mass transfer effects (Markus, 2004).

2.8.6. Kinetics in liquid reactions

Two interdependent effects complicate the application of kinetic theory to reactions in liquids. Diffusion is extremely reduced in liquids compared to a gas because: (1) relative movements of molecules are much more restricted due to the dense and closely packed liquid phase. (2) Some of the ions or solute molecules tend to bond with the solvent. These properties are separately difficult to characterize quantitatively in proper forms that enable their inclusion into mathematical equations that expresses their influence towards reaction rates. Thus for reactions in liquids two limiting conditions of rate control can be distinguished. Diffusion control mechanism applies when the rate of product formation depends on the rate at which reaction entities move through the liquid phase towards each other: In these instances, the activation energy (E_a) values are relatively

small. The activation process tends to controls the reaction rate, where E_a values are large, through energy obtained from neighbouring solvent (Basagaoglu, 2002).

2.8.7. Diffusion process

The process of diffusion is made up of two distinct entities namely the mechanics or how the process occurs and the rate of the diffusion process. Highly sophisticated and complex mathematical models are now being considered in the theory of new product in place of various diffusion time-series models and other curves of acceptance models which have proven to be outdated (Scitovski and Meler, 2002).

2.8.7.1. Ash layer diffusion controls

A situation in which resistance to diffusion through the ash material influences the rate of the reaction is illustrated in Figure 2.8. Here a partially reacted particle is shown with both reactant A and the edge of the un-reacted core of particle move inwardly towards the center of the particle. Although for gas-solid reactions the flow rate of reactant A is faster towards the un-reacted core than the rate at which the particle core shrinks due to the ratio of densities of solid to gas by a factor of about 1000. This leads us to assume that at any period during the reaction that the un-reacted core is stationary when considering the concentration gradient of A in the ash deposit (Levenspiel, 1999).

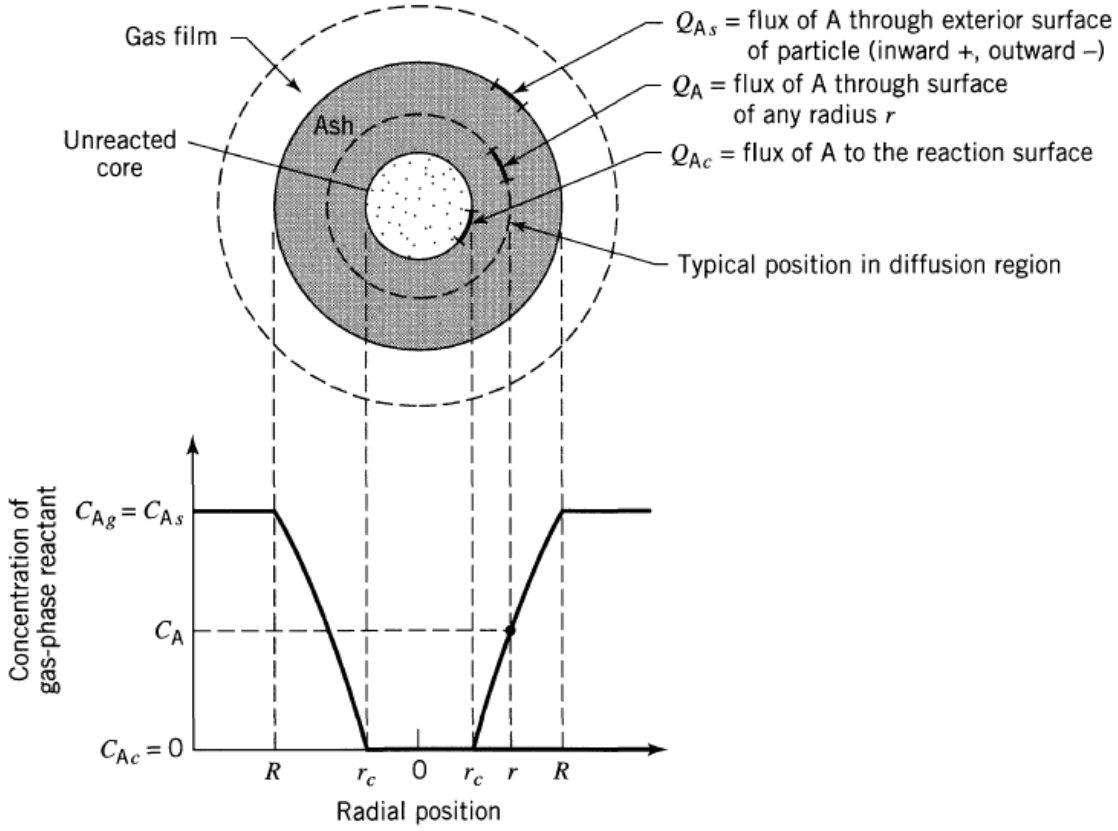

Figure 2.8: Representation of a reacting particle when diffusion through the ash layer is the controlling resistance (source: Levenspiel, 1999).

Liquid-solid systems, pose a great difficulty due to the fact that the velocity ratio is closer to unity than to 1000. It is assumed that the gas-solid systems are in a steady state. The reaction rate of reactant A is given by its rate of diffusion to the reaction surface or

$$-\frac{dN_A}{dt} = 4\pi r^2 Q_A = 4\pi R^2 Q_{AS} = 4\pi r_c^2 Q_{AC} = constant \qquad (2.32)$$

The flux of A, Q_A, within the ash layer is allowed to be expressed by Fick's law for equimolar counter diffusion to simplify mathematics. Noting that both $\frac{dC_A}{dr}$ and Q_A are positive, we have

$$Q_A = D_e \frac{dC_A}{dr} \quad (2.33)$$

where D_e is the effective diffusion coefficient of gaseous reactant in the ash layer. It is often impossible to assign a value to D_e before hand because of the sensitive nature of the ash (e.g. its sintering qualities) to small variations in the particle's environment and to presence of even amounts of impurities in the solid. For any size of unreacted core, the rate at which reactant A changes, $\frac{dN_A}{dt}$, is constant; however the rate of diffusion of A is reduced considerably as the core shrinks and the ash layer becomes thicker (Levenspiel, 1999).

2.8.7.2. Chemical reaction control

Figure 2.9 demonstrates the concentration gradients within a particle when chemical reaction controls. The reaction rate is proportional to the available surface of unreacted core, since the progress of the reaction is unaffected by the presence of any ash layer.

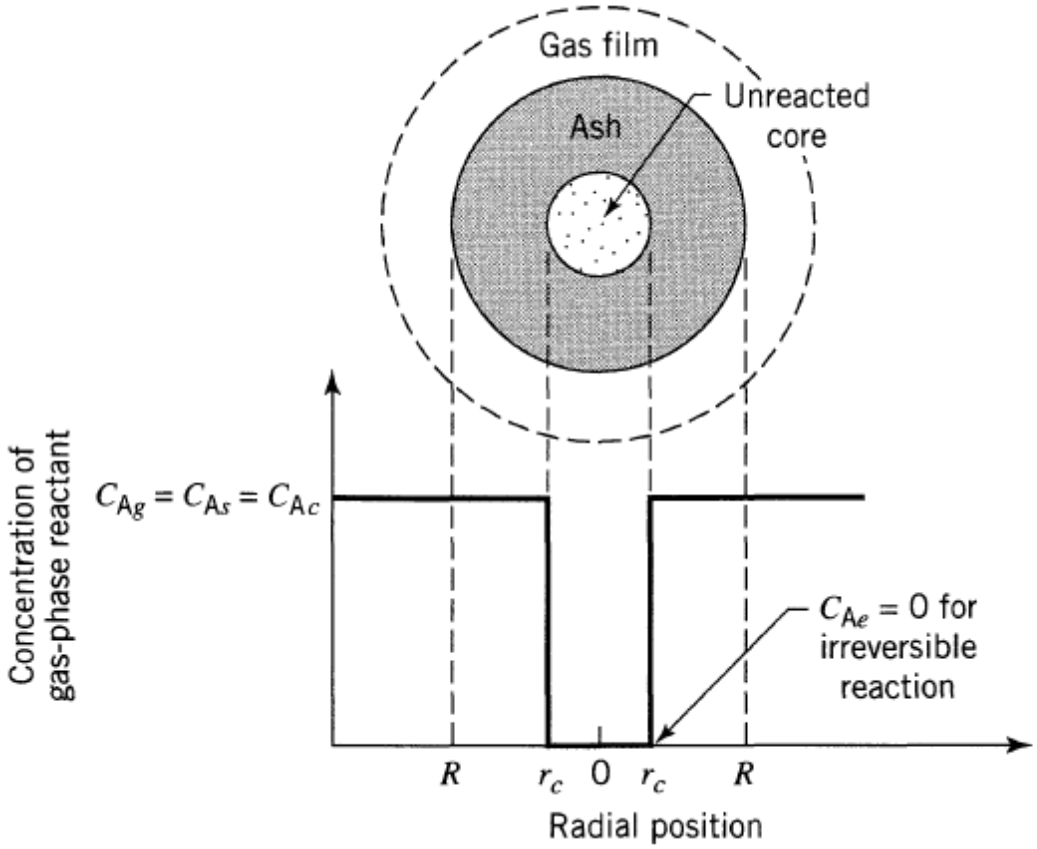

Figure 2.9: Representation of a reacting particle when chemical reaction is the controlling resistance (source: Levenspiel 1999)

The equations for these models follow below:

When the diffusion through inert/ash layer controls

$$\frac{t}{\tau} = 1 - 3(1 - X_B)^{2/3} + 2\,(1 - X_B) \tag{2.34}$$

where

$$\tau = \frac{\rho_B\, R^2}{6b\mathcal{D}_e C_{Ag}} \tag{2.35}$$

When surface chemical reaction controls

$$\frac{t}{\tau} = 1 - \frac{r_c}{R} = 1 - (1 - X_B)^{1/3} \tag{2.36}$$

where

$$\tau = \frac{\rho_B R}{bk'' C_{Ag}} \tag{2.37}$$

For full derivation of Equations 2.34-2.37, see Levenspiel, 1999 (page 571-576).

CHAPTER 3

Experimental

3.1. Introduction

This chapter presents the experimental procedures, chemicals and the description of the microwave system that was used to perform the experiments. Analytical methods, namely XRD, Raman and SEM that were used to characterize the residue, are also described shortly in this chapter.

3.2. Chemicals

Prime grade zircon (d_{50} particle size 125 µm) obtained from Namakwa Sands was used for all work reported here. The hafnium content is about 1.5%. Ammonium acid fluoride (AAF, $NH_4F{\cdot}1.5HF$) was obtained from Pelchem (Pty) Ltd. HF (40%) and H_3BO_3 were Merck analytical grade. All chemicals had a purity of >99%.

3.3. General description and features of the microwave digestion unit

3.3.1. The microwave system

For digestion experiments, a CEM microwave accelerated reaction system (MARS 5) was used (Figure 3.1) The Mars 5 programmable microwave unit is capable of digesting, hydrolyzing and dissolving a wide variety of materials in a laboratory environment. The unit heats up samples in ionic or polar solutions or by using microwave energy at high pressure and at an accelerated pace. In this study the

microwave system was used to study the kinetics for the reaction of zircon and ammonium acid fluoride.

The system consists of:

- A microwave power system with user programmable power settings (0-1600 W).
- An oven interior (fluoropolymer-coated microwave cavity).
- A cavity exhaust fan and tubing to expel fumes.
- A programmable microcomputer that controls and monitors the power, temperature, and pressure within the reaction vessels, and 100 programs also capable to store up to five reaction phases.
- 12 reaction vessels and one control vessel for monitoring the temperature and pressure of the reaction.
- An alternating turntable that allows the samples to rotates 360 °C in the microwave field.
- A door safety, interlock system that prevents microwave emissions when the door is open.

Figure 3.1: The microwave oven exterior attached to the microprocessor computer

CEM has a variety of vessel types designed for their ovens. In this particular system, the XP-1500 vessel were used which are able to withstand temperatures and pressures up to 240 °C and 800 psi respectively (Figure 3.2).

The digestion process is controlled by the temperature. A number of safeguards are incorporated into the MARS 5 system to prevent the possibility of any explosion related to high pressure material failure. Each and every reaction vessel is contained inside a microwavable sleeve made of Kevlar with each vessel-sleeve pair securely clamped within a support unit or carriage with a clamping bolt. A rupture disc made of a plastic membrane sits between the threaded blue cap and exhaust port in the vessel lid. Its purpose is to ensure that the digestion process occurs at lower pressures and under completely closed conditions. A pen-sized sunction device is used to insert the rupture disc (Figure 3.5). If the allowed gaseous pressure level is exceeded for the type of vessel the membrane will rupture, draining the gas into the oven via the exhaust port in the vessel lid and cap, which further drains into a fume hood. The microwave unit is also fitted with a pressure sensor that cuts power to the microwave unit should it detect an unexpected power change.

Figure 3.2: The microwave vessel with support module

3.3.2. Control vessels

Only one reaction vessel per carousel set of 12 vessels is monitored for temperature and pressure. The user-defined computer program regulates the rate of temperature and pressure increase within the vessels as well as the power supplied to the oven. It is actually the temperature and pressure measured within a control vessel that is used to adjust the oven power. It is imperative that the sample in the control vessel be identical to the samples in other vessels digested simultaneously as the amount of heating within a solution depends on the type of dipolar molecules and ions present.

The control vessel and the other reaction vessels are made of the same type of material with the exception that only the control vessel has a pressure sealed glass well (Thermowell) that penetrates into the vessel allowing a fiber optic temperature sensor to be lowered into the vessel. A pressure sensor is attached to the control vessel lid (Figure 3.3).

Figure 3.3: The control vessel

3.3.3. Thermowell and fiber optic temperature sensor

The thermowell is a glass tube open at only one end. The open end fits into a compression fitting in a threaded cap that tightens as it screws on to the control vessel lid and allows the temperature sensor to be lowered into the pressure sealed vessel. The closed end of the thermowell is submerged in the sample mixture.

Temperature in the sample mixture, as it is heated, is measured by a microwave-transparent infrared fiber optic sensor. One end of the sensor is lowered into the thermowell and the other is connected to a snap-in port in the oven. The temperature sensor can read temperatures up to 240 °C and is completely inert to all corrosive reagents.

3.3.4. Pressure sensor

The pressure control system is able to read pressures up to 800 psi and is composed of two parts:

- the electronic controls and a connector, factory built into the oven, and
- the sensor unit which is attached to the control vessel lid through a flexible transparent tube.

The sensor which is made up of a pressure sensing mechanism (pressure sensoring mechanism) situated within the black cylinder attached to the tubing and is mounted to the connector inside the oven cavity. During operation the pressure readings inside the reaction control vessel are transmitted to the load cell which then sends out a signal to the electronic control unit. The Mars unit, unlike older microwave systems that had pressure lines charged with water, depends on the vapour pressure directly acting on

the load cell within the control vessel. The temperature sensor and pressure sensor can both be calibrated and zeroed using the microwave oven's computer (Figure 3.4).

Figure 3.4: The temperature and pressure sensor

The reaction vessels are rotated through the microwave field using a carousel (which is a turntable that holds up to 12 reaction vessels and support modules) to facilitate heating is evenly distributed among and within all the reaction vessels in the microwave oven cavity (Figure 3.6). The turntable rides on ball rollers and fits on a drive drag inside the oven. The turntable is rotated 360 °C per cycle, with the direction of rotation changing per each cycle.

In the system, the temperature is controlled, while the pressure is monitored. Thus in our results we quote the temperature at which the work was done. For typical sample charges, the reaction pressure varied from 15 bar at 100 ºC to 44 bar at 240 °C.

Figure 3.5: The torque wrench and pen-sized suction device

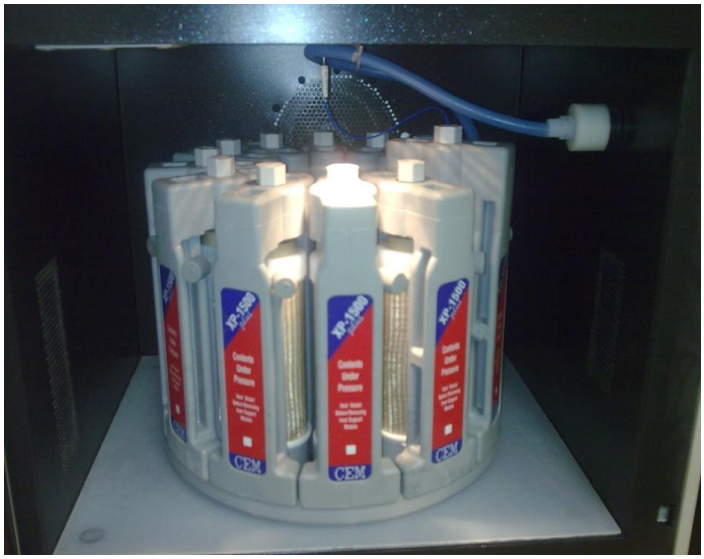

Figure 3.6: The carousel

3.4. Experimental procedure

The experimental work employed three procedures in the quest to determine the fractional conversion of zircon.

The three procedures can be summarized as follows:

Procedure 1: Twelve vessels were used, each charged with virgin zircon and AAF. The system was run and after consecutive 10 min periods, individual vessels were removed, and the fractional conversion of each was determined.

Procedure 2: Three vessels with identical contents were used per run. After 10 min the reaction was stopped and the fractional conversion was determined. This experiment was repeated for 3 further runs, with periods of 20, 30 and 60 min. For each run virgin zircon was used as starting material.

Procedure 3: The purpose of procedure 3 was to “wash” away any ash layer that might have formed and possibly prohibit full conversion. Procedure 3 was similar to procedure 2 except that only one sample was used per vessel. The fractional conversion of the sample was determined after time t, each sample was then washed with water to remove any product layer, and then re-introduced into the vessel for the next digestion period.

A full description of each procedure is given below:

Procedure 1

For each of twelve identical vessels, a starting mass of 0.5 g zircon and 5 g $NH_4F{\cdot}1.5HF$ were weighed and transferred to each vessel. The vessels were capped and loaded in the carousel. The microwave system was set at a temperature of 180 °C, power was 1600 W and the pressure was monitored at 5.5 MPa. The vessels were placed in the support modules with the load distributing caps, and tightened with a torque wrench to 5 ft*lbs (Figure 3.5). Blue pressure caps (with rupture membranes inserted) were hand tightened. The pressure sensor and thermowell were attached to the control vessel. The support modules were placed on the carousel and the top ring attached. Assuming that the reaction proceeds according to the equation below, this represents roughly a 5:1 molar excess based on AAF.

$$3ZrSiO_4 + 16NH_4F{\cdot}1.5HF \rightarrow 3(NH_4)_3ZrF_7 + 3(NH_4)_2SiF_6 + 12H_2O + NH_4F \quad (3.1)$$

The vessels were placed in the microwave system where the parameters for power, control temperature, pressure maximum, ramp time, hold time and stage settings were manually programmed in as required by the standard procedure. The carousel was placed on the drive drag in the oven and the pressure sensor and temperature sensor were attached. The microwave door was closed and the start button pressed. The cool down period was reached when the temperature sensor read below 35 °C. Only then it was safe to remove the carousel from the oven.

The first vessel was removed and the contents analyzed after 10 min. The second vessel was removed after another digestion period of 10 min. The third vessel was removed after a further period of 10 min, and so on, as illustrated in Table 3.1.

Table 3.1: Summary of digestion times for procedure 1

Vessel no	1	2	3	4	5	6	7	8	9	10	11	12
Number of 10 min periods	1	2	3	4	5	6	7	8	9	10	11	12
Full time	10	20	30	40	50	60	70	80	90	100	110	120

After removal, the vessels were cooled on their own to room temperature, uncapped, the pressure in the reaction vessels was released slowly by unscrewing the blue cap and venting any remaining vapors in a fume hood and the reaction stopped by addition of 50 ml of a 3% boric acid (H_3BO_3) solution to neutralise the remaining free and bound HF. The reaction proceeds according to the equations below, with the formation of water-soluble HBF_4 and NH_4BF_4:

$$H_3BO_3 + 4HF \rightarrow HBF_4 + 3H_2O \quad (3.2)$$

$$H_3BO_3 + 2NH_4F{\cdot}1.5HF \rightarrow NH_4F + NH_4BF_4 + 3H_2O \quad (3.3)$$

The reaction mixture was centrifuged and the supernatant liquid decanted. The solid residue was washed with propanol, dried at 80 °C for 3 hours and weighed.

Another set of eleven vessels were prepared and the temperature set at 200 °C, but this time each vessel was removed after 20 min, the last vessel was taken out after 220 min. The procedure was repeated for another set of eleven vessels and the time interval for removing each vessel was increased to 30 min at the same temperature of 200 °C, the last vessel was removed after 330 min.

Procedure 2

In procedure 2 only three microwave vessels were used per experimental cycle. The procedure was performed at temperatures ranging from 100 to 200 °C. The vessels were allowed to digest for 10 min, after completion, all the three vessels were cooled to room temperature, and the conversion was determined as in procedure 1. Another set of three samples were prepared and the heating time was increased to 20 min. The procedure was repeated further in 10 min steps up to 60 min. The digestion cycles were done at 100, 120, 140, 160, 180 and 200 °C. All experiments were conducted in triplicate and the averaged values are reported here.

Procedure 3

All the vessels are prepared in the same manner as in procedure 2 and three vessels were used per cycle. The initial digestion time for a fixed temperature was set at 10 min. After completion, all the three vessels were cooled to room temperature, the sample was washed with water and the conversion was determined the same route as in procedure 1. The residue of the first period was then used as a starting material for the next experiment. The material in the three vessels was again digested with 5 g of

$NH_4F{\cdot}1.5HF$ with digestion time increased to 20 min. The digestion time was increased by 10 min for each subsequent cycle up to a maximum of 60 min (total digestion time per series 260 min). The digestion cycles were done at 120, 140, 160, 180, 200, 220 and 240 °C.

The raw (nominal) and corrected time data (to be explained in Chapter 4) are displayed in Table 3.2.

Table 3.2: Nominal and corrected reaction times

Isothermal reaction time (t_r) (min)	Ramp-up time (t_h) (min)	Ramp-down time (t_c) (min)	Ramp time contribution factor	Adjusted reaction time (min)	Cumulative reaction time (min)
10	10	15	0.56	22.5	22.5
20	10	15	0.38	32.5	55.0
30	10	15	0.29	42.5	97.5
40	10	15	0.24	52.5	150.0
50	10	15	0.20	62.5	212.5
60	10	15	0.17	72.5	285.0

3.4.1. Sampling handling

- The vessels should be free of particulate matter or drops of liquid such as high salt solutions that can absorb microwaves, before being subjected to microwave energy, which in turn could cause localized heating and damage to the vessel.
- When heating samples always ensure that pressure relief devices are used.
- Unknown samples should be pre-digested for 15 min before sealing the vessel to allow for oxidized compounds to exhaust volatile gas and thus diminishing the pressure inside the vessel during heating.

- High boiling point acids such as concentrated sulfuric or phosphoric acid should never be heated in the microwave.
- The operation manual should be consulted frequently for the list of solutions and solvents not recommended for use in the system or in the particular reaction vessel you are using.

3.5. Analytical methods

3.5.1. X-ray diffraction (XRD)

X-ray diffraction technique (Bruker A-D8 Advanced) in conjunction with 2007 PDF-2 database, was employed for chemical phase identification.

The measurement parameters were**:**

Diffractometer: D8 Advance
Goniometer: θ-θ
Target Tube: Cu
Recording range: 20˚ to 130˚
Step size: 0.02˚
Time/step: 1.5 s

3.5.2. FT-Raman

A Bruker Vertex FT-Raman spectrometer fitted with an Nd:YAG NIR laser with an excitation line of 1064 nm was used.

- Laser- Nd: YAG with 50 mW power output onto the sample
- Scan period- 128 scans
- Sample holder- Glass sample holder for zircon and aluminum sample holder for other samples.
- Resolution – 4 cm^{-1}

3.5.3. Scanning Electron Microscope (SEM)

The morphology of the particles was observed using a Scanning Electron Microscope, model FEI QUANTA 200i 3D.

3.5.4. Inductively coupled plasma optical emission spectrometry (ICP-OES)

A Spectro Arcos ICP-OES was used to analyse the concentration of elements present in the sample. Multi-element standards purchased form Merck (Pty) Ltd (South Africa) were used for calibration.

CHAPTER 4

Results and discussions

4.1. Introduction

Experimental results are presented and discussed in this chapter. The chemical analyses involved the use of XRD, SEM, ICP-OES and Raman spectroscopy for characterization of the raw, intermediate and final products. The detailed experimental procedures are discussed in chapter 3.

It is assumed that the reaction between zircon and $NH_4F{\cdot}1.5HF$ proceeds according to Equation 4.1:

$$3ZrSiO_4 + 16NH_4F{\cdot}1.5HF \rightarrow 3(NH_4)_3ZrF_7 + 3(NH_4)_2SiF_6 + 12H_2O + NH_4F \quad (4.1)$$

The AAF and ammonium fluoride, as well as the two ammonium fluorometallates, $(NH_4)_3ZrF_7$ and $(NH_4)_2SiF_6$, are totally soluble in water (Frayret *et al*., 2006; Hala 1989). The fractional conversion, α, is thus readily obtained by washing, filtering, and drying the zircon residue after time t. The fractional residue α is defined as

$$\alpha = \frac{m_{residue}}{m_0} \quad (4.2)$$

with $m_{residue}$ and m_0 the mass of the residue and starting mass respectively.

After completion of each run, and after the vessel had been cooled to room temperature and uncapped, the reaction was terminated by the addition of a boric acid (H_3BO_3) solution to neutralise the remaining free and bound HF. The reaction proceeds

according to Equations 4.3 and 4.4, with the formation of water-soluble HBF_4 and NH_4BF_4:

$$4HF + H_3BO_3 \rightarrow HBF_4 + 3H_2O \quad (4.3)$$

$$2NH_4F{\cdot}1.5HF + H_3BO_3 \rightarrow NH_4F + NH_4BF_4 + 3H_2O \quad (4.4)$$

4.2. Dissolution results

4.2.1. The reaction of zircon with AAF according to procedure 1

Gravimetric results for the zircon that was leached in $NH_4F{\cdot}1.5HF$ at 180 °C and 200 °C where one vessel was removed after a specific time are shown numerically and graphically in Table 4.1 - 4.3 and Figure 4.1 - 4.3.

From the results in Table 4.1 and Figure 4.1 it can be seen that a conversion of only 60% was obtained at 180 °C after 120 min. The standard error and standard deviation for these results were 0.04 and 0.13 respectively.

Table 4.1: Fractional residue (α) of zircon at 180 °C and in 10 minute intervals

Time (min)	Fractional residue (α)
0	1.00
10	0.76
20	0.76
30	0.75
40	0.72
50	0.73
60	0.68
70	0.65
80	0.64
90	0.66
100	0.61
110	0.63
120	0.42

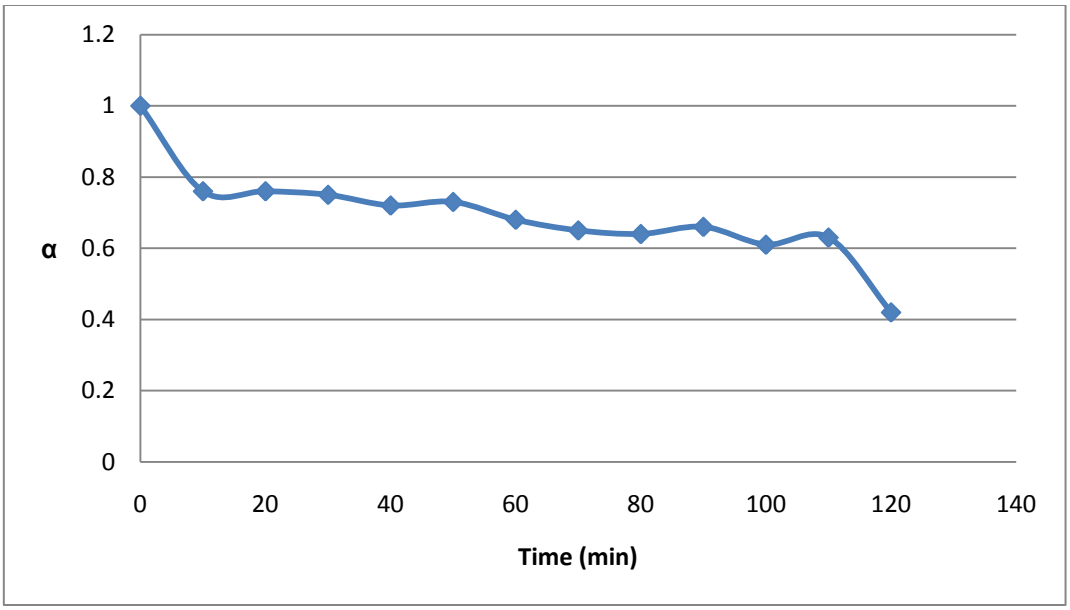

Figure 4.1: Fractional residue (α) of zircon at 180 °C and in 10 minute intervals

From the results in Table 4.2 and Figure 4.2, where the time interval was set to 20 min intervals, it can be seen that there was a slight change in the conversion of zircon, a nearly 70% conversion was produced at 200 °C after 220 min.

Table 4.2: Fractional residue (α) of zircon at 200 °C and 20 minute intervals

Time (min)	Fractional residue (α)
0	1.00
20	0.82
40	0.71
60	0.70
80	0.69
100	0.65
120	0.63
140	0.67
160	0.63
180	0.58
200	0.56
220	0.35

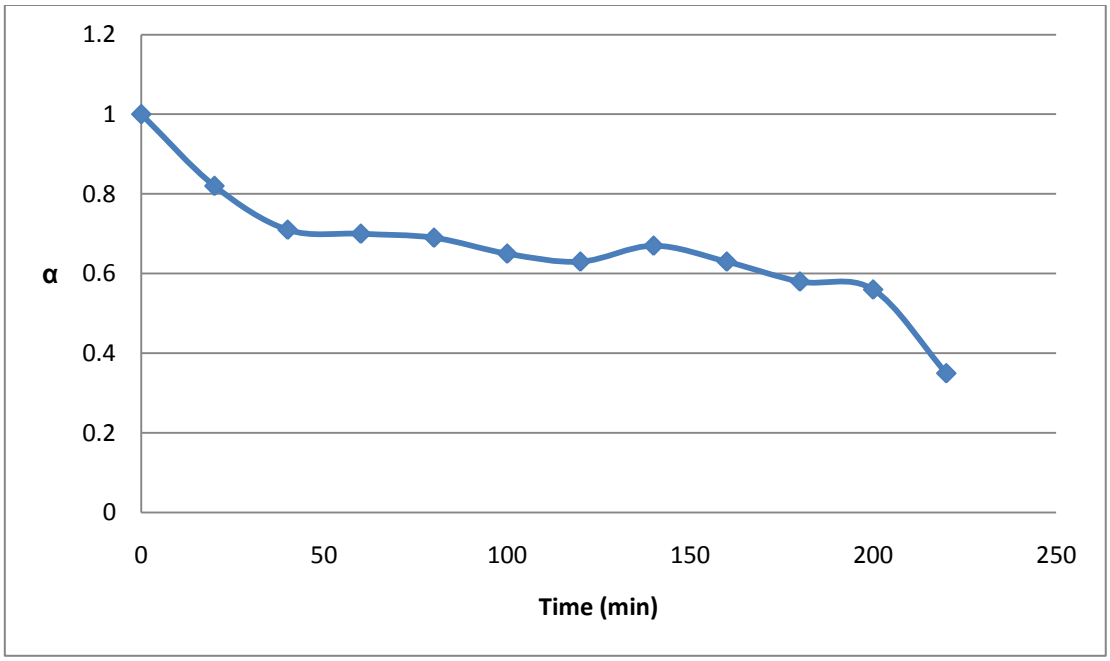

Figure 4.2: Fractional residue (α) of zircon at 200 °C and 20 minute intervals

The standard error and standard deviation for these results were 0.04 and 0.15 respectively.

Both Figures 4.1 and 4.2 display a dip at the final data point, seeming to suggest the possibility of further conversion. In order to investigate this, at the maximum temperature of 200 °C, the digestion periods were increased as illustrated in Table 4.3 and Figure 4.3. Unfortunately, however, the results were not encouraging. The conversion graph displays the same 40% conversion plateau well beyond the 220 min mark. It also gives a final dip at the last data point, this time at 330 min - an observation we can't explain at this stage. The general conclusion is that this procedure gives a maximum conversion of 70%. The standard error and standard deviation for this result were 0.05 and 0.16 respectively.

Table 4.3: Fractional residue (α) of zircon at 200 °C and 30 minute intervals

Time (min)	Fractional residue (α)
0	1.00
30	0.78
60	0.71
90	0.66
120	0.69
150	0.65
180	0.61
210	0.63
240	0.57
270	0.58
300	0.53
330	0.33

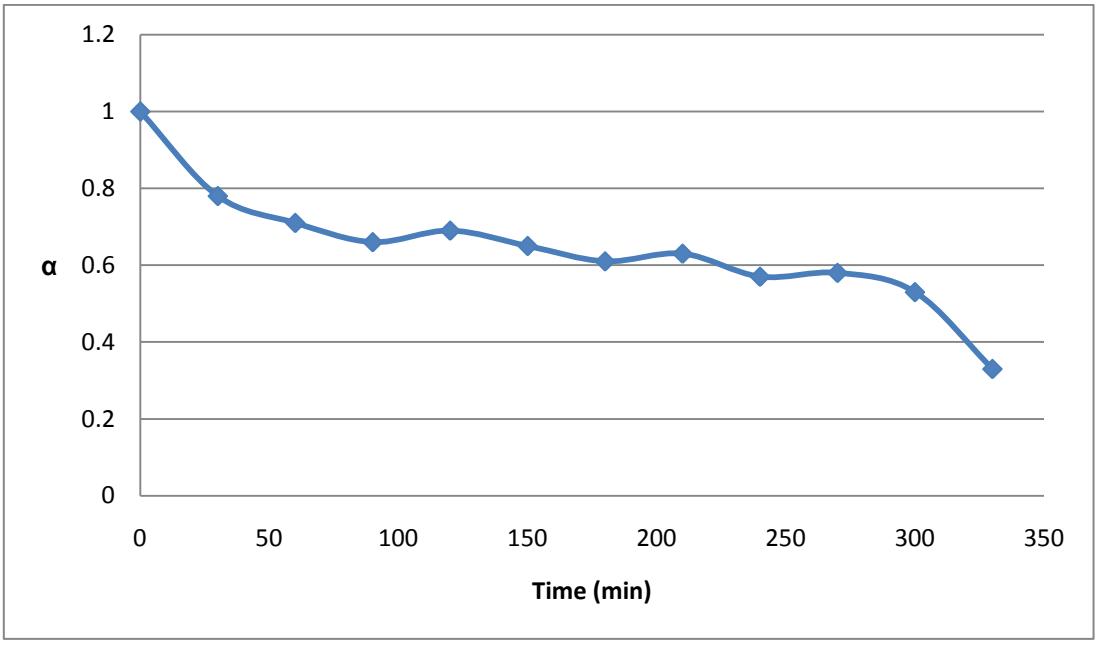

Figure 4.3: Fractional residue (α) of zircon at 200 °C and 30 minute intervals

4.2.2. The reaction of zircon with AAF according to procedure 2

The overall objective of procedure 2 was to obtain more detail of the effect of temperature on the process. Gravimetric results for the zircon that was leached in $NH_4F{\cdot}1.5HF$ at different temperatures and washed once are shown in Table 4.4 and Figure 4.4. The results show that the highest percentage conversion (about 30%) after 60 min occurs when the reaction temperature was set at 200 °C. This corresponds with Procedure 1 results. Also, it can be seen from Figure 4.4 that the conversion rates of zircon are temperature dependent, since the conversion rates increase with an increase in temperature. The average standard error and standard deviation were 0.03 and 0.06 respectively.

Since we did not anticipate further improvement in conversion, the experiments were not extended to longer times. Instead a different approach was conceptualized, as illustrated in the next section.

Table 4.4: Fractional residue of zircon *versus* temperature

	100 °C	120 °C	140 °C	160 °C	180 °C	200 °C
Time (min)	α	α	α	α	α	A
0	1	1	1	1	1	1
10	0.97	0.92	0.91	0.83	0.84	0.81
20	0.97	0.93	0.88	0.84	0.81	0.75
30	0.94	0.93	0.87	0.81	0.76	0.72
60	0.95	0.89	0.82	0.77	0.69	0.69

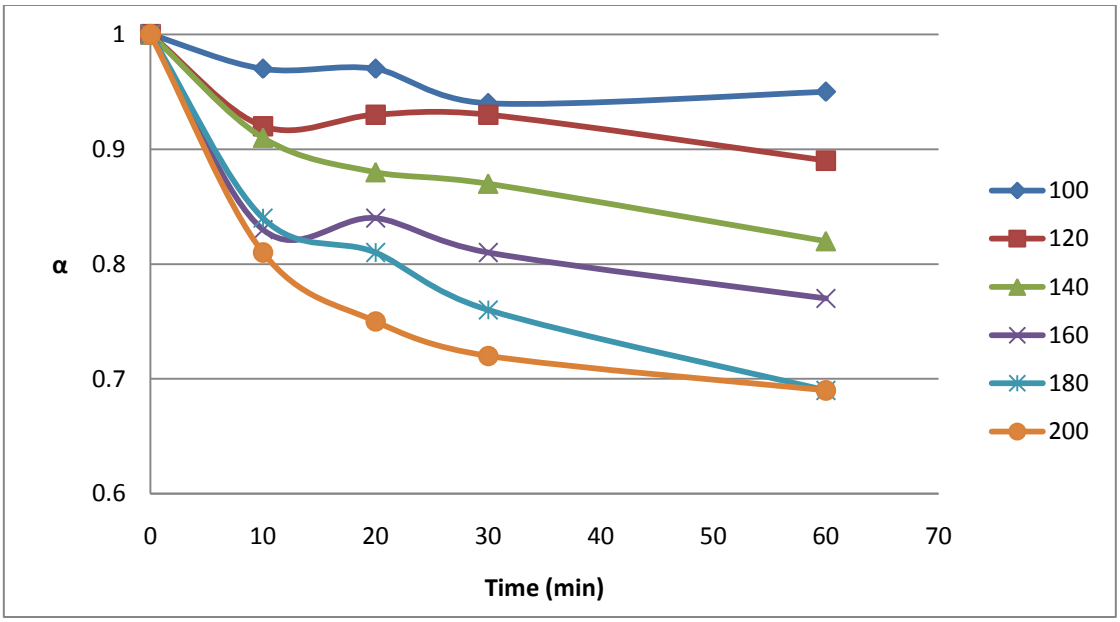

Figure 4.4: Fractional residue of zircon *versus* temperature

4.2.3. The reaction of zircon with AAF according to procedure 3

It was expected that the inability to achieve full conversion was due to the build up of product ash layer on the surface of each particle, preventing further reaction. Since vigorous agitation was not possible during digestion inside the microwave vessel, it was decided to interrupt the process after short periods and to remove the ash layer by washing. The experimental fractional residue as function of time and temperature is given in Table 4.5 and Figure 4.5 which show that an increase in temperature clearly increases the rate of conversion of zircon. After 285 min about 30% (α = 0.70) of the zircon was converted at 120 °C, while >99% (α = 0.007) conversion was achieved at 240 °C, the highest temperature investigated. The average standard error and deviation were 0.10 and 0.25 respectively.

Table 4.5: The effect of temperature and repeated addition of $NH_4F{\cdot}1.5HF$ on the fractional residue

Sample	Digestion time (min)	120 °C α	140 °C α	160 °C α	180 °C α	200 °C A	220 °C α	240 °C α
	0	1	1	1	1	1	1	1
Original	10	0.93	0.93	0.87	0.84	0.74	0.64	0.67
Residue 1	30	0.85	0.85	0.77	0.65	0.55	0.53	0.34
Residue 2	60	0.82	0.79	0.69	0.55	0.38	0.36	0.19
Residue 3	100	0.77	0.75	0.58	0.37	0.31	0.29	0.07
Residue 4	150	0.73	0.70	0.48	0.25	0.17	0.16	0.05
Residue 5	210	0.70	0.64	0.40	0.13	0.12	0.09	0.01

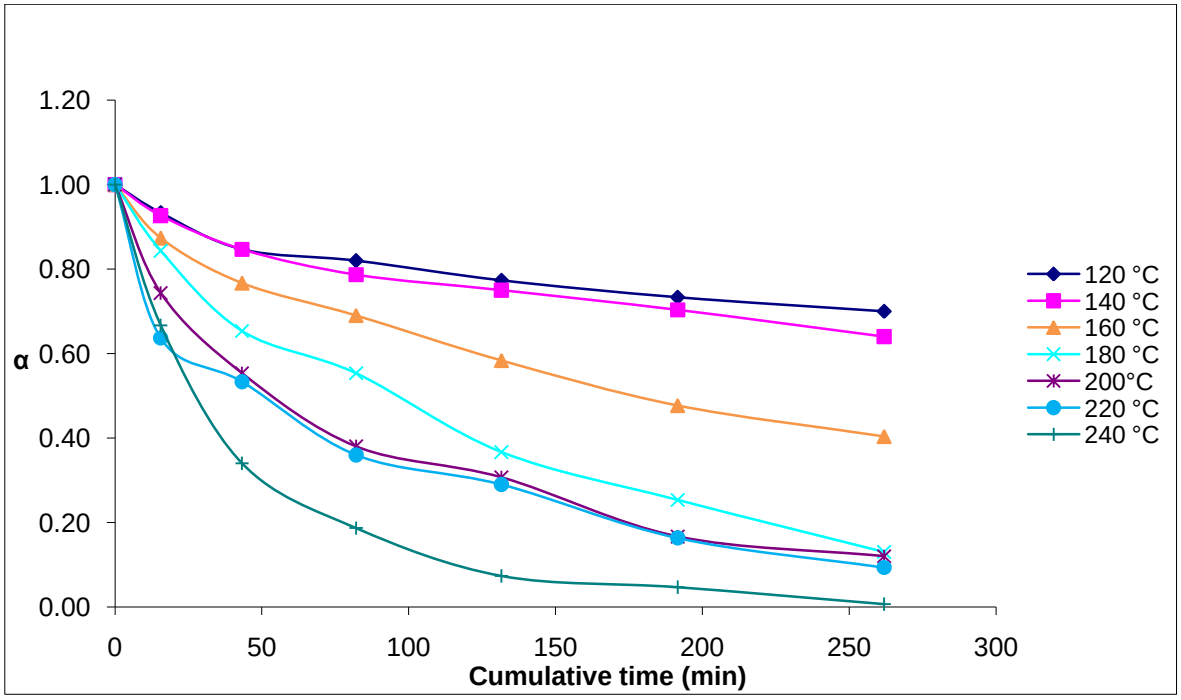

Figure 4.5: The effect of temperature and repeated addition of $NH_4F{\cdot}1.5HF$ on the fractional residue

4.3. Chemical analysis

ICP-OES results for the reaction of zircon with AAF according to procedure 3

ICP-OES analysis results of untreated zircon are shown in Table 4.6. Zirconium and silicon are the main components, with hafnium the main contaminant. 0.14% aluminium was observed and traces of components such as sulphur. Tables 4.7-4.9 contain analyses of the leached residues. No further presence of aluminium and about 1% less silicon are observed, indicating slight selective leaching of free silica and alumina.

Table 4.6: ICP-OES results of untreated zircon

Element	Concentration (%)
Aluminium (Al)	0.14
Hafnium (Hf)	1.26
Silicon (Si	15.60
Zirconium (Zr)	48.40
Copper (Cu)	Trace
Iron (Fe)	Trace
Nickel (Ni)	Trace
Sulphur (S)	Trace

Table 4.7: ICP-OES results of zircon leached in $NH_4F{\cdot}1.5HF$ and re-digested for 55 min at 200 °C

Element	Concentration (%)
Hafnium (Hf)	1.06
Silicon (Si)	14.60
Zirconium (Zr)	48.60
Yttrium (Y)	Trace

Table 4.8: ICP-OES results of zircon leached in $NH_4F{\cdot}1.5HF$ and re-digested for 150 min

Element	Concentration (%)
Hafnium (Hf)	1.02
Silicon (Si)	14.50
Zirconium (Zr)	48.00
Iron (Fe)	Trace

Table 4.9: ICP-OES results of zircon leached in $NH_4F{\cdot}1.5HF$ and re-digested for 285 min at 200 °C

Element	Concentration (%)
Hafnium (Hf)	10.99
Silicon (Si)	13.90
Zirconium (Zr)	46.40

4.3.1. XRD analysis of the residue after leaching

XRD results for the reaction of zircon with AAF according to procedure 1

Background subtracted diffraction patterns of untreated zircon and the zircon leached in AAF overlaid with stick patterns from the database are shown in Figures 4.6-4.8. With the exception of the peak at 42° in 2θ (which haven't been identified), the analysis confirms that the material is indeed $ZrSiO_4$ (70-7135), see Figure 4.6. The sample digested for 180 min shows no significant changes on the initial material (with the exception of peak intensities), Figure 4.7. With further digestion time, the minority phases of ammonium hydrogen fluoride and ammonium zirconium fluoride, in addition to the initial material, are also present, Figure 4.8.

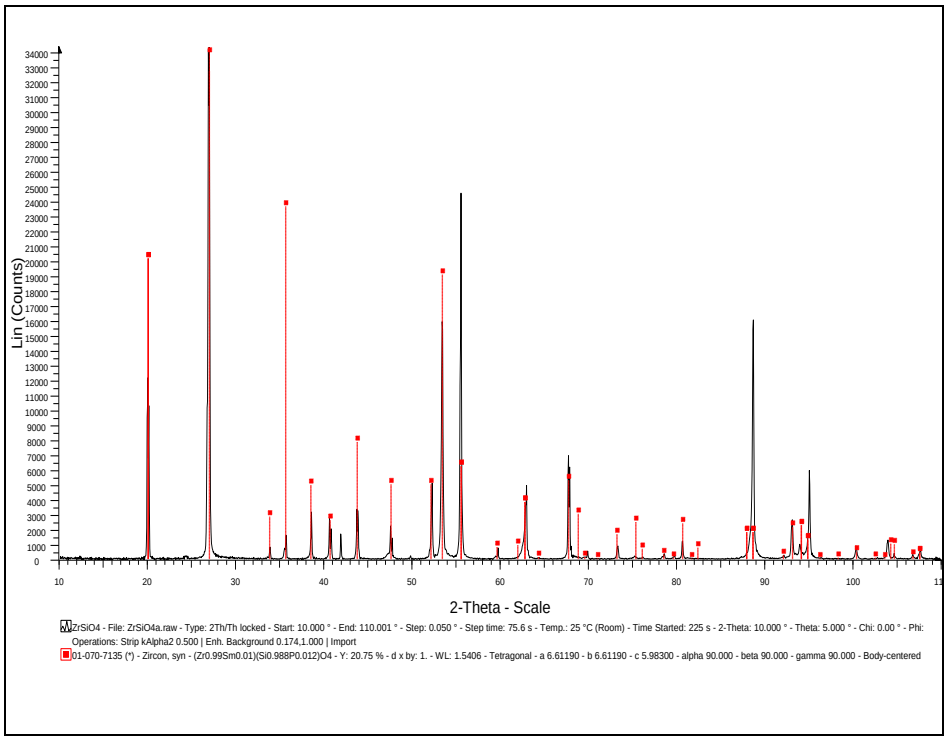

Figure 4.6: X-ray diffraction pattern of untreated zircon sample overlaid with the proposed stick pattern from the ICDD database.

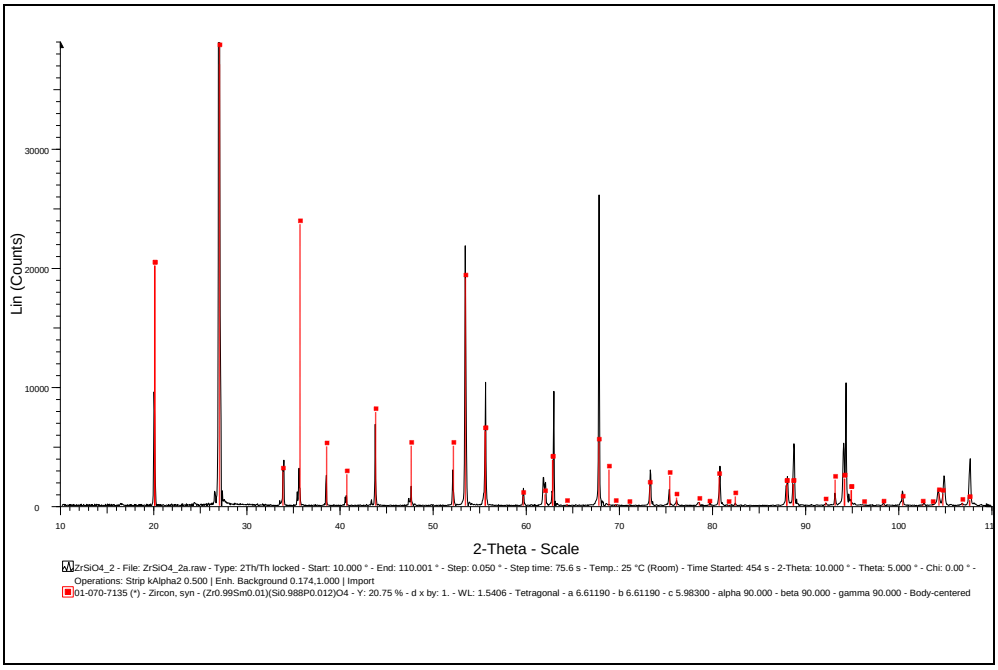

Figure 4.7: X-ray diffraction pattern of the zircon leached in AAF for 180 min at 200 °C, overlaid with the proposed stick pattern from the ICDD database.

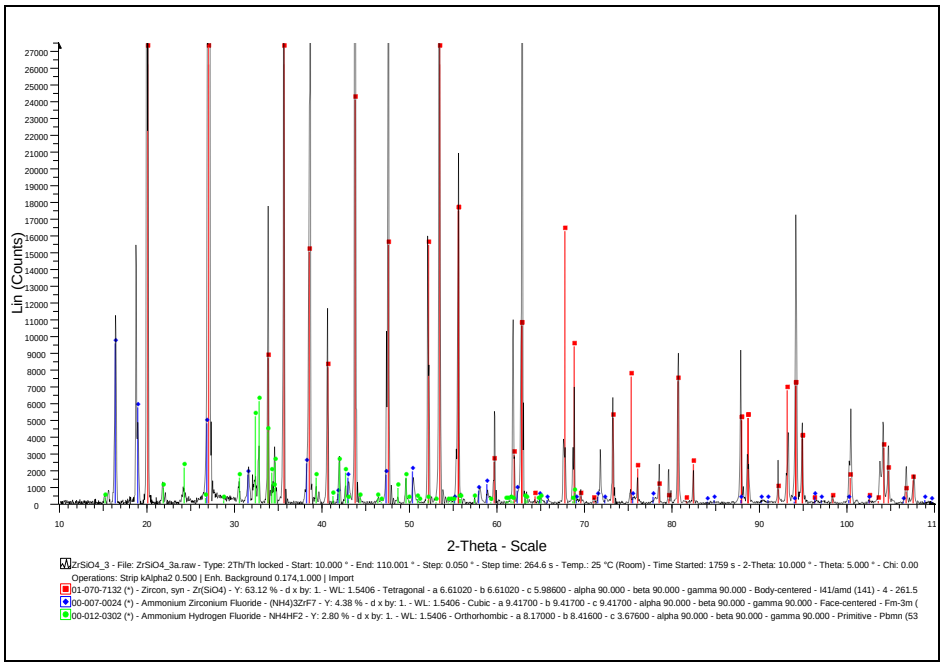

Figure 4.8: X-ray diffraction pattern of the zircon leached in AAF for 330 min at 200 °C, overlaid with stick patterns from the ICDD database of the proposed phases present.

XRD results for the reaction of zircon with AAF according to procedure 2

The X-ray diffraction pattern of zircon leached in $NH_4F{\cdot}1.5HF$ for 60 min at 200 °C overlaid with the proposed stick pattern from the ICDD database is shown in Figure 4.9. The pattern shows $ZrSiO_4$ to be the major phase with minority phases of $(NH_4)_2SiF_6$ and $(NH_4)_3ZrF_7$.

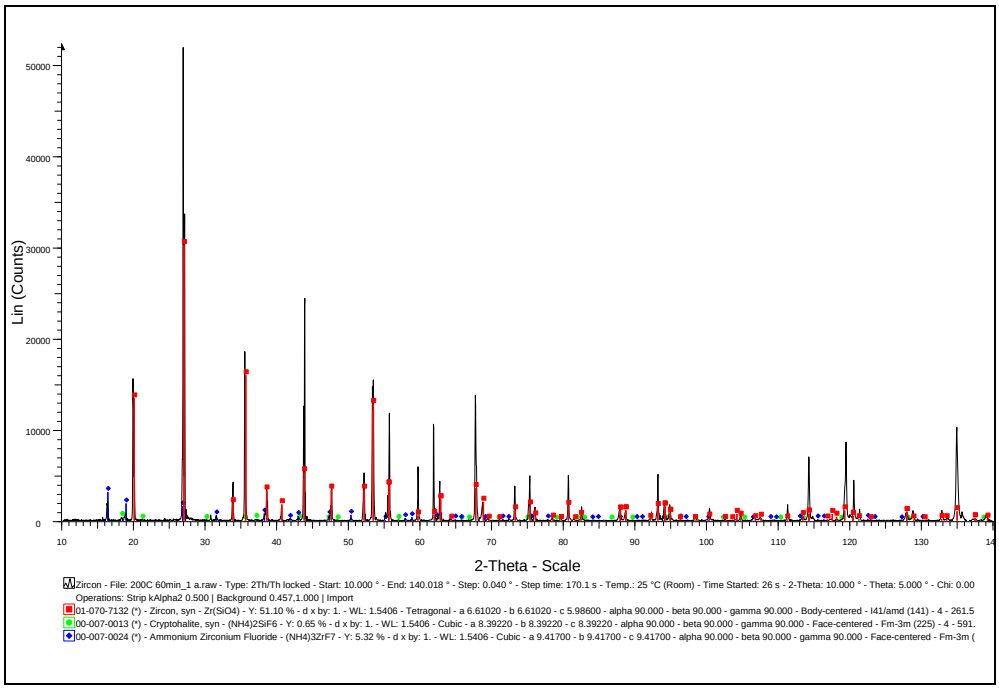

Figure 4.9: X-ray diffraction pattern of zircon leached in $NH_4F{\cdot}1.5HF$ for 60 min at 200 °C overlaid with the proposed stick pattern from the ICDD database.

XRD results for the reaction of zircon with AAF according to procedure 3

X-ray diffractograms of zircon leached in $NH_4F{\cdot}1.5HF$, washed and re-digested at different times are shown in Figures 4.10 to 4.12. Figure 4.10 and 4.11 show that the major component of the residue is $ZrSiO_4$. The pattern in Figure 4.12 shows $ZrSiO_4$ to be the major components with minority phases of $(NH_4)_2SiF_6$ and $(NH_4)_3ZrF_7$. A close examination of the XRD pattern shows some mismatch between the zircon reference and experimental spectra, as well as unindexed reflections at 16, 24, 25 and 29 degrees 2θ.

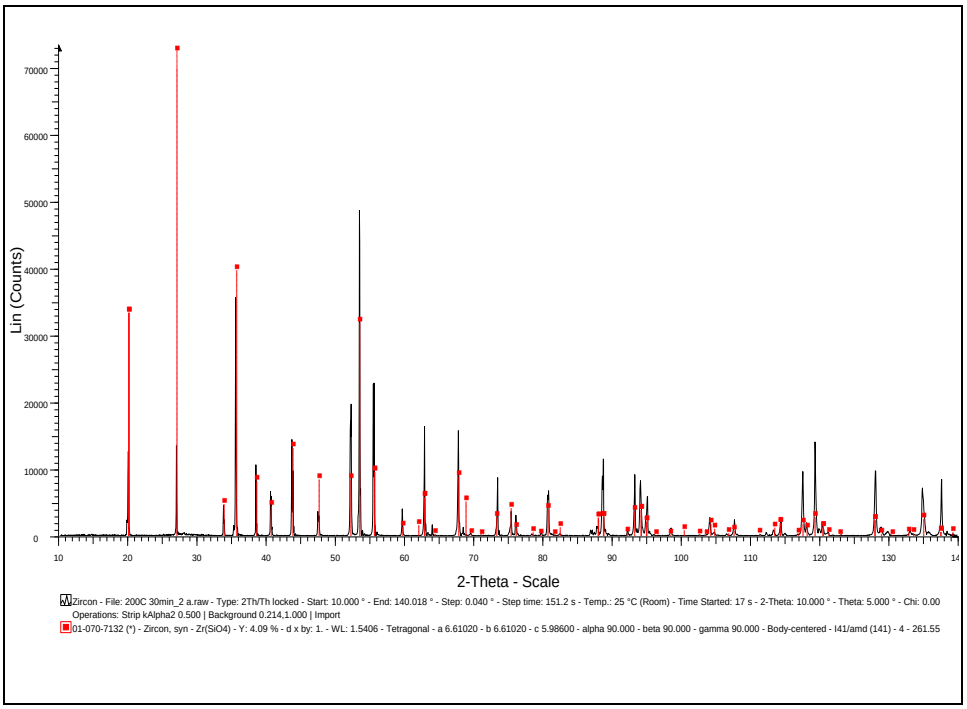

Figure 4.10: X-ray diffraction pattern of zircon leached in $NH_4F{\cdot}1.5HF$ and re-digested for 55 min at 200 °C overlaid with the proposed stick pattern from the ICDD database.

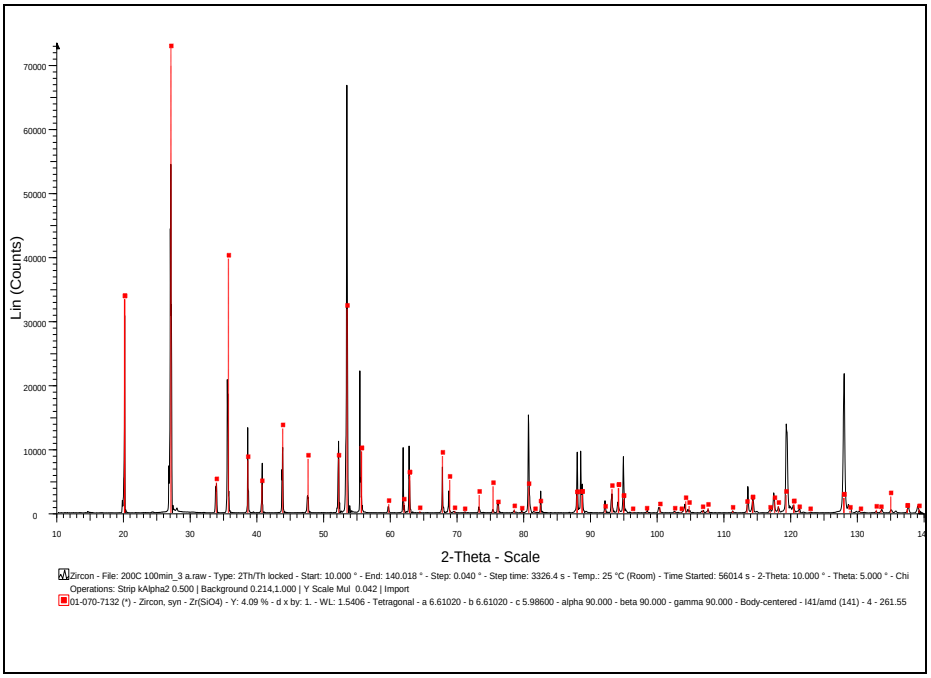

Figure 4.11: X-ray diffraction pattern of zircon leached in $NH_4F{\cdot}1.5HF$ and re-digested for 150 min at 200 °C overlaid with the proposed stick pattern from the ICDD database.

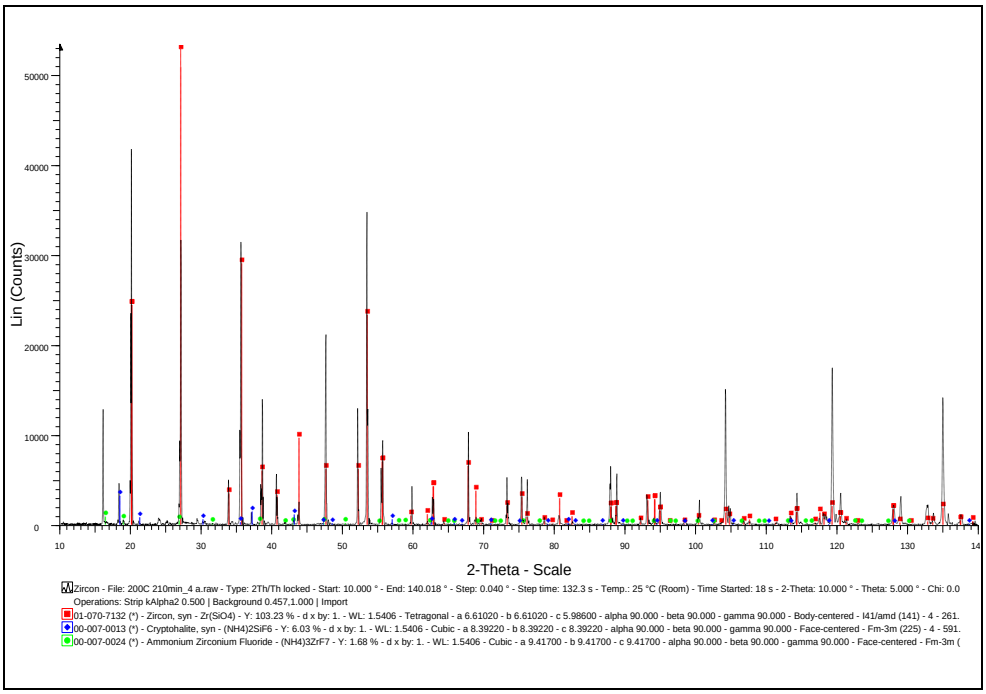

Figure 4.12: X-ray diffraction pattern of zircon leached in $NH_4F{\cdot}1.5HF$ and re-digested for 285 min at 200 °C overlaid with the proposed stick pattern from the ICDD database.

Background subtracted diffraction patterns of the zircon leached in $NH_4F{\cdot}1.5HF$, washed and redigested for 285 min at different temperatures overlaid with stick patterns of the proposed phases are shown in Figure 4.13-4.15. Details of the measured pattern and the overlaid sticks are shown on the caption. Table 4.10 below shows the summary of the proposed phases in each sample.

Table 4.10: Phases proposed to be present in the zircon digested samples.

Sample	PDF chemical/crystallographic phases
Zircon 120 °C	Zircon, ammonium zirconium fluoride, zirconium hafnium silicate
Zircon 160 °C	Zircon, zirconium hafnium silicate
Zircon 240 °C	Zircon, ammonium zirconium fluoride zirconium hafnium silicate and ammonium boron fluoride

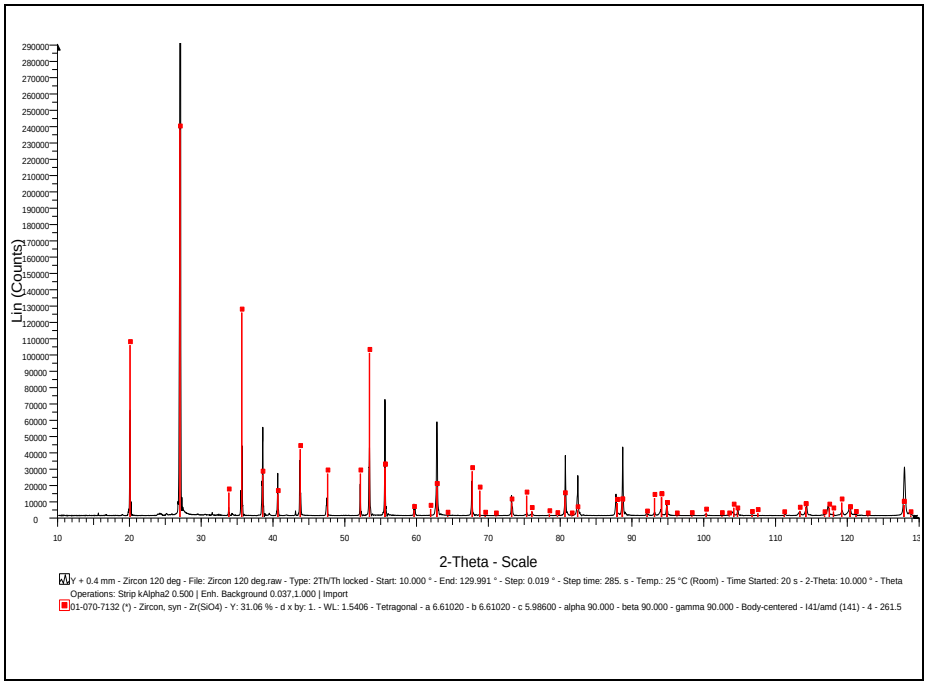

Figure 4.13: Background subtracted diffraction pattern of the zircon leached in $NH_4F{\cdot}1.5HF$ and redigested for 285 min at 120 °C overlaid with stick pattern of zircon.

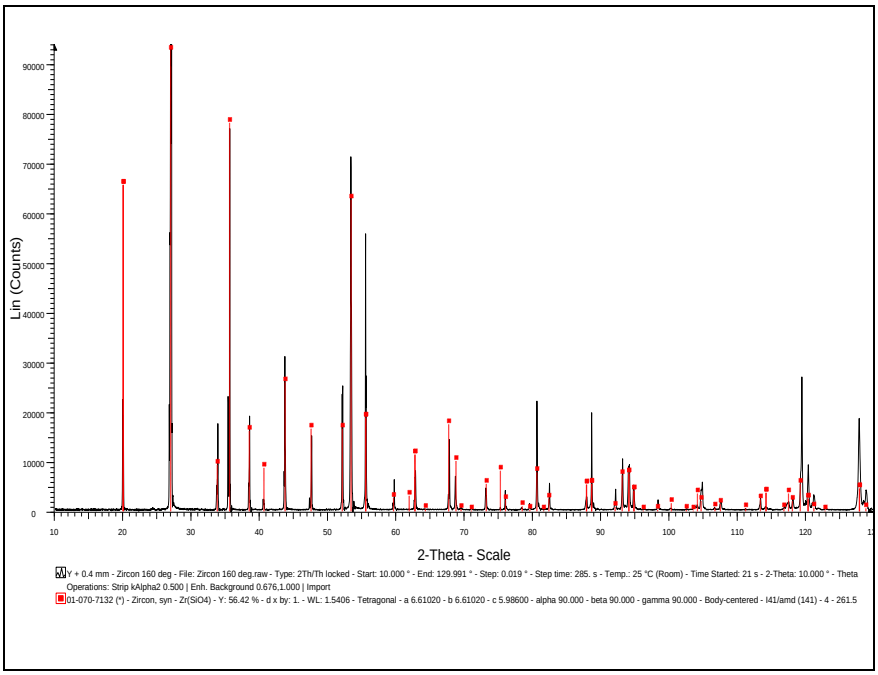

Figure 4.14: Background subtracted diffraction pattern of the zircon leached in $NH_4F{\cdot}1.5HF$ and redigested for 285 min at 160 °C overlaid with the stick pattern of zircon.

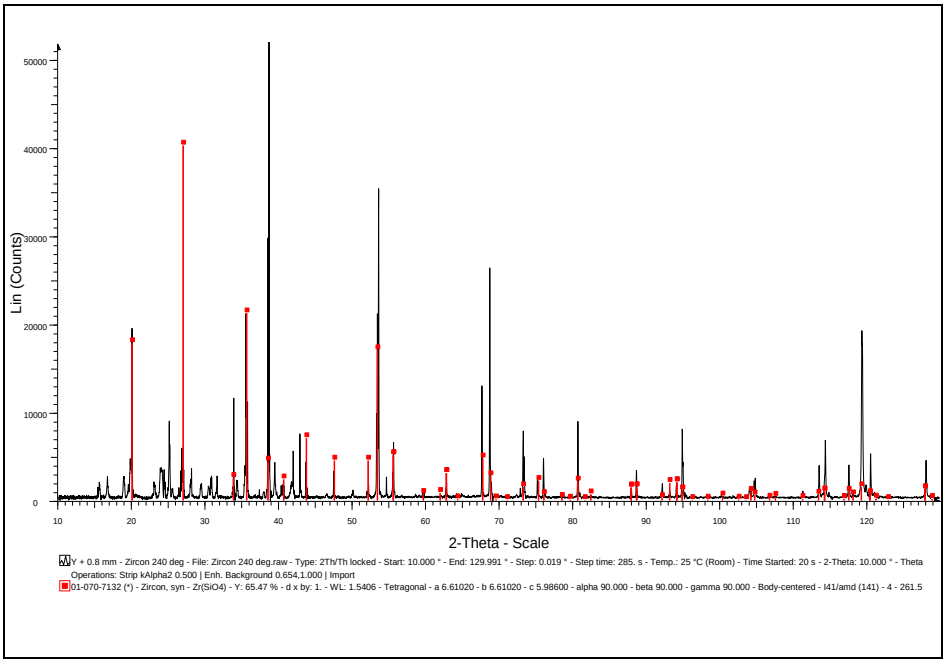

Figure 4.15: Background subtracted diffraction pattern of the zircon leached in $NH_4F{\cdot}1.5HF$ and re-digested for 285 min at 240 °C sample overlaid with stick pattern of zircon.

4.3.2. Raman spectroscopy

Raman results for the reaction of zircon with AAF according to procedure 2

No Raman spectra were recorded for procedure 1. Raman spectra of zircon leached in $NH_4F{\cdot}1.5HF$ at various times and temperatures are represented in Figures 4.16-4.19. Three peaks are observed at 357, 440 and 1008 which are associated with zircon. Zircon slowly reacts to form a mixture of $(NH_4)_2SiF_6$ and $(NH_4)_3ZrF_7$ which were confirmed by XRD analysis (see fig 4.9). This explains the reason why longer period leached samples tend to show low intensity peaks on Raman. Compare Figure 4.16 and 4.17, also 4.18 and 4.19.

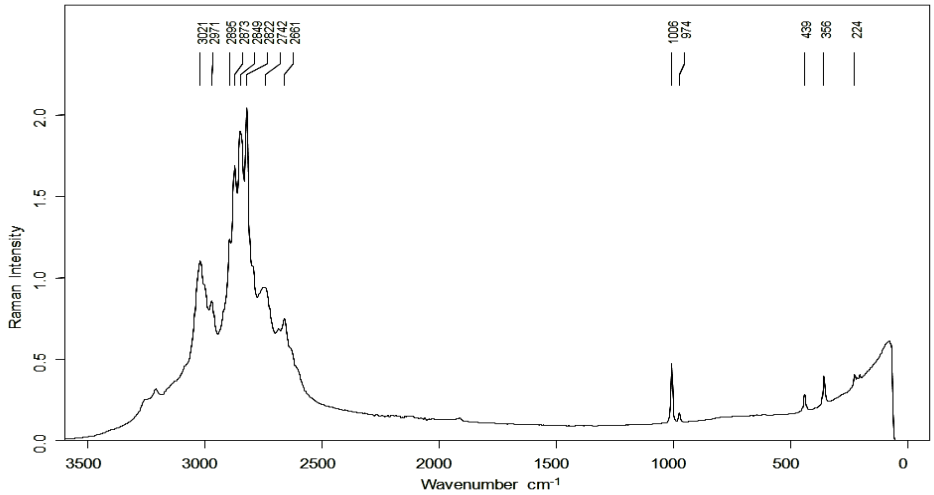

Figure 4.16: Raman spectrum of zircon leached in $NH_4F{\cdot}1.5HF$ for 30 min at 120 °C

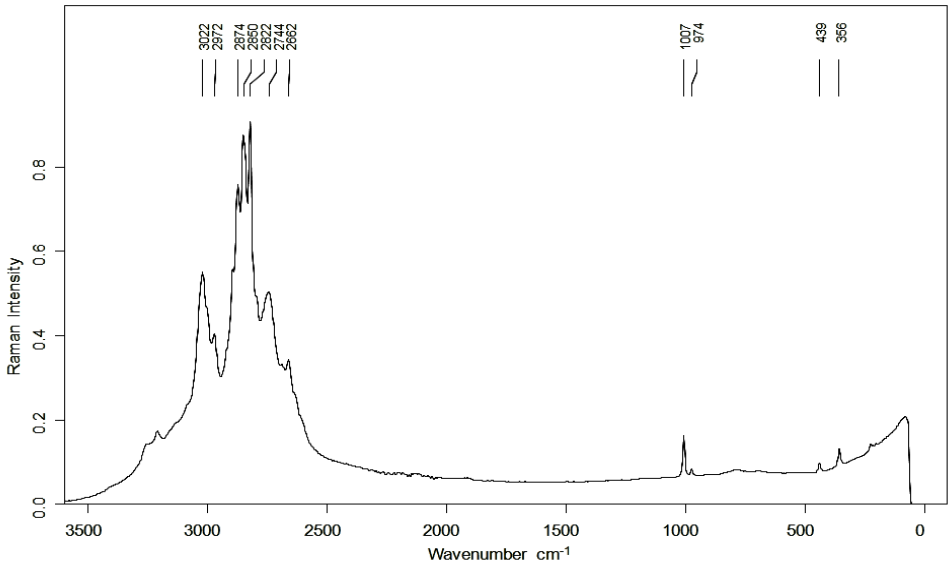

Figure 4.17: Raman spectrum of zircon leached in $NH_4F{\cdot}1.5HF$ for 60 min at 120 °C

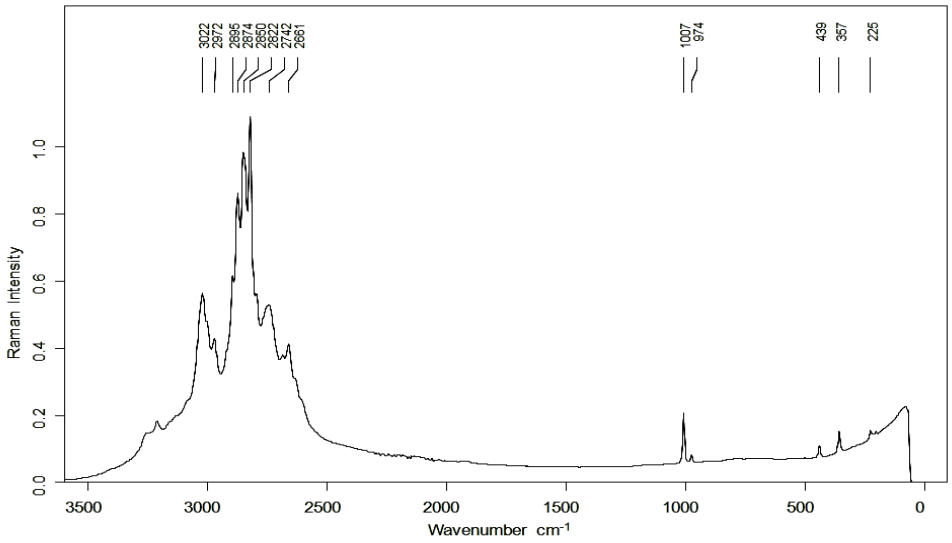

Figure 4.18: Raman spectrum of zircon leached in $NH_4F{\cdot}1.5HF$ for 30 min at 200 °C

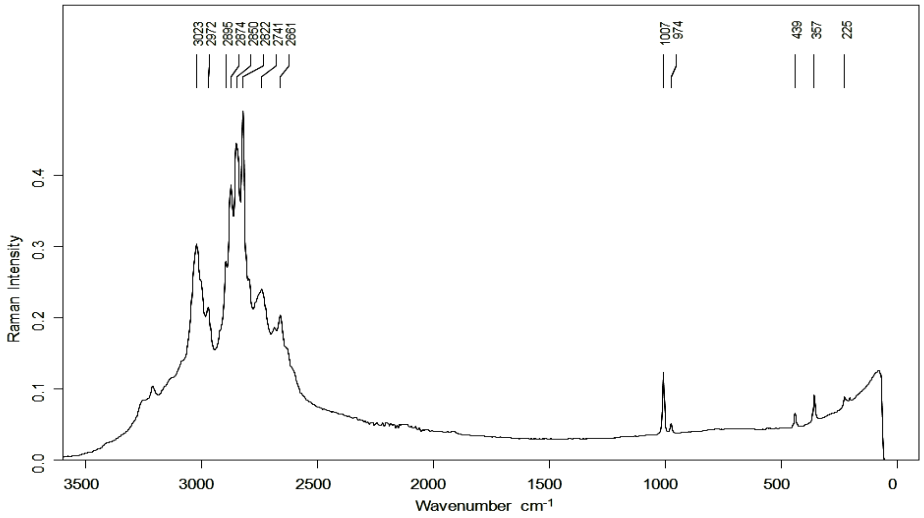

Figure 4.19: Raman spectrum of zircon leached in $NH_4F{\cdot}1.5HF$ for 60 minutes at 200 °C

Raman results for the reaction of zircon with AAF according to procedure 3

Raman spectra of untreated zircon (Figure 4.20) and the zircon leached in $NH_4F{\cdot}1.5HF$, washed and re-digested for different times at 200 °C are shown in Figure 4.21 to Figure 4.23. The Raman spectra show three peaks at 357, 440 and 1008 cm^{-1}, which are associated with zircon. These peaks belong to the lattice mode, Si-O bend and Si-O anti-symmetric zircon modes respectively. The silicate ion has three degrees of freedom and symmetry related to a C_{nV} molecule, with an order of 3. The Raman spectroscopic investigation of the sample before leaching indicates that the E_g at 357 cm^{-1} (lattice mode) and the symmetric A_{1g} at 439 cm^{-1} mode of zircon's Si-O group (Presser and Glotzbach, 2008) are of low intensities relative to the cluster of peaks around 2800 cm^{-1} (Figure 4.20). However, when the sample is leached with AAF and digested in a microwave, the relative intensities of the two modes, A_{1g} and the E_g to the peak at 2800 cm^{-1} increase with the increasing leaching period (Figure 4.21-4.23). This could be due to the increasing purity of zircon because some impurities might be selectively leached out. The other peak observed on the spectrum of zircon is the anti-symmetric stretching

of the Si-O group at 1008 cm^{-1}. This ν_3 band has a B_{1g} symmetry (De Waal *et al*., 1996; Knittle and Williams, 1993) and has the highest intensity of all the Si-O modes in zircon

.

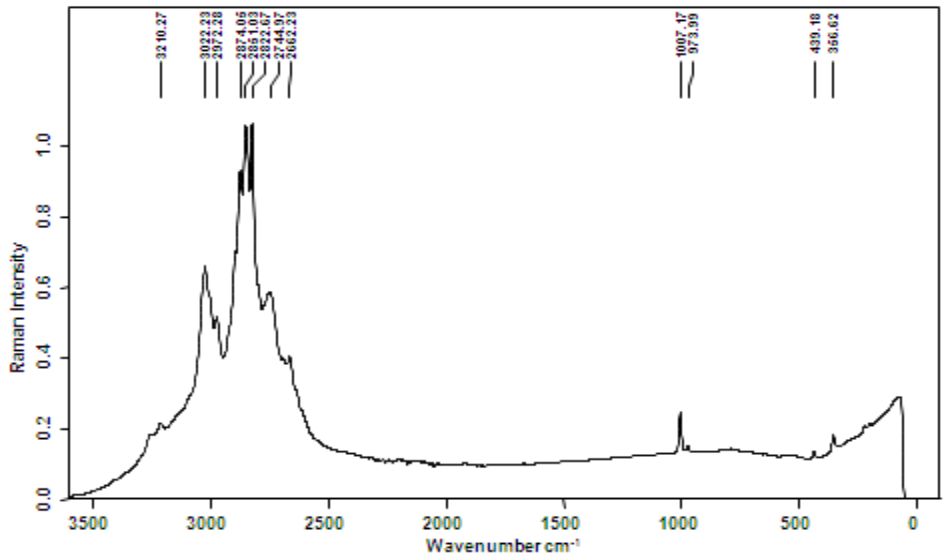

Figure 4.20: Raman spectrum of untreated zircon

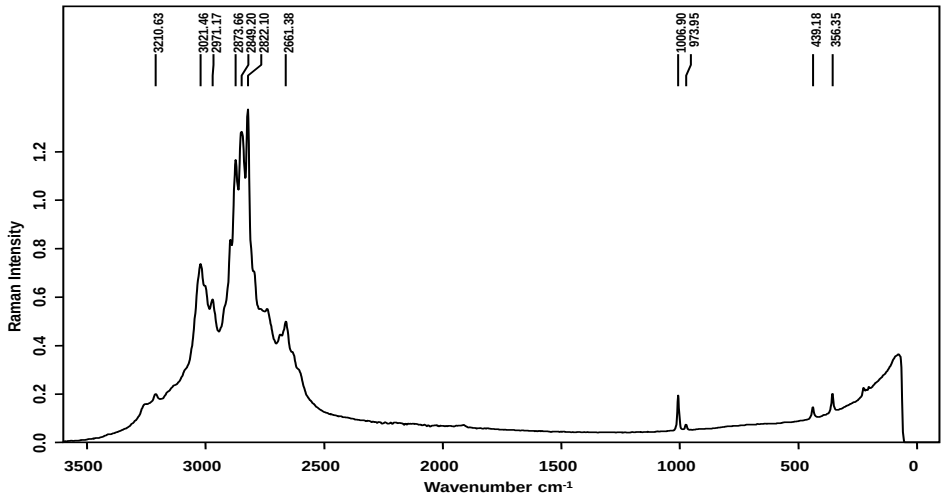

Figure 4.21: Raman spectrum of zircon leached in $NH_4F{\cdot}1.5HF$ for 55 min at 200 °C

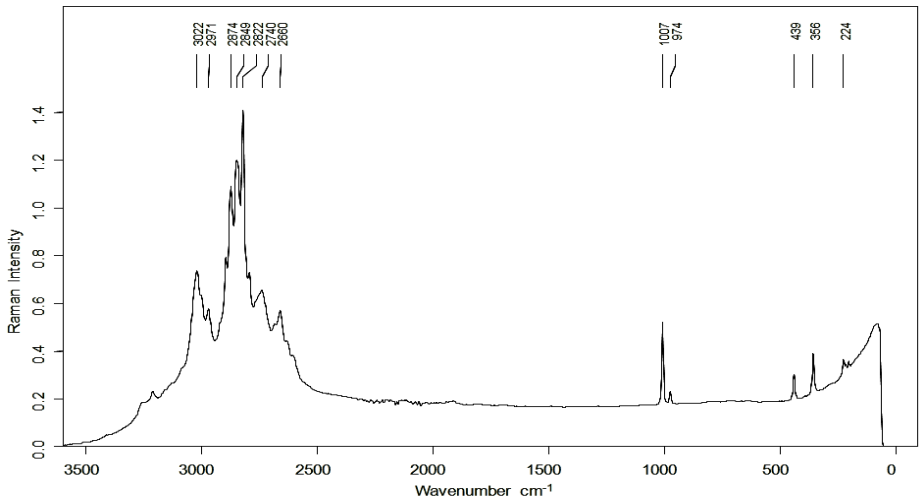

Figure 4.22: Raman spectrum of zircon leached in $NH_4F{\cdot}1.5HF$ for 150 min at 200 °C

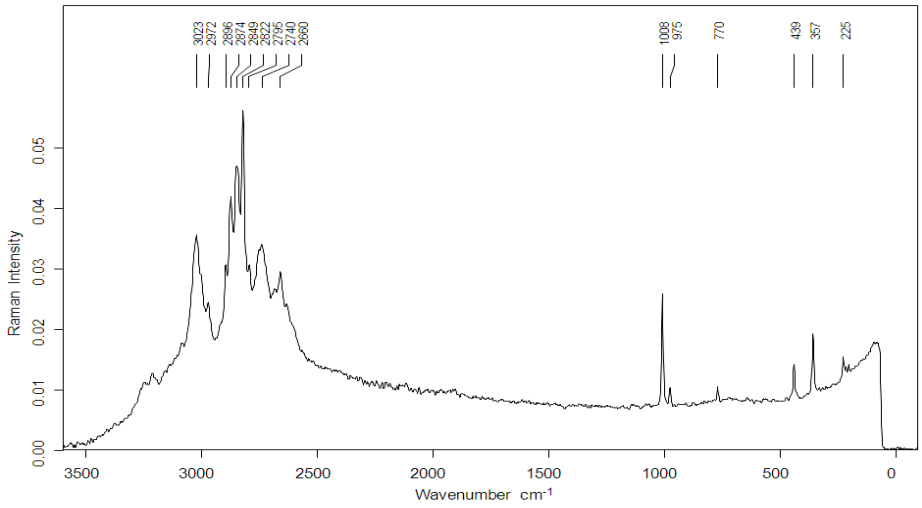

Figure 4.23: Raman spectrum of zircon leached in $NH_4F{\cdot}1.5HF$ for 285 min at 200 °C

4.3.3. Particle morphology

SEM results for the reaction of zircon with AAF according to procedure 1

The morphology of untreated zircon particles and zircon leached in $NH_4F{\cdot}1.5HF$ at different times is shown in Figures 4.24 to 4.26. The particles for pure zircon show a

smooth surface without pores (Figure 4.24). Light grey areas contain high percentages of zirconium, and darker areas contain higher percentages of silicon (Kaiser *et al*., 2008). After the zircon was leached in $NH_4F{\cdot}1.5HF$ for 120 min the surface of the particles became rough and had some pores caused by the leaching of zircon by the acid (Figure 4.25). Figure 4.26 shows the particles for the zircon that were leached for longer time (220 min) is more etched and have some cracks.

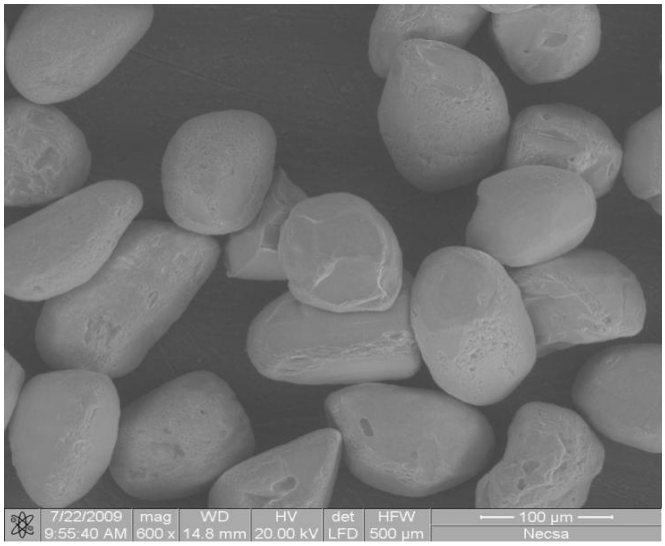

Figure 4.24: SEM micrograph of untreated zircon

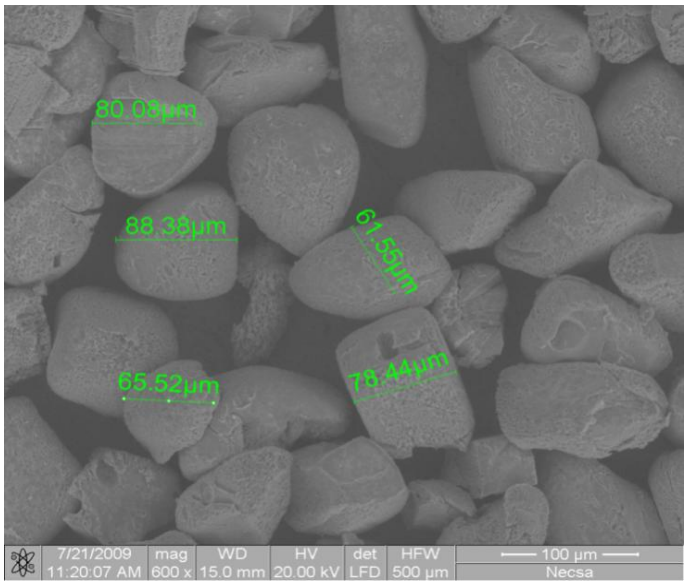

Figure 4.25: SEM micrograph of zircon leached in $NH_4F{\cdot}1.5HF$ for 120 min at 200 °C

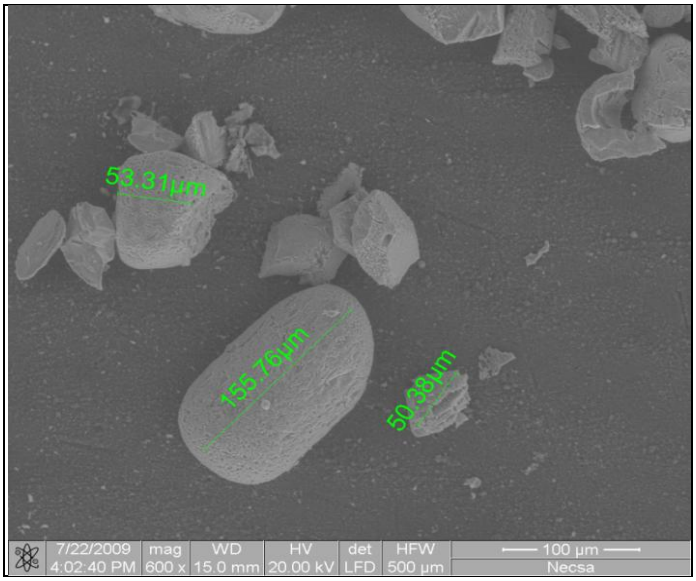

Figure 4.26: SEM micrograph of zircon leached in $NH_4F{\cdot}1.5HF$ for 220 min at 200 °C

SEM results for the reaction of zircon with AAF according to procedure 2

The comparison of the SEM analysis between untreated and treated zircon samples are also shown in Figure 4.27 to Figure 4.30. From different SEM images the difference in roundness of the zircon particle and the zircon leached in $NH_4F{\cdot}1.5HF$ can be noticed. It proves that untreated zircon particles are more spherical in shape (Figure 4.27) compared to particles of zircon leached in $NH_4F{\cdot}1.5HF$, which are characterized by more cylindrically shaped particles Figure 4.28, Figure 4.29 and Figure 4.30.

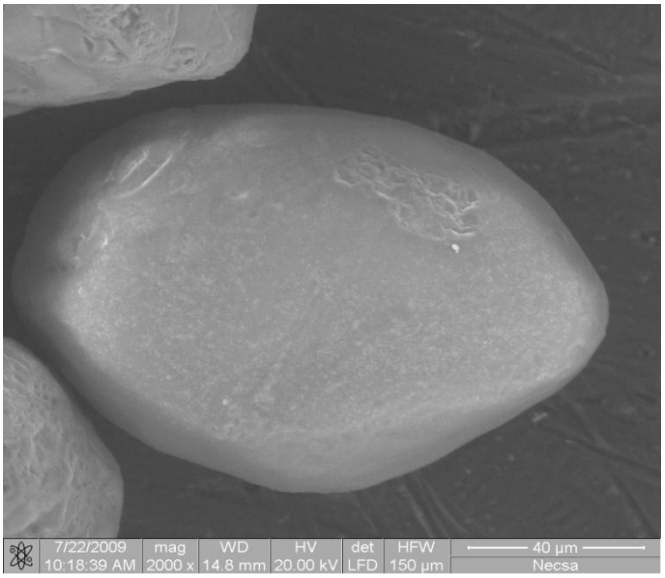

Figure 4.27: SEM micrograph of untreated zircon

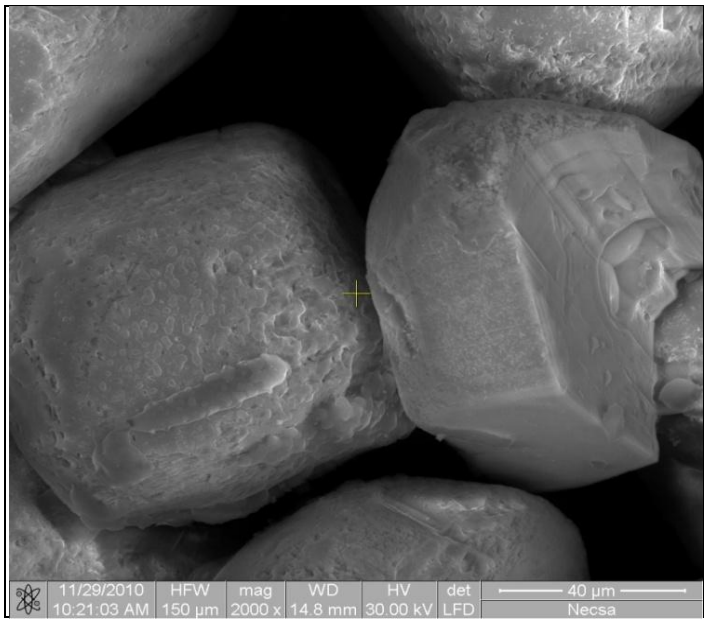

Figure 4.28: SEM micrograph of zircon leached in $NH_4F{\cdot}1.5HF$ for 30 min at 160 °C

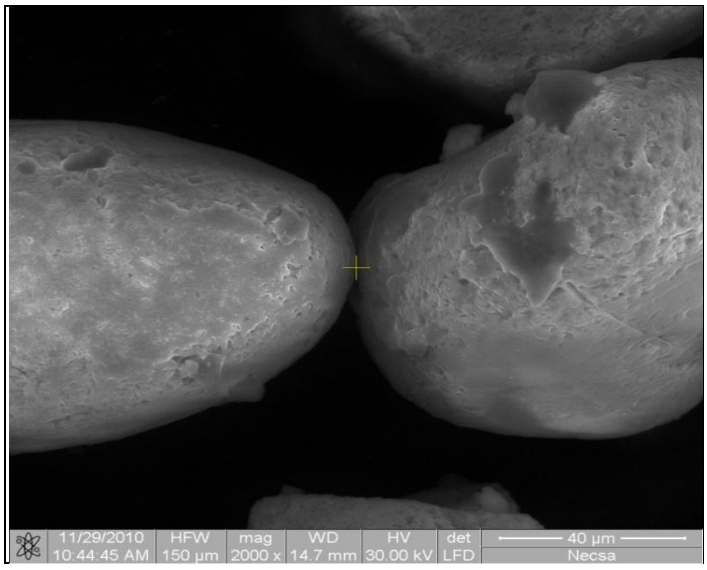

Figure 4.29: SEM micrograph of zircon leached in $NH_4F{\cdot}1.5HF$ for 60 min at 120 °C

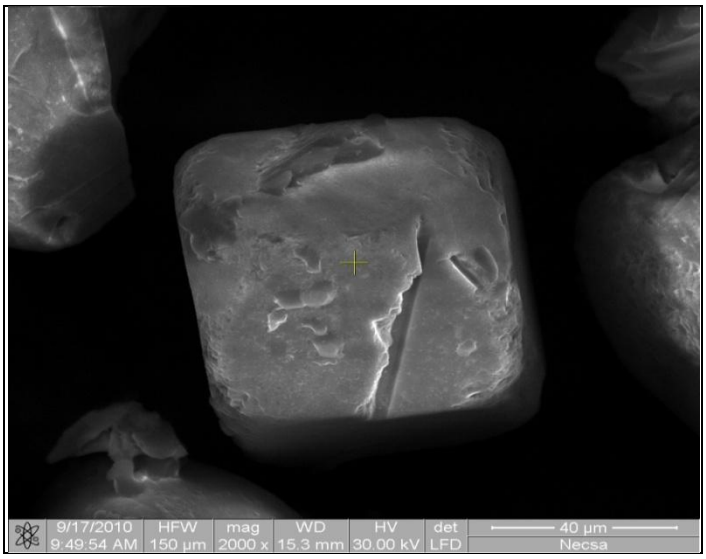

Figure 4.30: SEM micrograph of zircon leached in $NH_4F{\cdot}1.5HF$ for 60 min at 160 °C

SEM results for the reaction of zircon with AAF according to procedure 3

The morphology of the zircon leached in $NH_4F{\cdot}1.5HF$, washed and re-digested at different times is shown in Figures 4.31 to 4.33. It can be seen from Figure 4.31 that after 55 min of leaching the particle is etched and have some pores. As the leaching time increases to 150 min the etching of the zircon is more, and there are also some cracks. The pores on the surface are paving a way for the $NH_4F{\cdot}1.5HF$ to penetrate through the zircon (Figure 4.32). It is clear from Figure 4.33 that the longer the sample is leached (285 min) a more etched surface is observed and the particle is becoming amorphous with many cracks, which simply mean that it is becoming easy for the $NH_4F{\cdot}1.5HF$ to go through the zircon. Also the morphology of the zircon leached in $NH_4F{\cdot}1.5HF$, washed and redigested for 285 min at different temperatures is shown in Figures 4.34-4.36. At lower temperatures, some cracks are visible on the surface as indicated in Figure 4.34. The higher the leaching temperature results in small amount of zircon lost to form new compounds: $(NH_4)_2SiF_6$, $(NH_4)_3ZrF_7$ as described in this chapter. The SEM micrographs indicate the porous surfaces as evidence for the loss of zircon particles, which reacted during leaching as in Figures 4.35 and 4.36. Figure 4.36, where

the zircon was leached at the highest temperature, shows a more exposed surface of a particle.

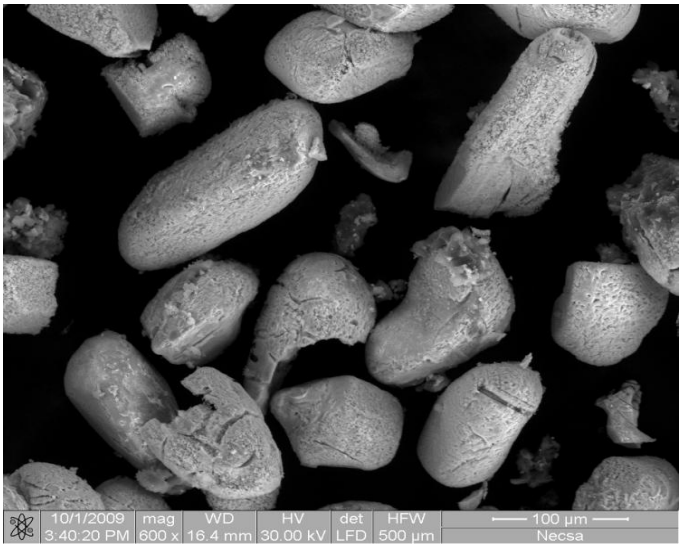

Figure 4.31: SEM micrograph of zircon leached in $NH_4F{\cdot}1.5HF$, washed and re-digested for 55 min at 200 °C

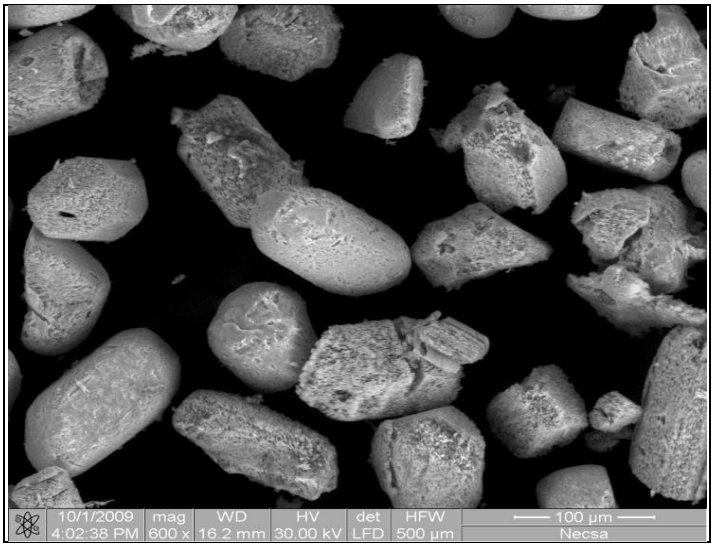

Figure 4.32: SEM micrograph of zircon leached in $NH_4F{\cdot}1.5HF$, washed and re-digested for 150 min at 200 °C

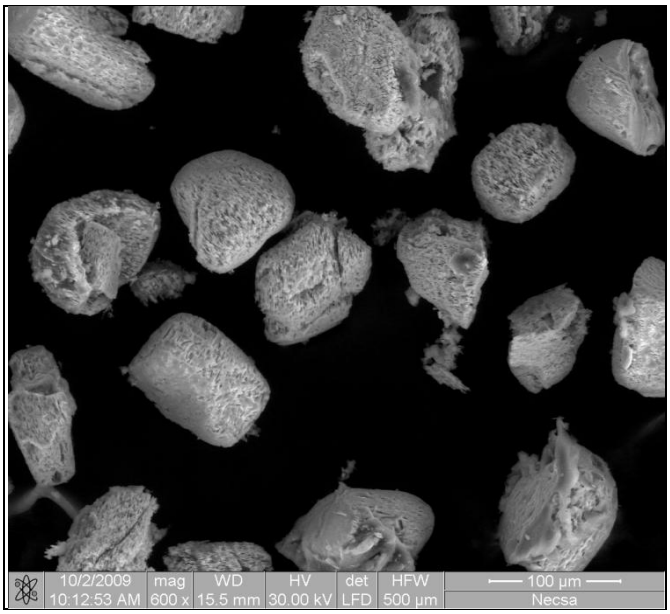

Figure 4.33: SEM micrograph of zircon leached in $NH_4F{\cdot}1.5HF$, washed and re-digested for 285 min at 200 °C

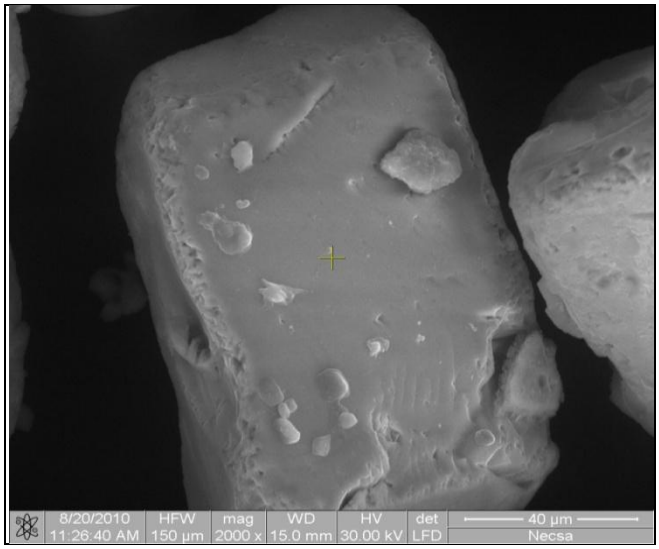

Figure 4.34: SEM micrograph of zircon leached in $NH_4F{\cdot}1.5HF$ and re-digested for 285 min at 120 °C

Figure 4.35: SEM micrograph of zircon leached in $NH_4F{\cdot}1.5HF$ and re-digested for 285 min at 160 °C

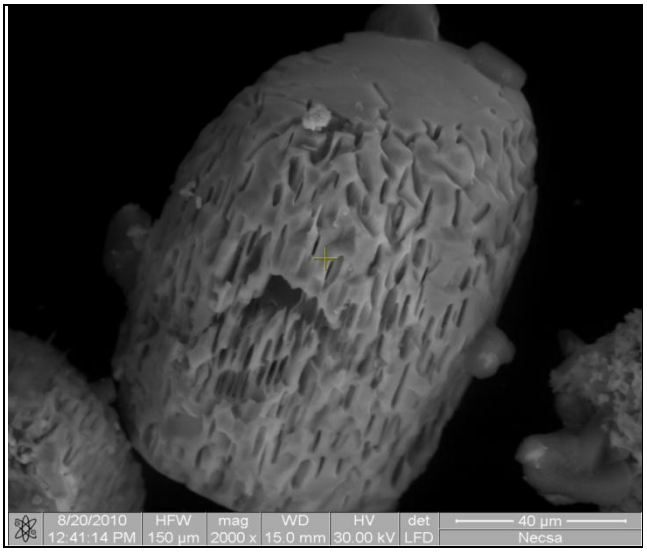

Figure 4.36: SEM micrograph of zircon leached in $NH_4F{\cdot}1.5HF$ and re-digested for 285 min at 240 °C

4.4. Reaction kinetics

This section presents the reaction kinetics which was derived from the data in procedure 3. Two models were considered for this reaction and, will be discussed.

The fact that digestion takes place during heating to temperature and during cooling complicates the extraction of kinetic data. Temperature ramp-up time (t_h) and ramp-down time (t_c), were 10 and 15 minutes respectively. The following simplifying assumptions were made in for processing the experimental data. A linear contribution to the total reaction time was assumed for these periods and added to the isothermal reaction times, t_r, at the preset temperature (T). The total reaction time was then calculated using the time-temperature integral (surface under the heating curve), *viz*.

$$Tt_{total} = Tt_r + Tt_h / 2 + Tt_c / 2 \quad (4.5)$$

Division by T simplifies Equation 4.5 to:

$$t_{total} = t_r + t_h / 2 + t_c / 2 \quad (4.6)$$

A number of kinetic models are possible for fluid-solid reactions (Levenspiel 1999). For this work the two most likely models were considered to be (1) a progressively shrinking particle, and (2) reaction rate control by diffusion through the product layer. For simplicity the particles are assumed to be spherical.

The expression for the progressive conversion model is

$$\alpha^{1/3} = 1 - \frac{t}{\tau} \quad (4.7)$$

with

$$\tau = \frac{\rho_5 r_0}{b M_5 k c} \quad (4.8)$$

Here τ is the full time for complete conversion, M_s and ρ_s are the molecular weight (183.3 g.mol^{-1}) and density (4.65 g.cm^{-3}) of the solid zircon respectively, r_0 is the initial radius of the zircon particles (63 μm), *t* is the reaction time, b and c are the stoichiometric coefficient and the concentration of the active species (taken to be HF) in the melt, and k is the rate constant in m.s^{-1}.

For the diffusion controlled model the rate expression is

$$3\alpha^{2/3} - 2\alpha = 1 - \frac{t}{\tau} \quad (4.9)$$

with

$$\tau = \frac{\rho r_0^2}{6 b D_e c} \quad (4.10)$$

Here D_e is the effective diffusion coefficient of the active species in the fluid through the product layer. In order to obtain the appropriate descriptive constant for each model, k or D_e, the left hand side of either Equation 4.7 or Equation 4.9 is generally plotted against time, τ is obtained from the slope, and the relevant constant is calculated from τ. To decide between the two models, the linear curve fits of the data plots are then compared. The better fit suggests the more correct model. Plots for the experimental data at 120, 160, 200 and 240 °C are presented in Figure 4.37 and Table 4.11 for the chemical control model and in Figure 4.38 and Table 4.12 for the ash-layer diffusion control model. It is clear from Figure 4.37 and Figure 4.38 that although both models fit the data, the ash layer diffusion is the best fit because if the ash layer is removed then it will be easy for the AAF to pass through the particle. For this case, because of the experimental procedure followed, this method is not strictly correct. The particles were washed with water after each successive digestion step, effectively destroying the processing history of the material. The use of the cumulative processing time is thus not valid and r_0 in Equations 4.9 and 4.11 should be replaced by the initial particle radius for

each step, obtained after washing the product of the previous step. For the chemical control model, this can be expressed explicitly as

$$\alpha_{i+1}^{1/3} - \alpha_i^{1/3} = \frac{bM_s kc}{\rho_s r_{0,i}}\left[t_{i+1} - t_i\right] \tag{4.11}$$

For the diffusion controlled model the expression is

$$3(\alpha_{i+1}^{2/3} - \alpha_i^{2/3}) + 2(\alpha_{i+1} - \alpha_i) = \frac{bM_5 kc}{\rho_5 r_{0j}^2}[t_{i+1} - t_i] \tag{4.12}$$

For both Equations 4.11 and 4.12 per definition α_i = 1, t_{i+1} = zero, and $r_{0,i}$ is the initial particle radius for each digestion step. Each digestion step at a given temperature thus yields either a k or a D_e value. For each temperature series an average value is calculated, and the average values for the different temperature ranges are used in Arrhenius plots to obtain the usual constants for deriving temperature-dependent values, as illustrated in Figure 4.39 and Table 4.13, and Figure 4.40 and Table 4.14. Both plots (Figure 4.39 and 4.40) display reasonable linearity, with very similar R^2 values. A pre-exponential factor k_0 = 1.315×10^{-7} m.s^{-1} and activation energy E_a = 27.672 kJ.mol^{-1} are obtained from Figure 4.39 for the reaction constant for a progressively shrinking particle. For the diffusion constant the corresponding values D_0 = 7.583×10^{-10} m^2.s^{-1} and E_a = 53.930 kJ.mol^{-1} are obtained from Figure 4.40. The magnitude of the diffusion constant for this case lies between 10^{-15} and 10^{-17} m^2 s^{-1}, depending on temperature. This is several orders of magnitude lower than for molecular diffusion through liquids, and typical for molecular diffusion through solids (Geankoplis, 1978; Bird *et al.*, 1960) as reproduced in Table 4.15. This, coupled to the fact that the process has to be interupted by washing steps to go to completion, suggests that diffusion control is the more realistic model. A reasonable interpretation is thus that an adhesive layer of ammonium fluoro-silicate-zirconate forms around each particle, thereby inhibiting access by the diffusing HF/HF_2^-, and controlling the process kinetics.

Table 4.11: Linear data for a reaction rate control model at 120, 160, 200 and 240 °C

t (sec)	T=120 °C $(\alpha')^{1/3}$	T=160 °C $(\alpha')^{1/3}$	T=200 °C $(\alpha')^{1/3}$	T=240 °C $(\alpha')^{1/3}$
0.00	1.00	1.00	1.00	1.00
1350	0.98	0.96	0.91	0.88
1950	0.97	0.96	0.91	0.80
2550	0.99	0.97	0.88	0.82
3150	0.98	0.95	0.93	0.73
3750	0.98	0.93	0.82	0.86
4350	0.98	0.95	0.90	0.52

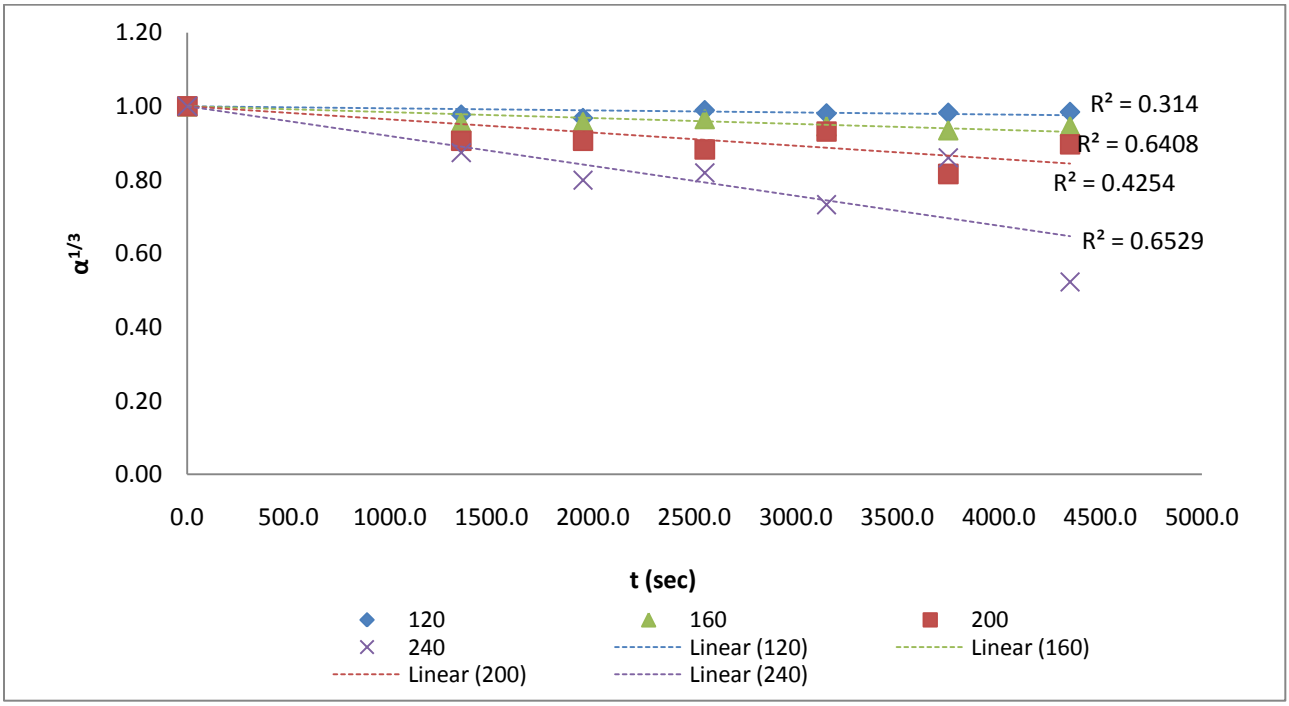

Figure 4.37: Linear plots for a reaction rate control model at 120, 160, 200 and 240 °C

Table 4.12: Linear data for a diffusion control model at 120, 160, 200 and 240 °C

t(sec)	T=120 °C $3(\alpha')^{2/3}-2\alpha'$	T=160 °C $3(\alpha')^{2/3}-2\alpha'$	T=200 °C $3(\alpha')^{2/3}-2\alpha'$	T=240 °C $3(\alpha')^{2/3}-2\alpha'$
0.00	1.00	1.00	1.00	1.00
1350	1.00	0.99	0.98	0.96
1950	1.00	0.96	0.98	0.90
2550	1.00	1.00	0.96	0.91
3150	1.00	0.99	0.99	0.82
3750	1.00	0.99	0.91	0.95
4350	1.00	0.99	0.97	0.53

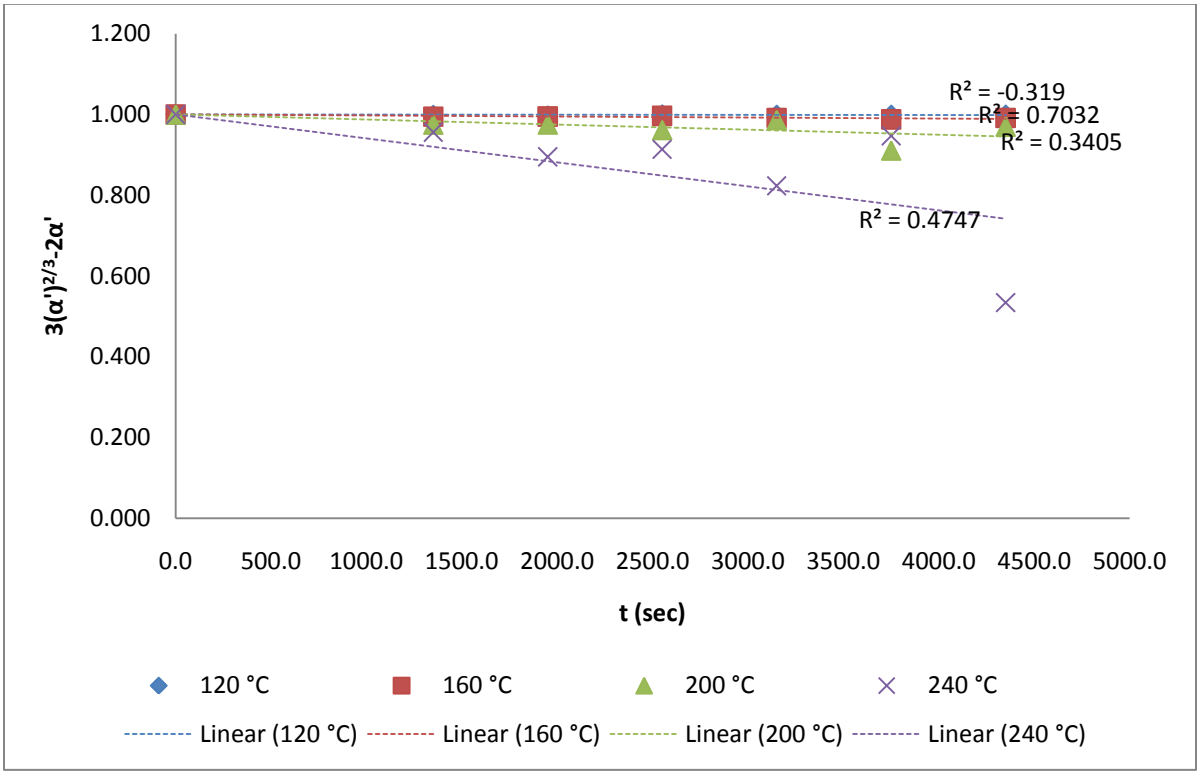

Figure 4.38: Linear plots for a product layer diffusion control model at 120, 160, 200 and 240 °C

Table 4.13: Arrhenius data for the chemical control model

1/T (1/K)	ln(k)
2.545×10^{-03}	-23.83
2.421×10^{-03}	-23.60
2.309×10^{-03}	-22.96
2.208×10^{-03}	-22.29
2.114×10^{-03}	-22.31
2.028×10^{-03}	-22.28
1.949×10^{-03}	-21.82

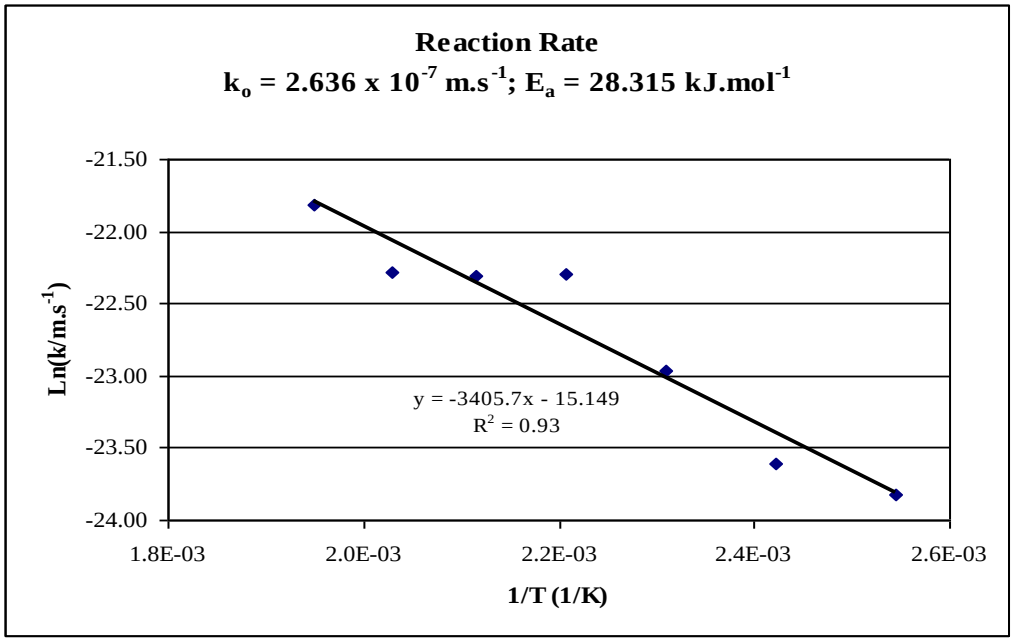

Figure 4.39: Arrhenius plot for a chemical control model

Table 4.14: Arrhenius data for the diffusion control model

1/T (1/K)	ln(D)
2.545×10^{-03}	-36.39
2.421×10^{-03}	-36.03
2.309×10^{-03}	-34.78
2.208×10^{-03}	-33.43
2.114×10^{-03}	-33.47
2.028×10^{-03}	-33.39
1.949×10^{-03}	-32.61

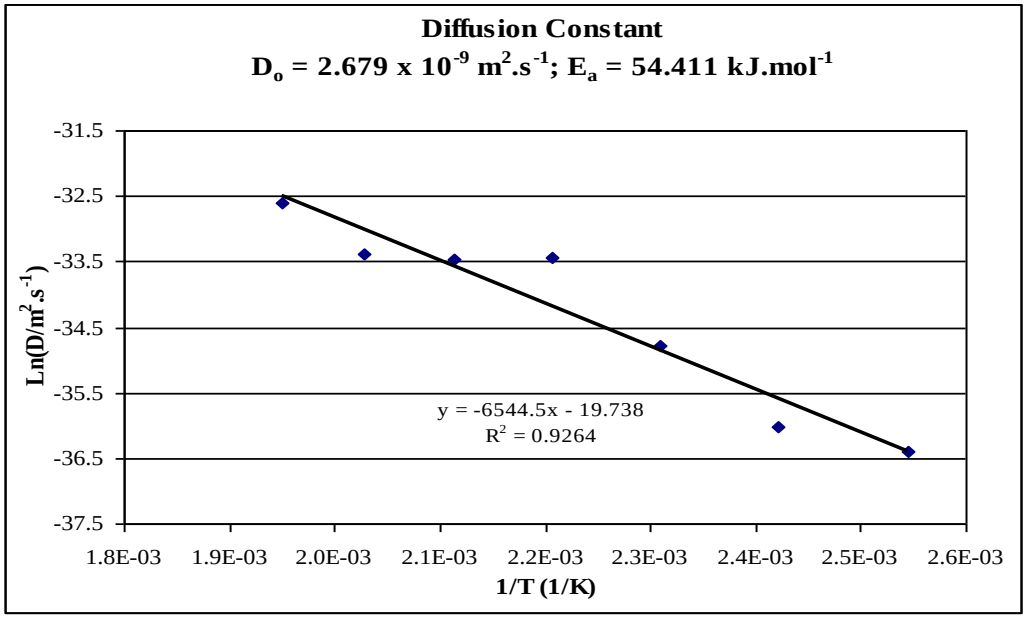

Figure 4.40: Arrhenius plot for a diffusion control model.

Table 4.15: Typical diffusivity values for various compounds (after Geankoplis, 1978; Bird *et al.*, 1960)

System	*T* (°C)	*D* ($m^2.s^{-1}$)
Gas phase		
CO_2 in N_2	25	1.65×10^{-5}
Ar in O_2	20	2.00×10^{-5}
Air in H_2	0	6.11×10^{-5}
Liquid phase		
Ethanol (50 mass %) in water	25	9.00×10^{-10}
Water (50 mass %) in n-butanol	25	2.67×10^{-10}
Acetone in water	25	1.28×10^{-9}
Solid state		
He in Pyrex®	20	4.5×10^{-15}
	500	2.0×10^{-12}
Hg in Pb	20	2.5×10^{-19}

4.5 Conclusion

From these results we can conclude that zircon can be converted practically quantitatively to water soluble products such as $(NH_4)_2SiF_6$ and $(NH_4)_3ZrF_7$) by microwave assisted digestion with $NH_4F{\cdot}1.5HF$ coupled with repeated removal of the product layer and addition of fresh reagent. This was achieved in four hours at a temperature of 240 °C. The kinetics of the fluorination process is mathematically equally well explained by both a progressively shrinking particle model and a product layer diffusion control model. The order of magnitude value of the diffusion constant calculated from this work corresponds to that for diffusion in solids. Because of this, and the fact that the process requires intermittent wash steps, the diffusion model is preferred and regarded as being physically more realistic.

CHAPTER 5

Summary conclusions and recommendations

In this work the reaction of zircon sand, obtained from Namakwa Sands (Pty) Ltd with ammonium acid fluoride under microwave condition was investigated. Three series of experiments were performed:

(1) Twelve vessels were used, each charged with virgin zircon and AAF. The system was run and after consecutive 10 min periods, individual vessels were removed, and the fractional conversion of each was determined.
(2) Three vessels with identical contents were used per run. After 10 min the reaction was stopped and the fractional conversion was determined. This experiment was repeated for 3 further runs, with fresh samples, for periods of 20, 30 and 60 min. For each run virgin zircon was used as starting material.
(3) Again three vessels with identical samples were used per run. The fractional conversion of the samples were determined after time t. Each sample was then washed with water to remove any product layer, and then re-introduced into the vessel for the next digestion period.

It was found that:

- Series 1 and 2 did not result in full conversion;
- The maximum conversion for series 1 was 70% after 330 min at 200 °C;
- The maximum for series 2 was 30% after 60 min at 200 °C;
- However, in series 3 after washing the sample with water between exposure periods to remove the ash layer, 99% conversion after 285 min at 240 °C was achieved.
- In general good data were obtained, with all gravimetric curves showing interpretable trends. A few inconsistencies and outliers were observed. This

could be due to our experimental techniques. Another explanation could be factors that were not monitored closely enough, such as non-analysed admixtures of alkali and alkali-earth metals.

As analytical tools SEM, Raman, ICP-OES and XRD were used. A kinetic analysis of the data of series 3 was performed. The main findings were as follows:

- Chemical analyses indicate the slight removal of Si and Al. This might be due to the removal of non-bound silica and alumina. This is at the ~1% level only;
- Zircon particles leached several times by AAF showed etch pores on their surface (SEM results);
- XRD and Raman confirmed that the main component of the residue was zircon;
- Two models that were considered to explain the reaction kinetics. They were the progressive shrinking particle model and the ash-layer diffusion control model;
- A kinetic analysis indicates that both models fit the data. The product-layer diffusion control model was selected as physically the most realistic;
- To by-pass the diffusion limitation, intermittent wash-steps were introduced to remove the product layer between digestion periods;
- At 240 °C 80 % conversion is achieved within one hour, and practically full conversion was obtained after four hours.

Unfortunately microwave digestion does not lend itself to vigorous agitation. A way forward would be to include an autoclave with a high torque stirrer. To further progress the technology as developed to this stage, the washed product would need additional careful attention and the chemistry of determining useful products from the aqueous solution investigated. This might include evaporation to dryness, and dried the residue further treated with heating to evaporate the $(NH_4)_2SiF_6$ leaving a residue of $(NH_4)_3ZrF_7$ from which ZrF_4 can be obtained by heating.

REFERENCES

- Abdelkader, AM, Daher, A and El-Kashef, E (2008) “Novel decomposition method for zircon” *J. Alloys Compd*, 460, 577-580.

- Acierno, D, Barba, AA, and Amore, M (2004) “Heat transfer phenomena during processing materials with microwave energy” *Heat and Mass Transfer*, 40(5), 413-420.

- Agazzi, A and Pirola, C (2000) “Fundamentals, methods and future trends of environmental microwave sample preparation” *Microchemical Journal*, 67(1-3), 337-342.

- Al-Harahsheh, M, Kingman, S, and Bradshaws, S (2006) “The reality of non-thermal effects in microwave assisted leaching systems” *Hydrometallurgy*, 84 (1-2), 1-13.

- Al-Harahsheh, M, Kingman, S, Hankins, N, Somerfield, C, Bradshaw, S and Louw, W (2005) “The influence of microwaves on the leaching kinetics of chalcopyrite” *Minerals Engineering*, 18(13-14), 1259-1268.

- Al-Harahshesh, M and Kingman, SW (2004) “Microwave-assisted leaching - a review” *Hydrometallurgy,* 73(3-4), 189-203.

- Baeraky, TA. (2002) “Microwave Measurements of the Dielectric Properties of Silicon Carbide at High Temperature” *Egypt. J. Sol*, 25(2), 263-273.

- Basagaoglu, H, McCoy, BJ, Ginn, T.R, Loge, FJ and Dietrich, J.P (2002), “A diffusion limited sorption kinetics model with polydispersed particles of distinct sizes and shapes”, *Advances in Water Resources*, 25, 755-772.

- Bidaye, AC, Venkatachalam, S and Gupta, C.K (1999) “Studies on the chlorination of zircon: Part I. Static bed investigations” *Metall. Mater. Trans. B* 30B, 205-213.

- Bird, RB, Stewart, WE and Lightfoot, EN (1960) “Transport phenomena” 2nd edn, John Wiley and Sons, New York.

- Bookse, JH, Cooper, RF and Freeman, SA (1997) “Microwave enhanced reaction kinetics in ceramics” *Mat Res Innovat*, 1(2), 77-84.

- Callebaut, J (2007) “Dielectric Heating” http://www.leonardo-energy.org/drupal/dielectrics-heating.com, accessed 2009/06/09.

- Camel, V (2000) “Microwave-assisted solvent extraction of environmental samples” *Trends in analytical chemistry*, 19(4), 229-248.

- Chou, S, Lo, S, Hsieh, C and Chen, C (2009) “Sintering of MSWI fly ash by microwave energy” *Journal of Hazardous Material*, 163(1), 357-362.

- Clark, DE, Folz, DC and West, JK (2000) “Processing materials with microwave energy” *Materials Science and Engineering*, 287(2), 153-158.

- Conner, WC and Tompsett, GA (2008) “How could and do microwaves influence chemistry at interfaces?” *J. Phys. Chem. B*, 112 (7), 2110-2118.

- Das, S, Mukhopadhyay, AK, Datta, S and Basu, D (2008) “Prospects of microwave processing: An overview” *Bulletin of material science*, 32(7) 943-956.

- De Waal D., Heyns AM., Pretorius G (1996) “Raman spectroscopic investigations of $ZrSiO_4$: V^{4+}, the blue zircon vanadium pigment” *Journal of Raman Spectroscopy,* 27(9), 657-662.

- Deshayes, S, Marion, L, Loupy, A, Luche, J and Petit, A (1999) "Microwave Activation in Phase Transfer Catalysis" *Tetrahedron,* 50 (36), 10851-10870.

- Elijofor, JU, Okonie, BA and Reddy, RG (1997) "Powder processing and properties of zircon-reinforced Al-13.5 Si-2.5 Mg alloy composites" *Journal of materials engineering and performance,* 6 (3), 326-334.

- Etherington, RC, Dalzell, RC and Lillie, DW (1955) "Zirconium and its application to nuclear reactors" in: Lustman, B. Kerze F. and Urban SF. (Editors), The Metallurgy of Zirconium. McGraw-Hill, New York, pp 1-18.

- Filliaudeau, D and Picard, G (1991) "Temperature dependence of the vapor pressures and electrochemical windows of the NH_4HF_2-HF mixtures, in Molten Salt Chemistry and Technology, *Material Science Forum* (Chemla, M and Devilliers, D eds.), volume 73-75, Zurich, p 669.

- Finch, JR and Hanchar, JM (2003) "Structure and chemistry of zircon and zircon-group minerals" *Reviews in mineralogy and geochemistry,* 53(1), 1-25.

- Flores, EMM, Barin, JS, Mesko, MF and Knapp, G (2007) "Sample preparation techniques based on combustion reactions in closed vessels - A brief overview and recent applications" *Spectrochimica Acta Part B* 62(9), 1051-1064.

- Frayret, J, Castetbon, A, Trouve G and Potin-Gautier, M (2006) "Solubility of $(NH_4)_2SiF_6$, K_2SiF_6 and Na_2SiF_6 in acidic solutions" *Chemical Physics Letters* 427, 356-364.

- Galema, SA, (1997) "Microwave chemistry" *Chemical Society Reviews* 26: 233-238.

- Galwey, AK (2003) “What is meant by the term ‘variable activation energy’ when applied in the kinetic analyses of solid state decompositions (crystolysis reactions, *Thermochimica Acta* 397, 249-268).

- Galwey, AK, (2000) “Structure and order in thermal dehydrations of crystalline solids”, *Thermochimica Acta*, 355,181-238.

- Gan, Q (2000) “A case study of microwave processing of metal hydroxide sediment sludge from printed circuit board manufacturing wash water” *Waste Management*, 20 (8), 695-701.

- Gbor, PK and Jia, CQ (2004) “Critical evaluation of coupling particle size distribution with the shrinking core model”, *Chemical Engineering Science*, 59 (1979-1987).

- Geankoplis, CJ (1978) “Transport processes and unit operations”, Allyn and Bacon, Inc., Boston.

- Gupta, M and Wong Wai Leong, E (2007) *Microwaves and Metals*, John Wiley & Sons, Asia.

- Guzeev, VV and D’yackenko, AN (2006) “Autoclave breakdown of zircon with ammonium fluorides” *Russian Journal of Applied Chemistry,* 79(11), 1757-1760.

- Hala, J (1989) “Halides, Oxyhalides and salts of halogen complexes of titanium, zirconium, hafnium, vanadium, niobium and tantalum”, IUPAC Solubility Data, Series, pp, 58

- Haque, KE (1999) “Microwave energy for mineral treatment processes-a brief review” *Int. J. Miner. Process*, 57(1), 1-24.

- Harzdorf, C, Rinneb, GJD, and Roggeb, M (1998) "Application of microwave digestion to trace organoelement determination in water samples" *Analytica Chimica Acta,* 374, (2-3), 209-214.

- Hill, JM and Marchant, TR (1996) "Modelling microwave heating" *Appl. Math. Modelling*, 20, 1-15.

- Hsu, J-P and Liu, B-T (1993), "Dissolution of solid particles in liquids: a reaction-diffusion model", *Colloids and Surfaces*, 69, 229-238.

- Industrial mineral (2010), "TiO_2/Zircon" http://www.indmin.com/MarketTracker/197202/TiO_2Zircon.html?id=ZISA-C,TDP-C, accessed 2011/09/02.

- Jafarifar, D, Daryanavard, MR and Sheibani, S (2005) "Ultra fast microwave-assisted leaching for recovery of platinum from spent catalyst" *Hydrometallurgy*, 78(3-4), 166-171.

- Janney, MA, Kimrey, HD, Allen, WR and Kiggans, JO (1997) "Enhanced diffusion in sapphire during microwave heating" *J. Mat. Sci.,* 32(5), (1347-1355).

- Kaiser, A, Lobert, M, and Telle, R (2008) "Thermal stability of zircon ($ZrSiO_4$)" *Journal of the European Ceramic Society*, 28, 2199-2211.

- Kappe, CO (2002) "High-speed combinatorial synthesis utilizing microwave irradiation" *Current opinion in chemical biology*, 6(3), 314-320.

- Kingston, (Skip) HM and Jassie, LB (1988) *Introduction to Microwave Sample Preparation*, American Chemical Society, Washington DC.

- Knittle E and Williams Q (1993) “High pressure Raman spectroscopy of zircon” *American Mineralogis*, 78, 245-252.

- Kollewin (2009) “The electromagnetic spectrum” http://www.kollewin.com/blog/electromagnetic-spectrum/accessed 2011/02/24.

- Kotzé, H, Bessinger, D and Beukes, J (2006) “Ilmenite Smelting at Ticor SA”, South African Institute of Mining and Metallurgy, Johannesburg.

- Krämer, D. (2003) “A new method for pressure measurement in microwave digestion vessels” Berghof Products and Instruments GmbH, Germany.

- Kuss, HM (1992) “Application of microwave digestion techniques for elemental analyses” *Fresenius J. Anal Chem*, 343(9-10), 788-793.

- Lamble, KJ and Hill, SJ, (1998) “Microwave digestion procedures for environmental matrices” *Analyst,* 123, 103-133.

- Langa, F, De La Cruz, P, De La Hoz, A, Diaz-Ortiz, A and Diez-Barra, E, (1997) “Microwave irradiation: more than just a method for accelerating reactions” *Contemporary Organic Synthesis*, 4, 373-386.

- LeBlanc, GN (2000) “Microwave-accelerated dissolution of polymers for molecular weight analysis” *American Laboratory*, 32(18), 32-37.

- Levenspiel, O (1999) “Chemical Reaction Engineering” 3rd edn, Wiley, New York.

- Levine, KE, Batchelor, JD, Rhoades, Jr, CB, and Jones, BT, (1999). “Evaluation of a high-pressure, high-temperature microwave digestion system”, *J. Anal. Atom. Spectr,* 14, 49-59.

- Lewis, GP, Wylie, SR, Shaw, A, AI-Shamma'a, AI, Phipps, D, Alkhaddar, R and Bond, G, (2007) "Monitoring and control system for turntable high frequency microwave assisted chemistry" *J. Phys: Conference Series,* 76(1), 1-6.

- Li, D, Liang, D, Fan, S, Li, X, Tang, L and Huang, N (2008) "*In situ* hydrate dissociation using microwave heating: Preliminary study", *Energy Conversion and Management,* 49(8), 2207-2213.

- Li, Y and Yang, W, (2008) "Microwave synthesis of zeolite membranes: A review" *J. Membr. Sci*, 316(1-2), 3-17.

- Lidstrom, P, Tierney, J, Wathey, B and Westman, J (2001) "Microwave assisted organic synthesis - a review" *Tetrahedron* 57(45), 9225-9283.

- Luque-Garcia, JL and Luque de Castro, MD (2003) "Where is microwave-based analytical equipment for solid sample pre-treatment going?" *Trends in Analytical Chemistry,* 22(2), 90-98.

- Ma, X and Li, Y (2006) "Determination of trace impurities in high-purity zirconium dioxide by inductively couple plasma atomic emission spectrometry using microwave-assisted digestion and wavelet transform-based correction procedure" *Anal. Chim. Acta*, 579(1), 47-52.

- Magnet lab s.a. "The magnetron" http://www.magnet.fsu.edu/education/tutorials/museum/magnetron.html accessed 2009/09/16.

- Manufacturer .s.a."Zircon sand" http://www.manufacturer.com/cimages/product/www.itrademarket.com/1018/q/288652, accessed 2010/17/09.

- Markus, H, Fugleberg, S, Valtakari, D, Salmi, T, Murzin, D and Lahtinen, M (2004) "Kinetic modeling of solid-liquid reaction: reduction of ferric iron to ferrous iron with zinc sulphide", *Chemical Engineering Science*, 59 (4), 919-930.

- McPherson, R and Shafer, RBV (1985) "The re-association of plasma dissociated zircon" *J. Mater*. *Sci,* 20, 2597-2602.

- Metaxas, AC (1991) "Microwave Heating" *Power Engineering Journal*, 5(5), 237-247.

- Metaxas, AC and Meredith, RJ (1983) *Industrial Microwave Heating*, Peter Peregrinus Ltd, London.

- Michael, D, Mingos, P and Baghurst, DR (1991) "Applications of Microwave Dielectric Heating Effects to Synthetic Problems in Chemistry" *Chem. Soc. Rev*, 2, 1-47.

- Microwaves s.a. "Waveguide primer" http://www.microwaves101.com/enclopedia/waveguide.cfm. accessed 2009/09/16.

- Milestone (2003) "Microwave Synthesis" http://www.milestonesci.com/synth-fund.php, accessed 2009/01/15).

- Milestone (2009) http://www.milestonesrl.com/analytical/products_digestion_start_mod.html, accessed 2009/16/09.

- Monnahela, OS (2008) "Synthesis of high purity zirconium tetrafluoride for nuclear applications" University of the Free State, Bloemfontein, (Dissertation M.Sc).

- Nel J.T., (1995) "The wet HF route," Patent, PCT/US/95/15556,.

- Obermayer, D, Gutmann, B, and Kappe CO (2009) ''Microwave chemistry in silicon carbide reaction vials: separating thermal from nonthermal effects" *'Angew. Int. Ed*, 48(44), 8321-8324.

- Opalovsky, AA, Fedorov, VE and Fedotova, TD (1973) "Reaction of alkali and ammonium bifluorides with aluminium and silicon", *Journal of Thermal Analysis*, 5, 475-482.

- Parrin (2009) "Parr microwave acid digestion bombs" http://www.parrinst.com/default.cfm?page_id=210,accessed 200916/09.

- Presser V, Glotzbach C (2009) "Metamictization in zircon: Raman investigation part II", *Journal of Raman Spectroscopy,* 40(5), 499-508.

- Puclin, T, Kaczmarek, WA and Ninham, BW (1995) "Dissolution of $ZrSiO_4$ after mechanical milling with Al_2O_3", *Mater. Chem. Phys.* 40,105-109.

- Rakov, EG and Mel'nichenko, EI (1984) "The properties and Reactions of Ammonium Fluorides", *Russian Chemical Reviews*, 53 (9), 851-869.

- Rasmussen, B (2005) "Zircon growth in very low grade meta-sedimentary rocks: evidence for zirconium mobility at 250 °C" *Contrib mineral petrol,* 150(2), 146-155.

- Rendtorff, NM, Garrido, LB and Aglietti, EF (2009) "Mechanical and fracture properties of zircon-mullite composites obtained by direction sintering" *Ceramics International*, 35(7), 2907-2913.

- Roskill Information Services Ltd (2004) "The economics of zirconium", Roskill.

- Schawe, JEK (2002) "A description of chemical and diffusion control in isothermal kinetics of cure kinetics", *Thermochimica Acta*, 388, 299-312.

- Scitovski, R and Meler, M (2002) “Solving parameter estimation problem in new product diffusion models” ,*Applied Mathematics and Computation* 127, 45–63.

- Shi, Y, Huang, X and Yan, D (1997) “Fabrication of hot-pressed zircon ceramics: mechanical properties and microstructure” *Ceramics International*, 23(5), 457-462.

- Snyders, E (2007) “The development of zircon as a superior opacifier” Tshwane University of Technology, Pretoria, (Dissertation D.Tech).

- Sosnowski, M and Skulski L (2005) “A comparison of Microwave-Accelerated and Conventionally Heated Iodination Reactions of Some Arenes and Heteroarenes, Using ortho-Periodic Acid as the Oxidant” *Molecules,* 10(2), 401-406.

- Stadler, A, Pichler, S, Horeis, G and Kappe, CO (2002) “Microwave-enhanced reactions under open and closed vessel condition. A case study” *Tetrahedron,* 58 (16) 3177-3183.

- Stevens, R (1986) “Zirconia and zirconia ceramics” Magnesium Elektron Ltd.,Twickenham

- Stuerga, D and Gaillard, P (1996) “Microwave heating as a new way to induce localized enhancements of reaction rates: Nonthermal and heterogeneous kinetics” *Tetrahedron*, 52(15), 5505-5510.

- Tada, S, Echigo, R and Yoshida, H (1998) “Numerical analysis of electromagnetic wave in a partially loaded microwave applicator” *Int. J. Heat Mass transfer*, 41:709-718.

- Tanase, A, Cornelia, AV and Patroescu, C (2004) "Optimized microwave digestion method for iron and zinc determination by flame absorption spectrometry in fodder yeasts obtained from paraffin, methanol and ethanol" *Chimie, Anul XIII (serie noua)* I-II: 117-124.

- Taylor, VE, Toms, A and Longerich, HP (2002) "Acid digestion of geological and environmental samples using open-vessel focused microwave digestion" *Anal Bioanal Chem,* 372(2), 360-365.

- Thostenson, ET and Chou, T (1999) "Microwave processing: fundamentals and applications" *Applied Science and Manufacturing*, 30(9), 1055-1071.

- Tripathi, A and Chattopadhyay, P (2007) "Digestion of titanium bearing geologic materials involving microwaves" *Annali di Chimica*, 97(10), 1047-1064.

- Tyler, RM and Minnitt, RCA (2004) "A review of sub-Saharan heavy mineral sand deposits: Implications for new projects in Southern Africa", *The Journal of The South African Institute of Mining and Metallurgy*, 104(2), 89-99.

- TZ Minerals International (2001) "The global zircon industry" (Pty) Ltd,, West Perth, Australia.

- U_xC Consulting Services (2010) "Nuclear zirconium alloy market" 1401 Macy Drive,Roswell, GA 30076.

- Vorotynstev,VM, Mochalov, GM and Suvorov, SS (2004) "Calculation of the constant of the electrolytic dissociation of hydrogen fluoride in NH_4F-HF melts variable composition of over the temperature range from 360 to 420 K" *Russian Journal of Physical Chemistry*,78(6),1050-1052.

- Vyazovkin, S (2000) “Kinetic concepts of thermally stimulated reactions in solids: a view from a historical perspective”, *International Reviews in Physical Chemistry*, 19 (1), 45-60.

- Walter, PJ, Chalk, S and Kingston, HMS (1998) *Overview of microwave assisted sample preparation,* American Chemical Society, Washington, DC
.
- Whittaker, G (2007) “Microwave heating mechanism”, http://www.tan_delta.com/mw_heating.html, accessed [2009/10/06.

- Wilks, PH, Ravinder, P, Grant, CL, Pelton, PA, Downer RJ and Talbot ML, (1972) “Plasma process for zirconium dioxide” *Chem. Eng. Prog*, 68, 82-83.

- Wilks, PH, Ravinder, P, Grrat, CL, Pelton, PA, Downer RJ and Talbot ML, (1974) “Commercial production of submicron ZrO_2 via plasma” *Chem. Eng. World* 9 pp 59-65.

- Will, H, Scholtz, P and Odruschka, B (2004) “Heterogeneous gas-phase catalysis under microwave irradiation - a new multi-mode microwave applicator” *Topics in Catalysis,* 29(3-4), 381-387.

- Williamson, JPH and Evans, AM (1979) “Investigations into the characteristics and some potential industrial applications of plasma dissociated zircon” *Trans. J. Br.Ceram. Soc,* 74, 68-77.

- Xie, Z, Yang, J, Huang, X and Huang, Y (1999) “Microwave Processing and Properties of Ceramics with Different Dielectric Loss” *J. Euro. Ceram. Soc,* 19(3), 381-387.

- Zhang, X and Hayward, DO (2006) “Application of microwave dielectric heating in environment-related heterogeneous gas-phase catalytic systems” *Inorg. Chim. Acta,* 359 (11), 3421-3433.

- Zhao, Y and Chen, J (2008) “Studies on the dissolution kinetics of ceramic uranium dioxide particles in nitric acid by microwave heating” *Journal of Nuclear Material,* 373(1-3), 53-58.